GRAPHENE: ELECTRON PROPERTIES AND TRANSPORT PHENOMENA

Leonid Levitov
MIT

Lecture notes and HW problems:
http://www.mit.edu/~levitov/

Summer School in Condensed Matter Physics, Princeton 2008

Table of contents

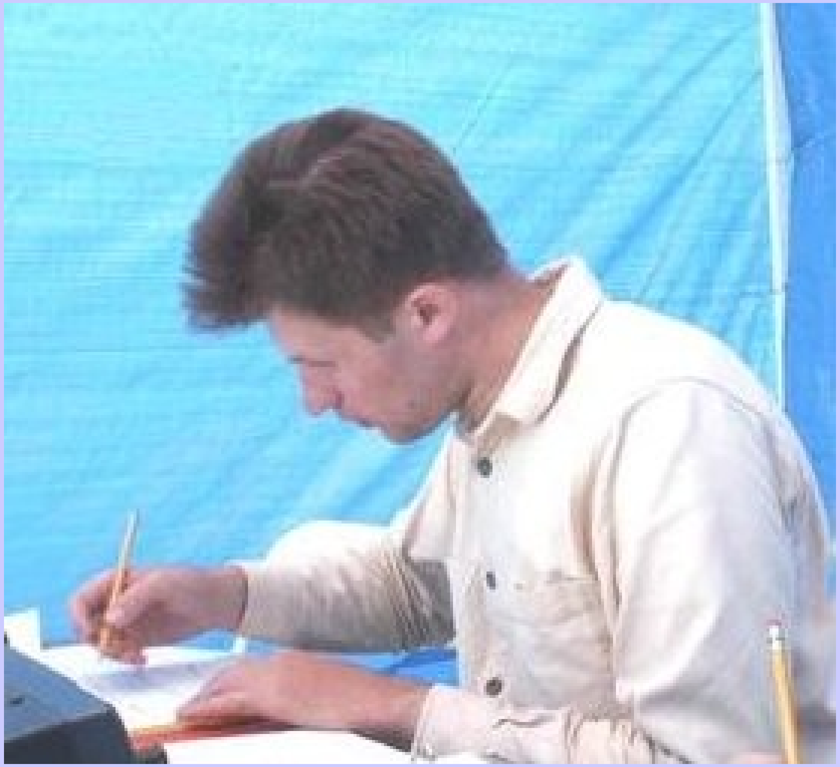

Dima Abanin (MIT)

Andrey Shytov (Utah)

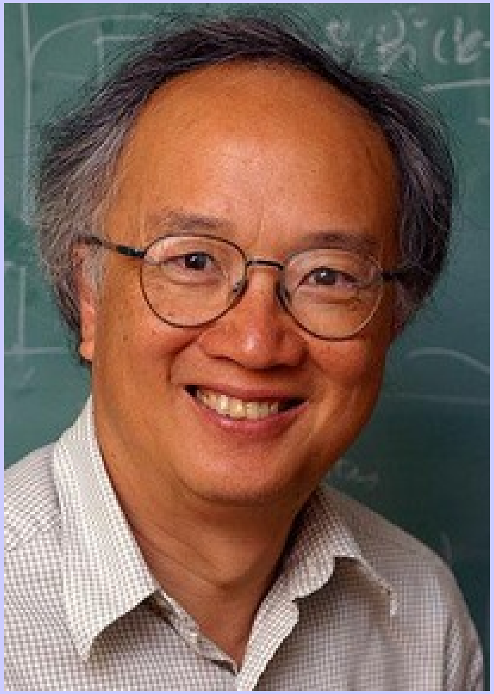

Misha Katsnelson (Nijmegen)

Patrick Lee (MIT)

Lecture I

Graphene background:

Transport properties, Quantum Hall effect, brief overview

Electron transport in graphene monolayer

New 2D electron system (Manchester 2004):
Nanoscale electron system with tunable properties;

Andrey Geim

Kostya Novoselov

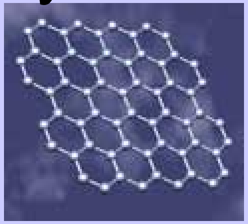

Monolayer graphene

Philip Kim

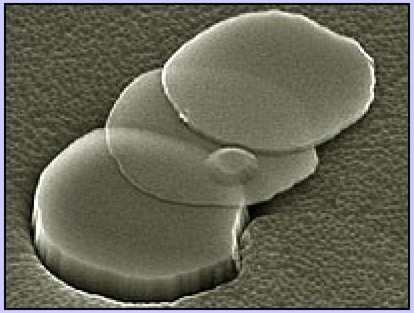

Field-effect enabled by gating:
tunable carrier density,
conductivity linear in density

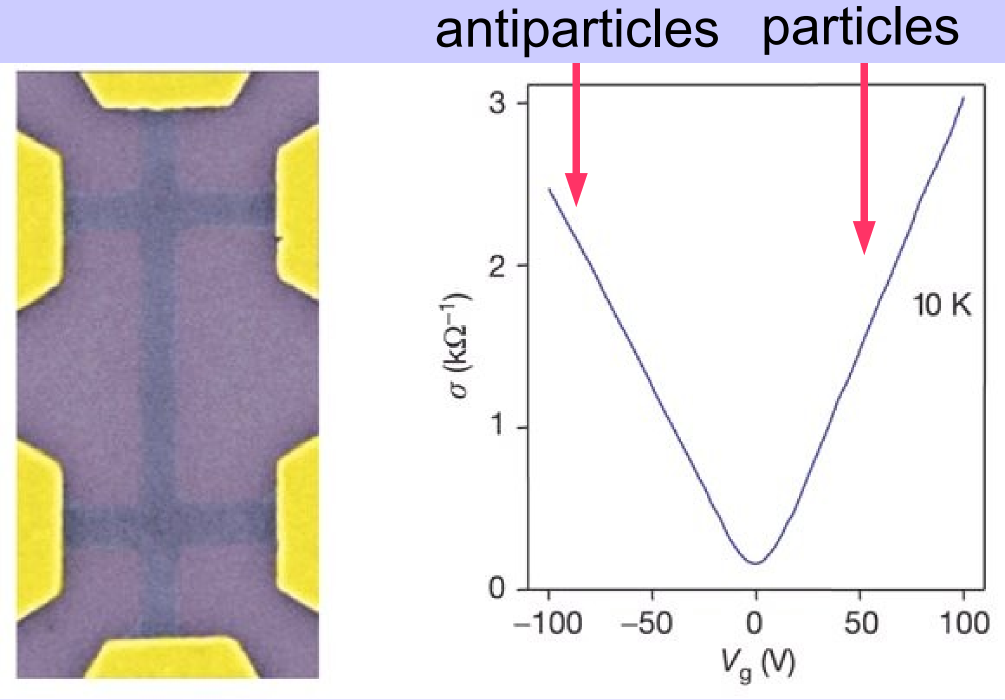

Novoselov et al, 2004, Zhang et al, 2005

Interesting Physical Properties

Semimetal (zero bandgap); electrons and holes coexist

Massless Dirac electrons, d=2

Electron band structure:
hexagonal BZ, at points K and K'
mimic relativistic Dirac particles

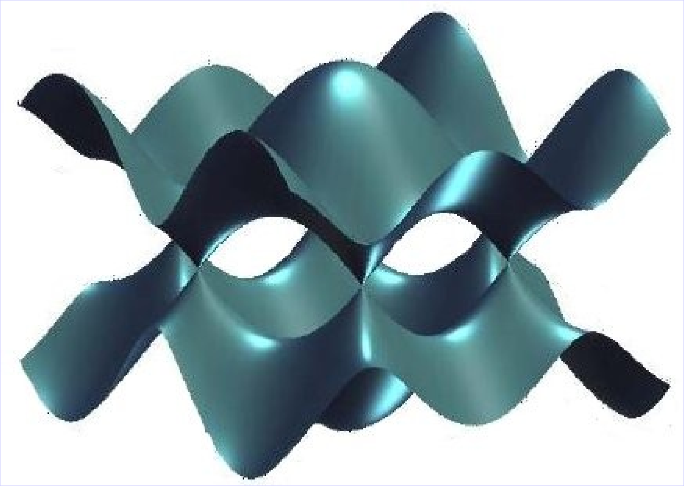

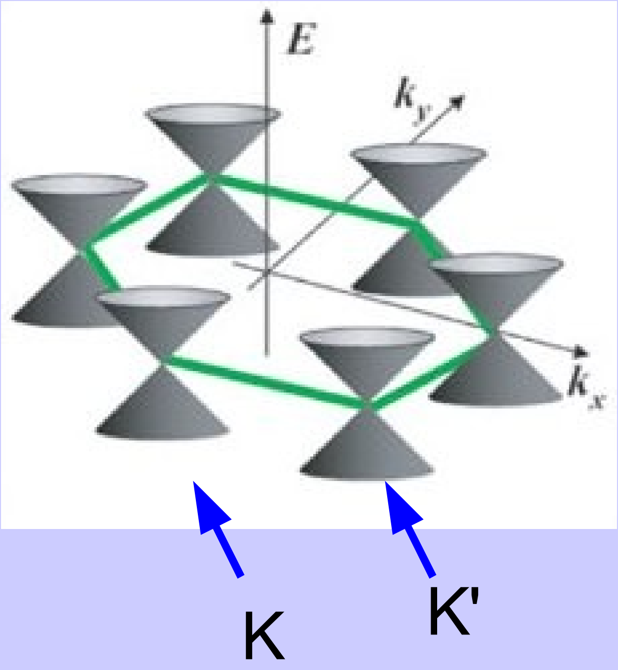

Manifestations: pseudo Lorentz invariance,
Fermi velocity instead of the light speed

"Half-integer" Quantum Hall Effect

Single-layer graphene:
QHE plateaus observed at

$$\nu = 4 \times (0, \pm 1/2, \pm 3/2 \ldots)$$

4=2x2 spin and valley degeneracy

Manifestation of relativistic Dirac electron properties

Landau level spectrum with very high cyclotron energy (1000K)

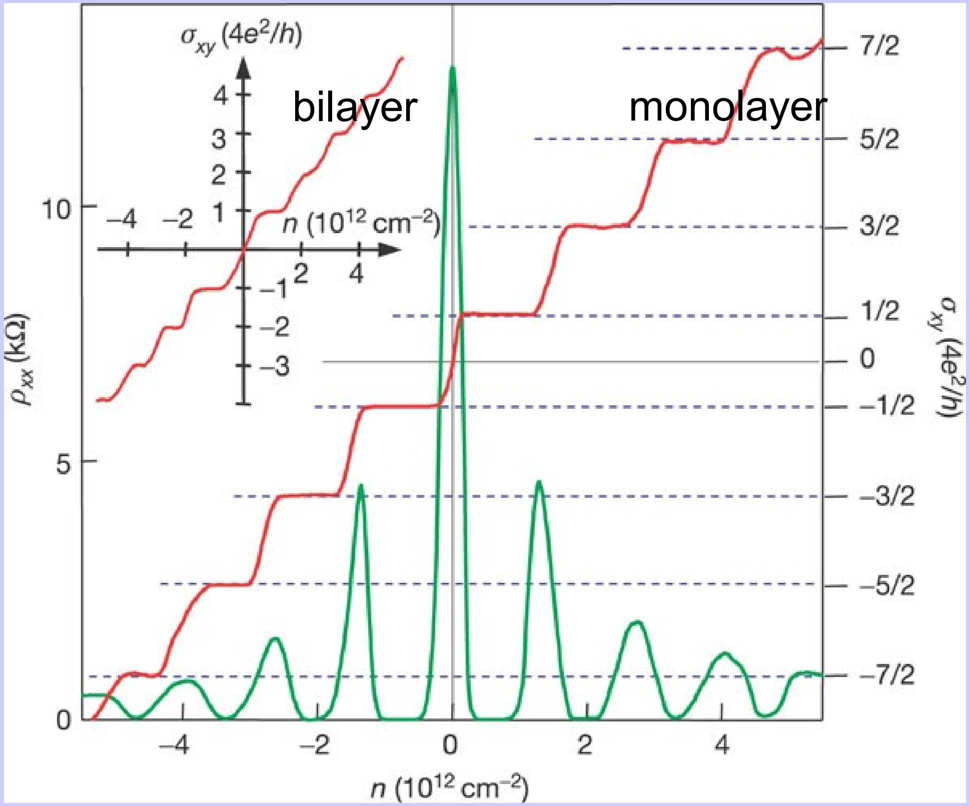

Novoselov et al, 2005, Zhang et al, 2005

<u>Recently: QHE at T=300K</u>

Recent experimental progress

- Spin and valley splitting of Landau levels in ultrahigh magnetic fields (Columbia, NHMFL)
- Increase in mobility (with and without substrate) (Manchester, Rutgers, Columbia)

Up to 200,000 cm^2/sV in suspended sheets

- Graphene with superconducting contacts (SGS Josephson junctions, Andreev scattering) (Delft, Rutgers)
- Energy gap induced by magnetic field (Princeton)
- Energy gap induced by substrate (Berkeley)
- Graphene devices (quantum dots, p-n junctions) (Manchester, Stanford, Harvard, Columbia)

Graphene-based devices

Devices in patterned graphene:
- quantum dots (Manchester),
- nanoribbons (IBM, Columbia);

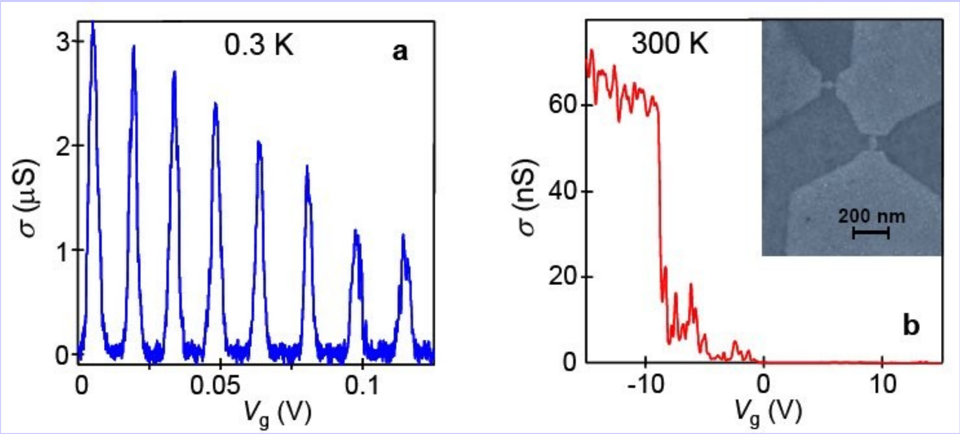

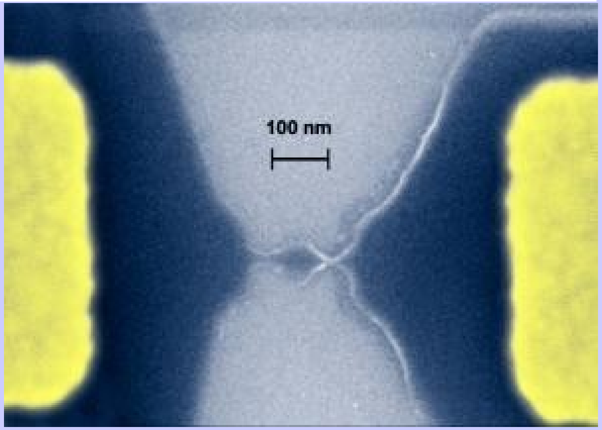

Local density control (gating):
- p-n and p-n-p junctions

(Stanford, Harvard, Columbia)

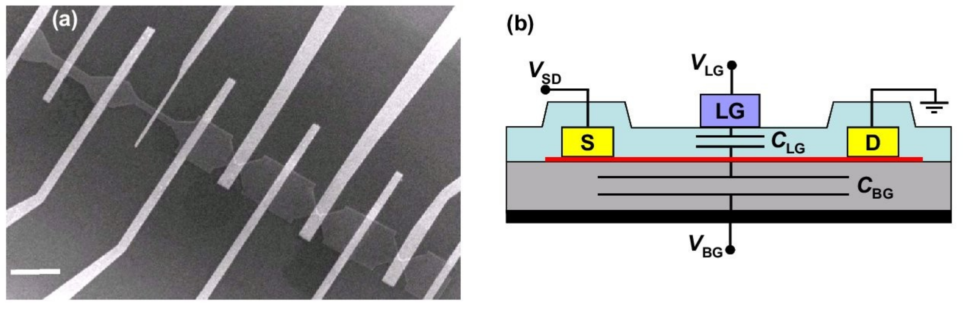

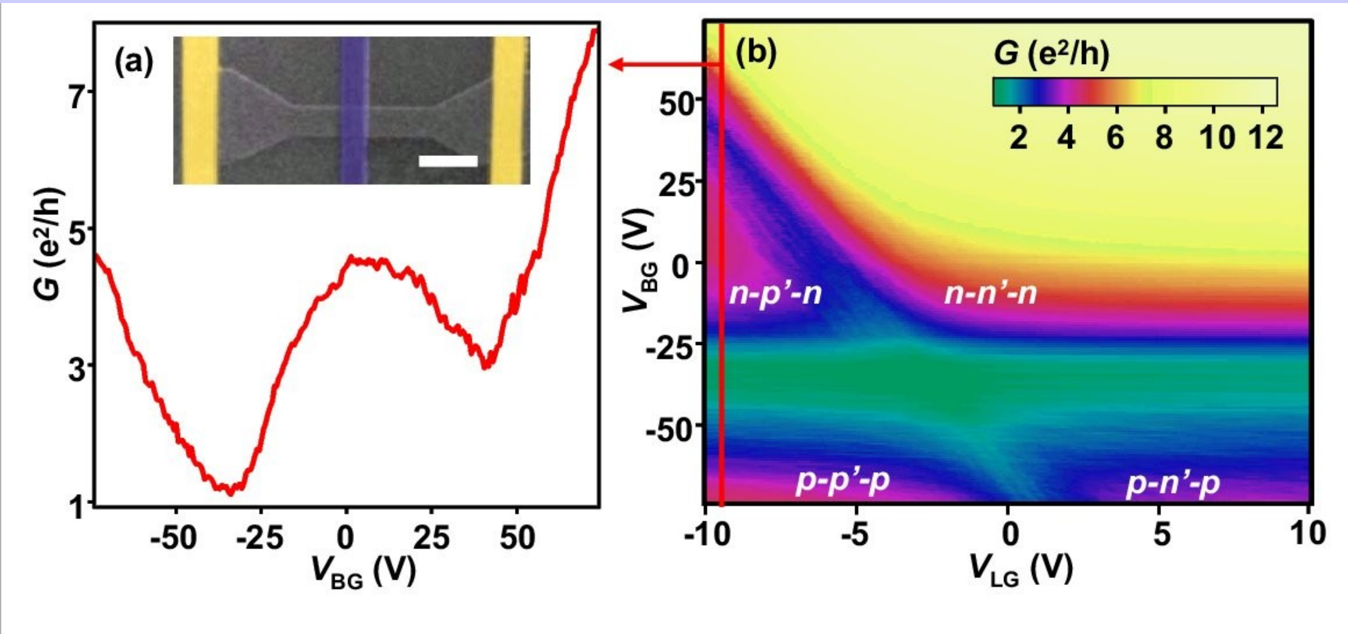

Equal or opposite polarities of charge carriers in the same system (electrons and holes coexist)

Lecture I

Electronic structure; Dirac model for charge carriers; Landau levels in graphene

Electron properties of graphene

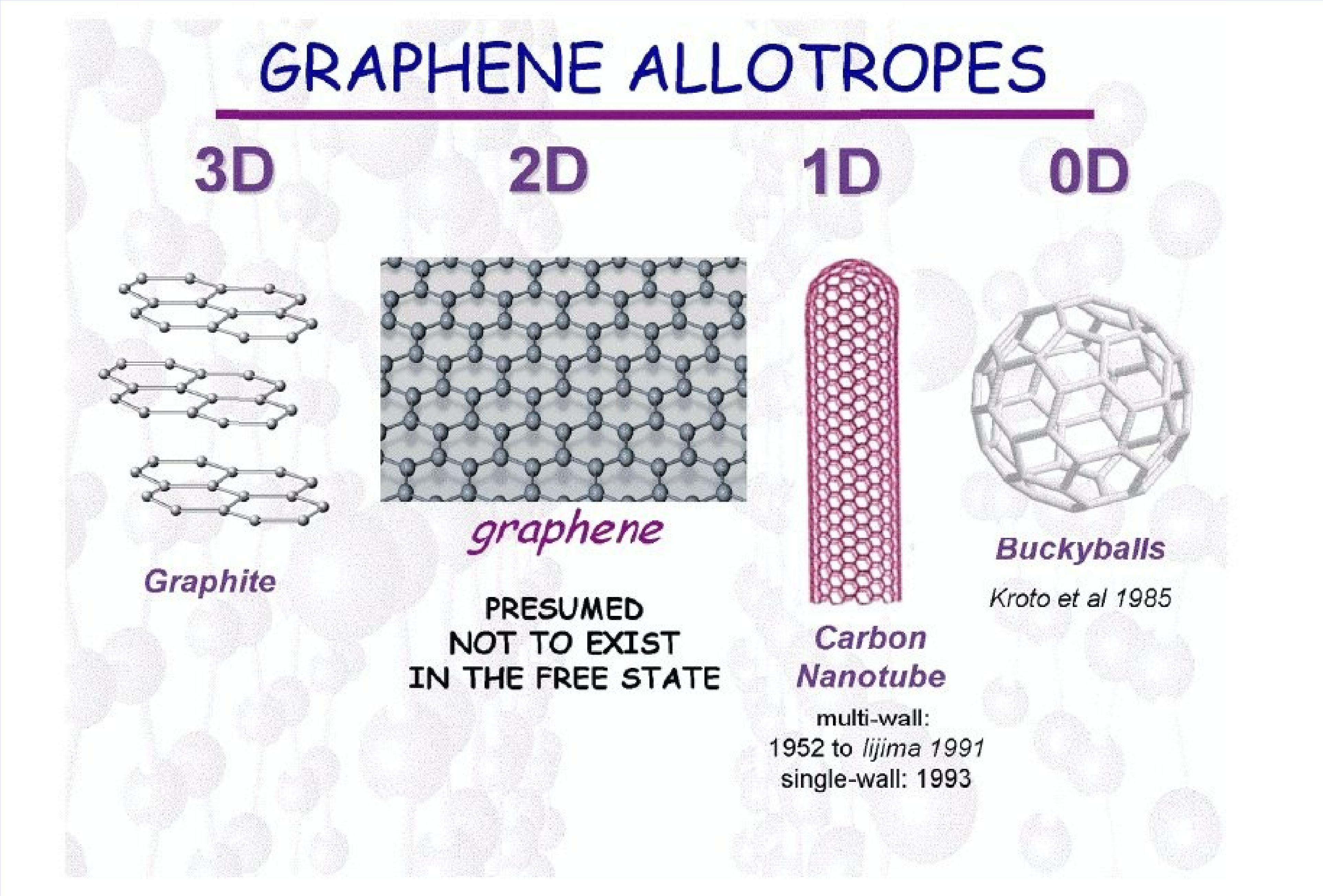

Tight-binding model
on a honeycomb lattice

Conduction band

Valence band

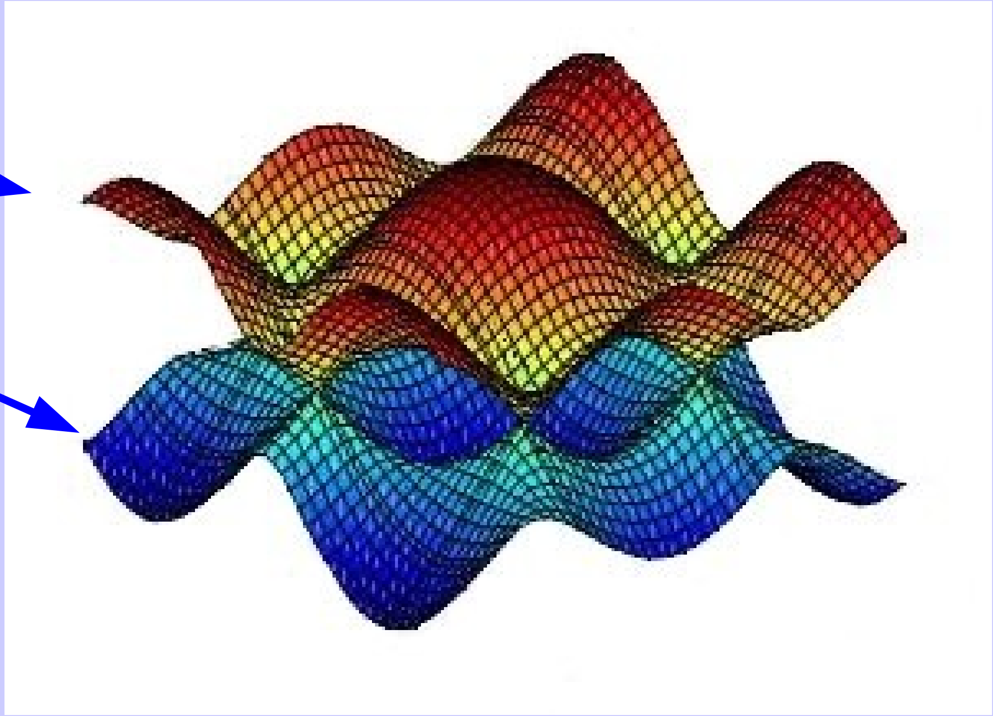

Dirac model:

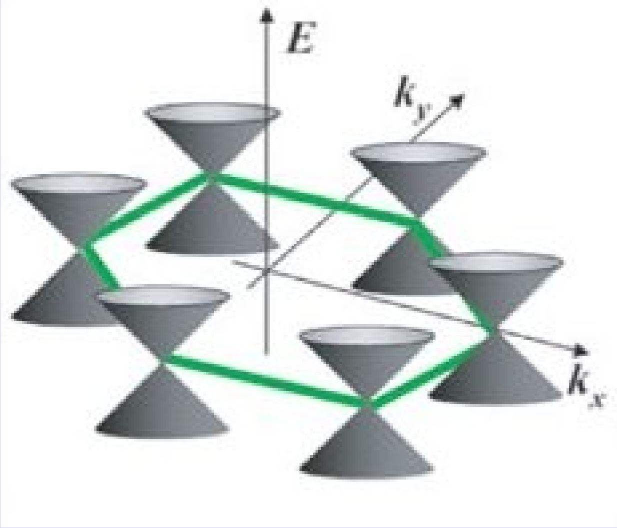

K K'

Velocity v = dE/dp=10^8 cm/s = c/300

Density of states linear in E,
particle/hole symmetry N(E)=N(-E)

Other effects: next-nearest neighbor hopping; spin-orbital coupling; trigonal warping (ALL SMALL)

S and P electron orbitals

after Paul McEuen

Carbon: 6 electrons $1s^2 2s^2 2p^2$ atomic.

$1s^2 2s 2p^3$ bonding.

sp bonds.

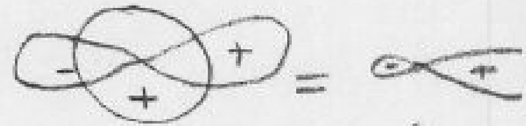

sp bond.

sp^2 bonds give honeycomb lattice. One p_z orbital left over per C-atom.

p_z responsible for conduction

sp^2 bond.

Unit cell:

Two atom basis.

Lattice.

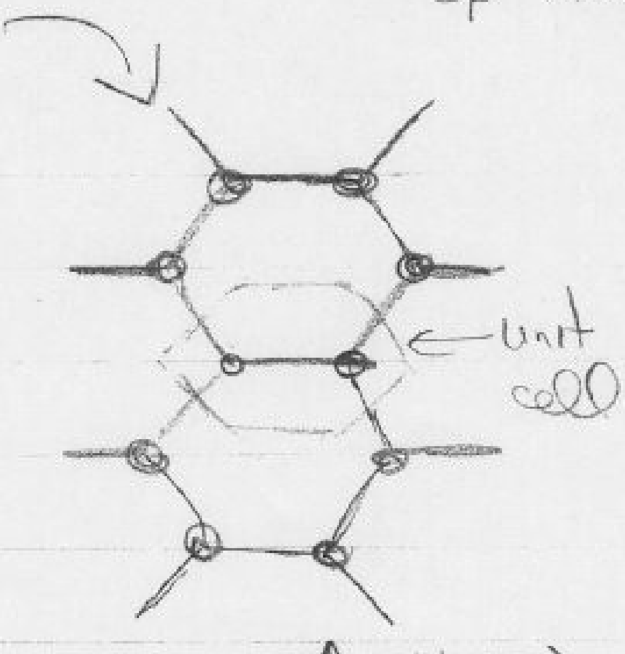

Side view:

π^*

π

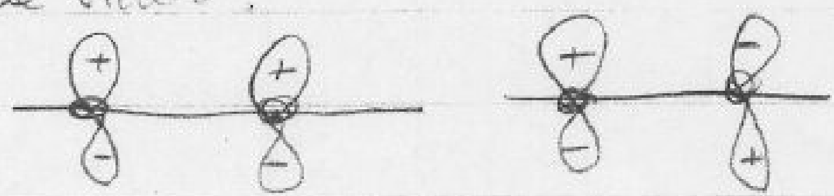

bonding antibonding,

called "pi" orbitals.

Real space, reciprocal space

Unit Cell. Real & Recip Space.

Set "a" = 1. $a = \sqrt{3} \cdot$ c-c bond length.

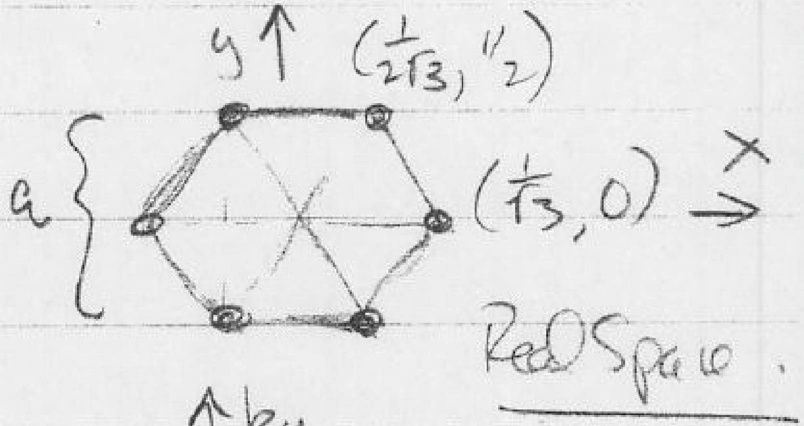

First Brillouin Zone ⇒ exactly filled by 2 atom lattice.

Two "special" points:

- ● $\vec{K} = (0, 4\pi/3)$
- ○ $\vec{K}' = (0, -4\pi/3)$

Note: other corners related by recip. lattice vectors.

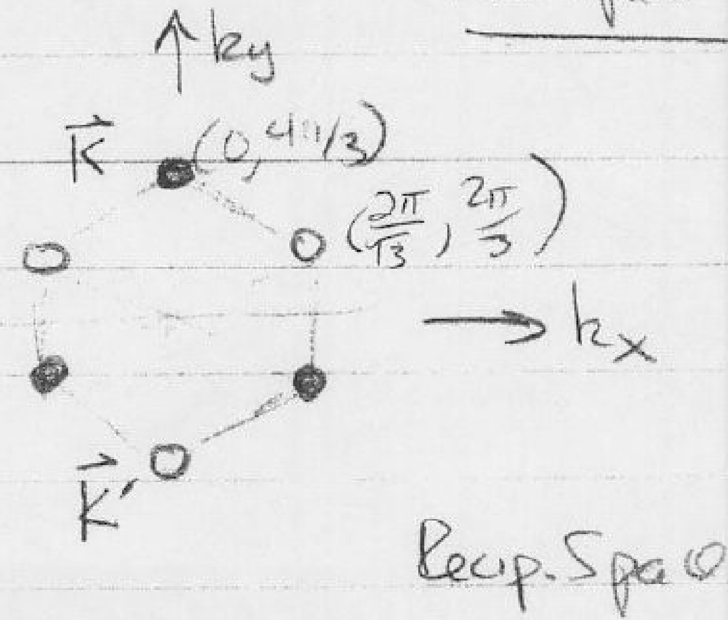

Graphene tight-binding model

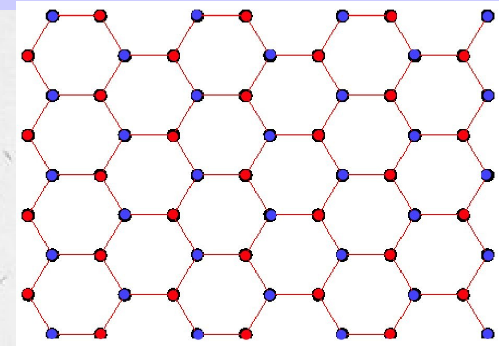

Tight Binding Model:

Assume N-N hopping with element t.

Need two #'s to describe basis

Write as column vector.

$\begin{pmatrix} 1 \\ 0 \end{pmatrix} \Rightarrow$ electron on A $\qquad \begin{pmatrix} 0 \\ 1 \end{pmatrix} \Rightarrow$ electron on B.

$\Rightarrow$ Hopping is off-diagonal (from A to B)

Assume $\psi(r) = \psi(0)\, e^{ik\cdot r}$ Bloch waves.

Then:

$$\mathcal{H} = \begin{pmatrix} 0 & \overbrace{t^* \sum_i e^{-i\vec{k}\cdot\vec{\rho}_i}}^{h^*} \\ \underbrace{t \sum_i e^{i\vec{k}\cdot\vec{\rho}_i}}_{h} & 0 \end{pmatrix} \quad \& \quad E = \pm |t|^2 \left| \sum e^{i\vec{k}\cdot\vec{\rho}_i} \right|^2 = \pm |h|$$

↑ Two roots correspond to π & π^* bands.

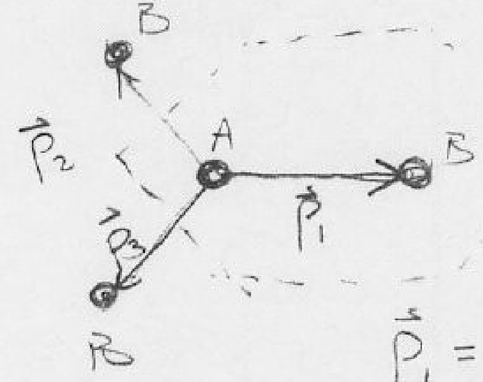

$\vec{\rho}_1 = \left(\frac{1}{\sqrt{3}}, 0\right)$

$\vec{\rho}_{2,3} = \left(-\frac{1}{2\sqrt{3}}, \pm\frac{1}{2}\right)$

Electronic Properties of Graphene

Graphene

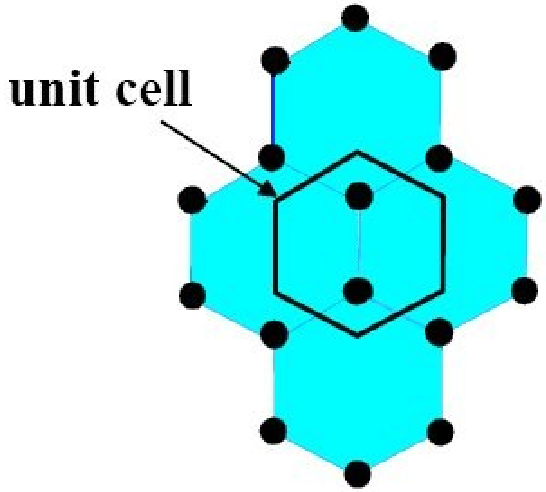

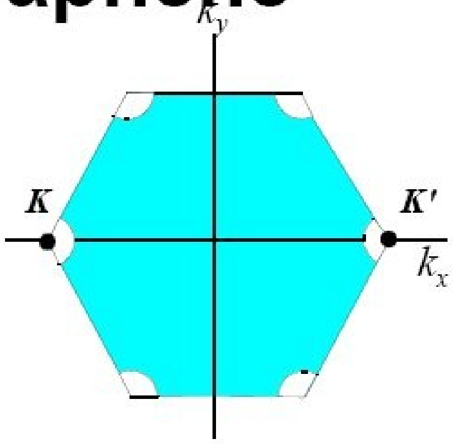

First Brillouin Zone

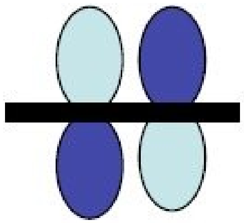

Anti-Bonding Orbitals

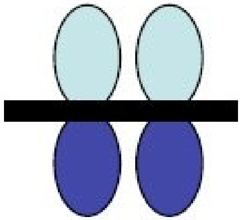

Bonding Orbitals

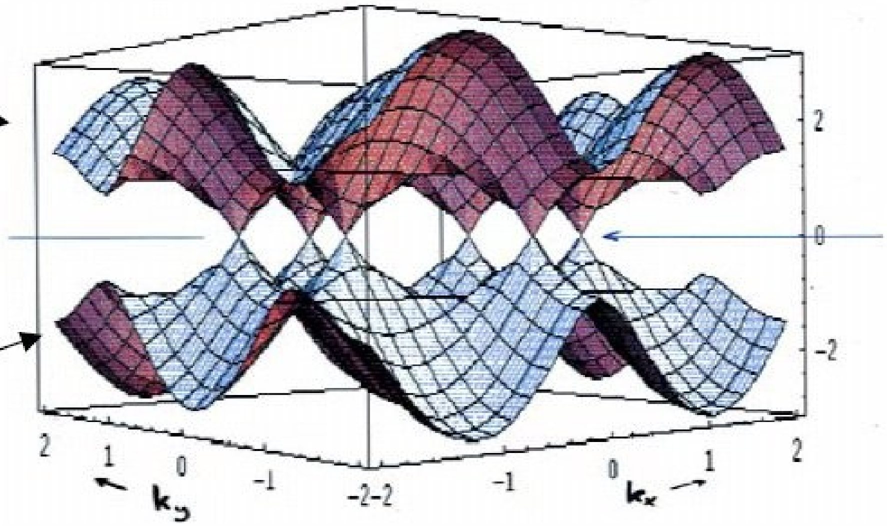

Linearize H near K and K'

$\Rightarrow$ see graph.

$$h = t\left[e^{ik_x/\sqrt{3}} + e^{-\frac{ik_x}{2\sqrt{3}}} 2\cos(k_y/2)\right]$$

Interesting case: $\vec{k} = \vec{K} = (0, 4\pi/3)$.

$$h = t\left[1 + 2\cos(2\pi/3)\right] = t\left[1 + 2(-\tfrac{1}{2})\right] = 0.$$

$E(\vec{K}) = \pm 0 \leftarrow$ same energy

$\Rightarrow$ **Gap Vanishes at $\vec{K}$ & $\vec{K}'$**

What about nearby $\vec{K}$ point?

$$\vec{k} = \vec{K} + \delta\vec{k} \Rightarrow k_x = \delta k_x \quad k_y = \tfrac{4\pi}{3} + \delta k_y \quad (\delta k \ll 1)$$

$$h = t\left[(1 + i\delta k_x/\sqrt{3}) + (1 - i\delta k_x/2\sqrt{3})\, 2\left[-\tfrac{1}{2} + (-\sin(\tfrac{2\pi}{3}))\delta k_y/2\right]\right]$$

$$= t\left[\tfrac{\sqrt{3}}{2} i\delta k_x - \tfrac{\sqrt{3}}{2}\delta k_y\right]$$

$$= \tfrac{\sqrt{3}}{2} t\,(i\delta k_x - \delta k_y) \quad \text{or:}$$

$$\mathcal{H} = -\frac{\sqrt{3}}{2} t \begin{pmatrix} 0 & i\delta k_x + \delta k_y \\ -i\delta k_x + \delta k_y & 0 \end{pmatrix} = A\,\vec{\sigma}\cdot\vec{p}$$

2D <u>Massless</u> <u>Dirac Hamilt.!</u>

Low energy properties I

Band Structure – low energies.

Massless Dirac Fermions.

Sublattice structure $\Longleftrightarrow$ "spin" $\to$ $\frac{1}{\sqrt{2}}(1,1)$ $\rightleftarrows$ bonding $\to$ $+S_x$

$\frac{1}{\sqrt{2}}(1,-1)$ $\to$ antibonding $\to$ $-S_x$ ...

"spin" points along propagation direction (won't prove).

Putting in units, etc.:

$$E_{\vec{k}}(\delta\vec{k}) = \pm\, \hbar v_F \left(\delta k_x^2 + \delta k_y^2\right)^{1/2}$$

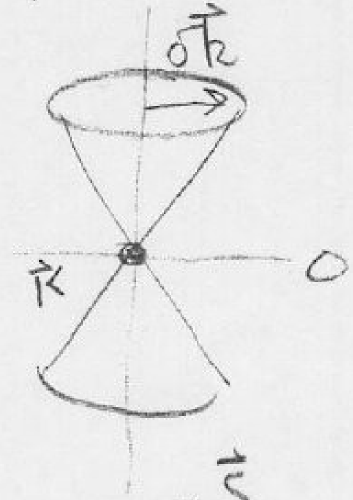

At K', same except "spin" is antiparallel to $\delta\vec{k}$.

$\Rightarrow$ left & right handed fermions

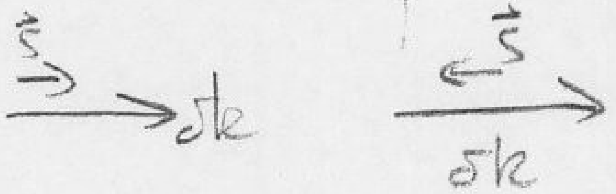

$\Rightarrow$ Very Unusual 2D system!

$\Rightarrow$ Zero Bandgap Semiconductor.

Low energy properties II

Unlike "massive" 2D system ⇒ DOS not constant.
LL's not equally spaced, etc.

New experiments (Geim et al, Kim et al) on single sheets underway!

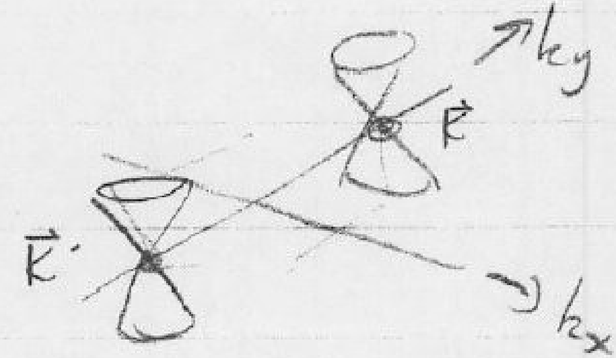

Summary ⇒ Band structure set by 2 2D Dirac cones

$v_F = 8 \cdot 10^5$ m/s.

Low energy theory: 2D massless Dirac Fermions

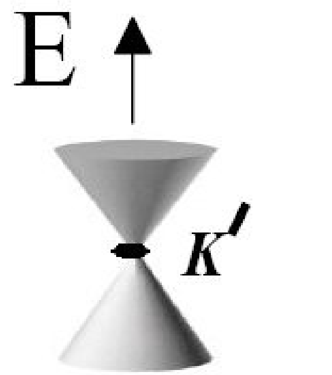

left -handed

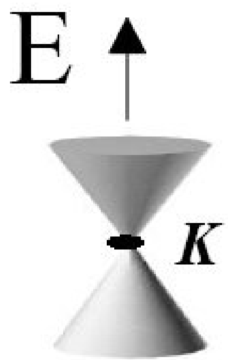

right-handed

Dirac (*k*•*p*) Hamiltonian

$$H = \hbar v_F \sigma \cdot k$$

$$E = b\hbar v_F |k|$$

$$|k> = \frac{1}{\sqrt{2}} e^{ik\cdot r} \begin{pmatrix} -ibe^{-i\theta_k/2} \\ e^{i\theta_k/2} \end{pmatrix}$$

"spin" = molec. orbital state

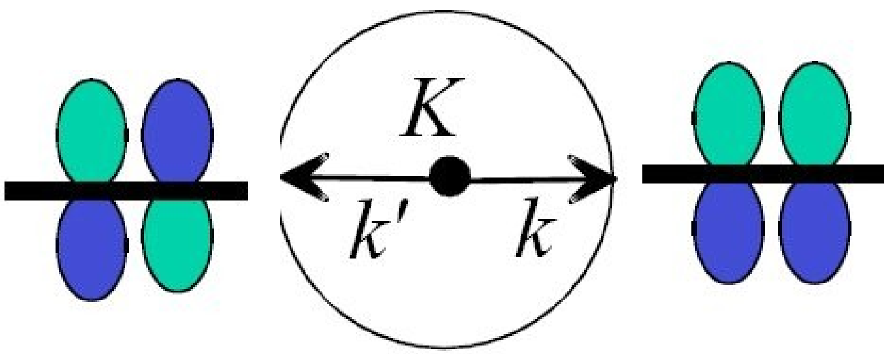

Relativistic electron in magnetic field: Landau levels

$$E_n = \mathrm{sgn}(n)|n|^{1/2}\epsilon_0, \quad \epsilon_0 = \hbar v_0\,(2eB/\hbar c)^{1/2}$$

Particle-hole symmetric; has a *zero mode*

$E_n \propto \sqrt{n}, \sqrt{B}$

Separation between low-lying LL is very large,
$1000\,\mathrm{K}$ at $B = 10\,\mathrm{T} \longrightarrow$ *room temperature QHE*

Homework problem 1: Dirac electron in magnetic field

Find the energy spectrum of a D=2 Hamiltonian:

$$H = v\, \sigma.(p-eA)$$

in a uniform B field || z-axis

Hint: $H_{Pauli\text{-}Schroedinger} = 2m(H_{Dirac})^2$

Homework problem 2: massive Dirac particles in graphene

Consider a carbon sheet with an on-site potential different for the A and B sublattice: $V_A = -V_B = \lambda$

(i) Show that the low energy states are described by a massive Dirac Hamiltonian

$$H = v\, \sigma.p + \lambda\sigma_3$$

(ii) Find the energy spectrum in a uniform B field

What is the most striking difference with the massless case $\lambda=0$?

Hint: $H_{Pauli\text{-}Schroedinger} = 2m(H_{Dirac})^2$

Dirac Landau levels by energy-resolved STM spectroscopy

Andrei group (2008):

particle/hole symmetry;

sqrt(B) scaling;

splitting of the n=0 Landau level

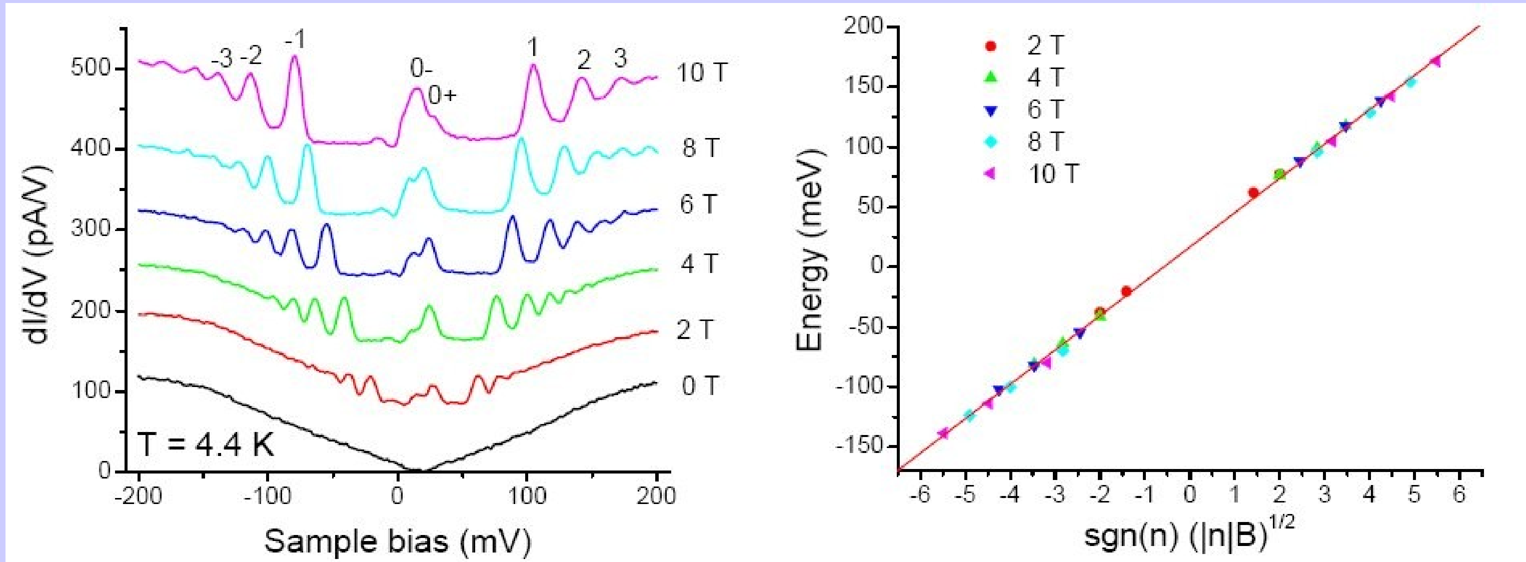

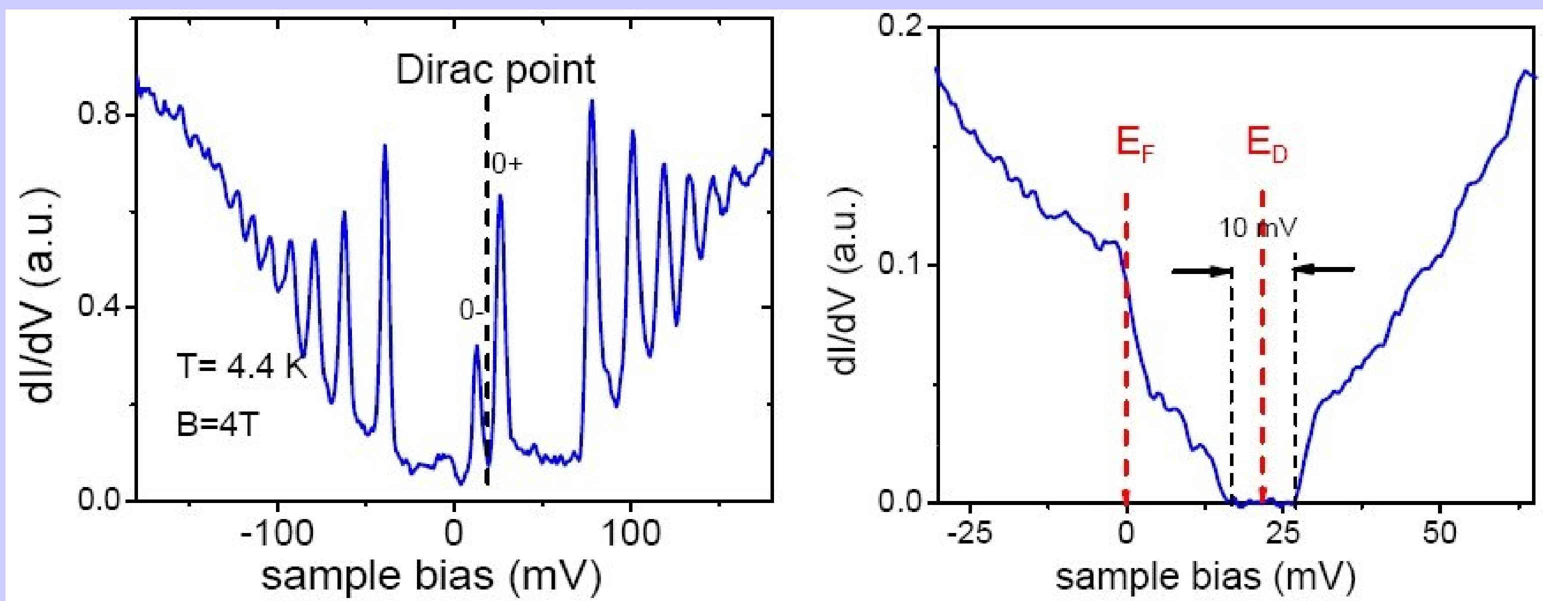

Square root dependence tested by infrared spectroscopy

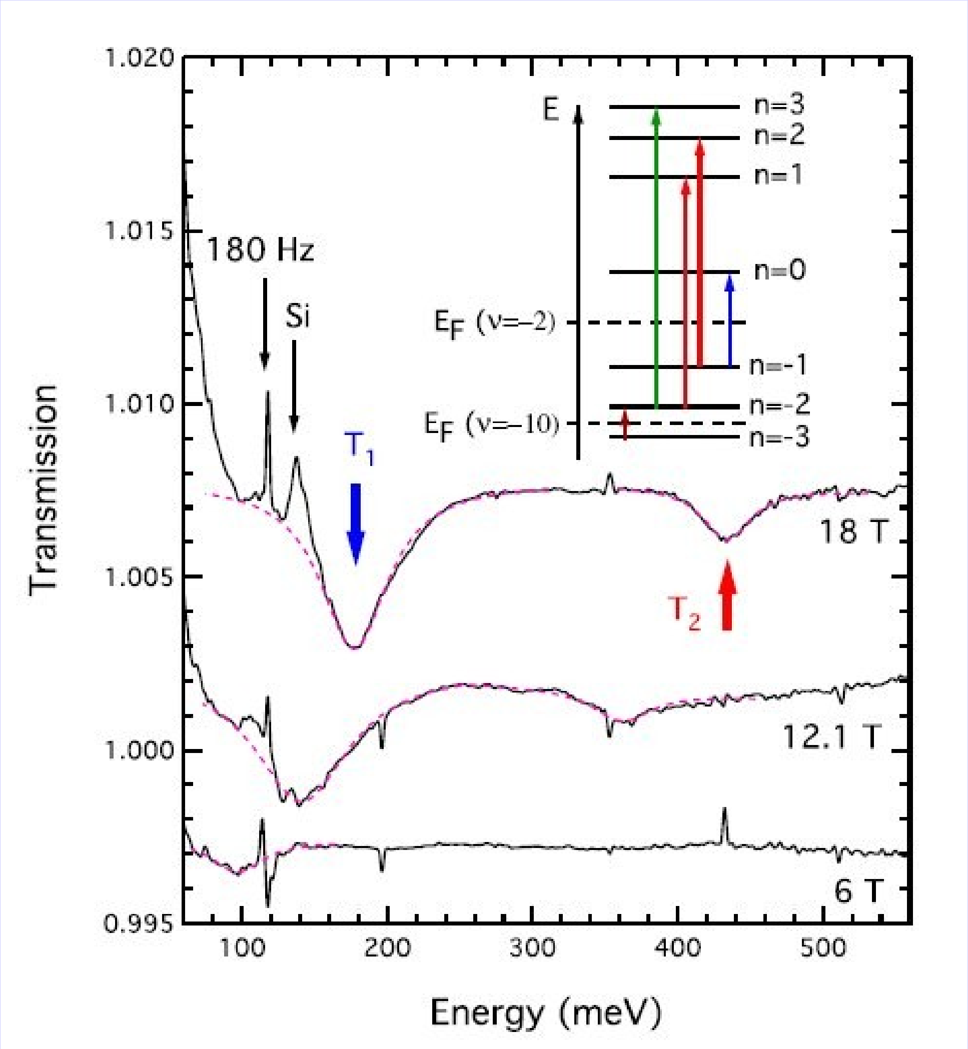

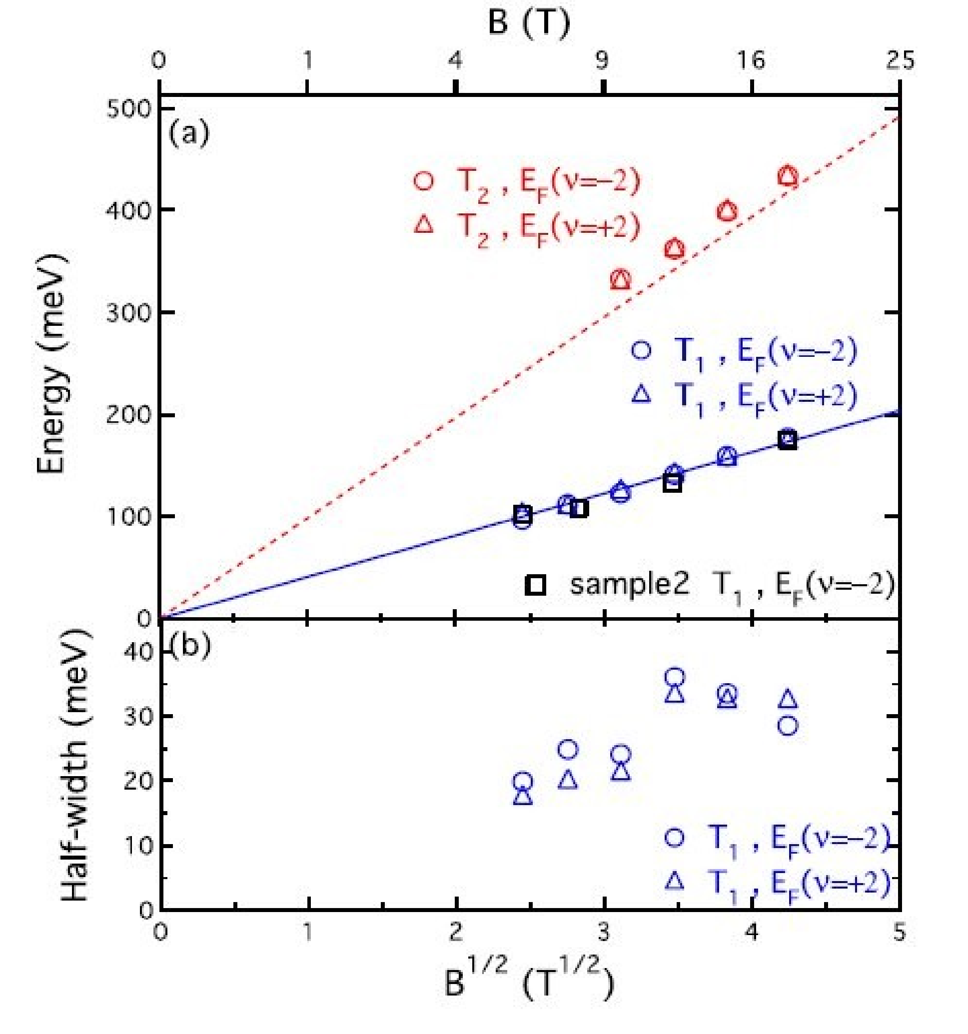

FIG. 3 (color online). (a) Resonance energies vs $\sqrt{B}$, from holes (ratio of $\nu = -2$ and $\nu = -10$ data, Fig. 2) and electrons

Stormer, Kim group (Columbia)

Lecture I

Dirac electrons
in external fields:

chiral dynamics,
Klein scattering,
transport in p-n junctions

Klein tunneling

Klein paradox: transmission of relativistic particles is unimpeded even by highest barriers
Reason: negative energy states;
Physical picture: particle/hole pairs

Katsnelson, Novoselov, Geim

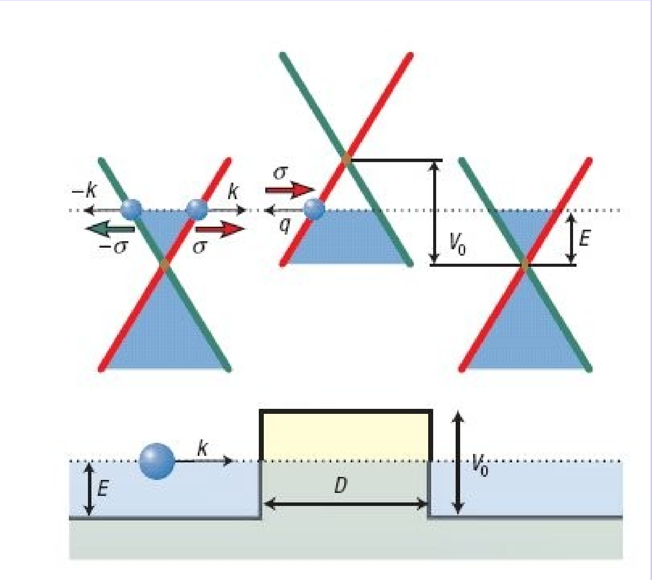

Example: potential step

$$V(x) = \begin{cases} V_0, & 0 < x < D, \\ 0 & \text{otherwise.} \end{cases}$$

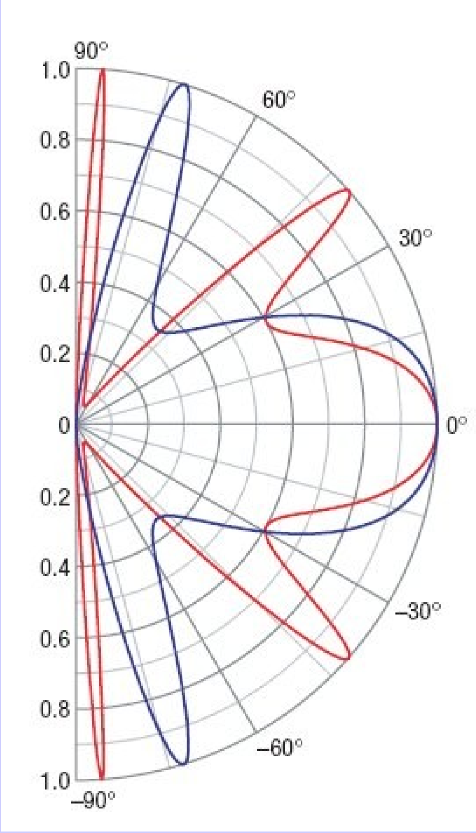

Transmission angular dependence

$$\psi_1(x,y) = \begin{cases} (e^{ik_x x} + re^{-ik_x x})e^{ik_y y}, & x < 0, \\ (ae^{iq_x x} + be^{-iq_x x})e^{ik_y y}, & 0 < x < D, \\ te^{ik_x x + ik_y y}, & x > D, \end{cases}$$

$$\psi_2(x,y) = \begin{cases} s(e^{ik_x x + i\phi} - re^{-ik_x x - i\phi})e^{ik_y y}, & x < 0, \\ s'(ae^{iq_x x + i\theta} - be^{-iq_x x - i\theta})e^{ik_y y}, & 0 < x < D, \\ ste^{ik_x x + ik_y y + i\phi}, & x > D, \end{cases}$$

Chiral dynamics of massless Dirac particles: no backward scattering (perfect transmission at zero angle)

Limit of extremely high barrier: finite T

$$T = \frac{\cos^2\phi}{1 - \cos^2(q_x D)\sin^2\phi}.$$

Confinement problem

Example: parabolic potential V(x) = ax^2 + E

Momentum conserved along y-axis:

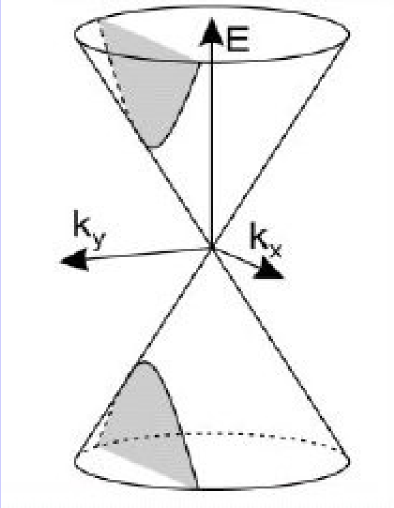

Effective D=1 potential

$$H_{\text{eff}} = \varepsilon = \pm c\sqrt{p_x^2 + p_y^2} + V(x).$$

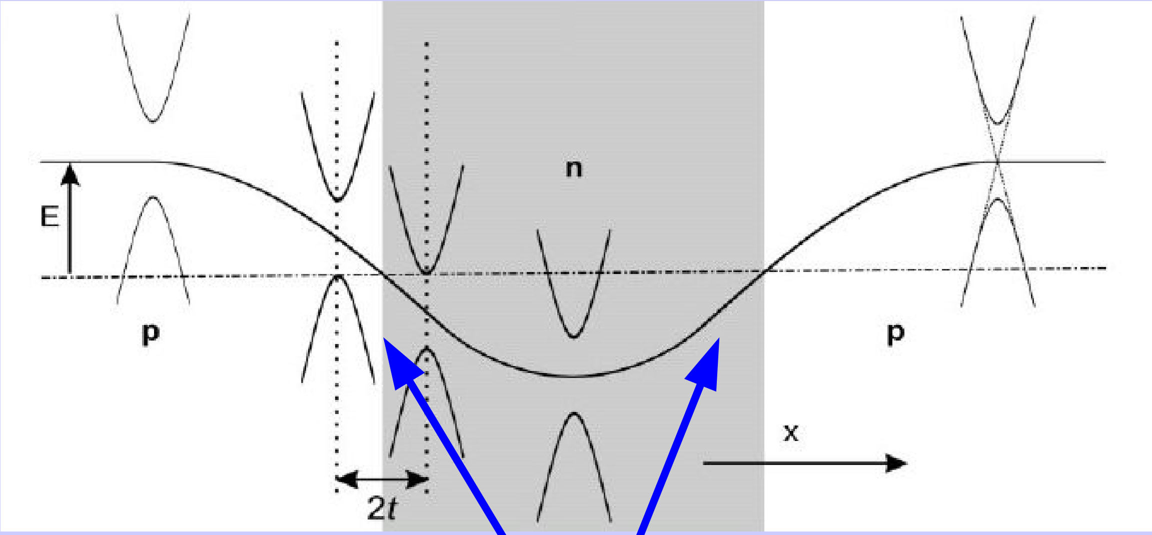

Tunneling

<u>Confinement by gates difficult!</u>

No discrete spectrum, instead: quasistationary states (resonances)

Quasiclassical treatment

Silvestrov, Efetov

Potential V(x) = U(x/x_0)^2 + E

$$H_{\text{eff}} = \varepsilon = \pm c\sqrt{p_x^2 + p_y^2} + V(x).$$

Bohr-Sommerfeld quantization

$$\int_{x_{\text{in}-}}^{x_{\text{in}+}} \sqrt{[\varepsilon_N - V(x)]^2 - c^2 p_y^2}\,\frac{dx}{c} = \pi\hbar\left(N + \frac{1}{2}\right).$$

Finite lifetime

$$\Gamma_N = \frac{\hbar}{\Delta t} w = \frac{\hbar v_0}{2x_0}\sqrt{\frac{U}{-2\varepsilon_N}}\exp\left(-\frac{\pi c p_y^2 x_0}{\hbar\sqrt{-2\varepsilon_N U}}\right).$$

Classical trajectories

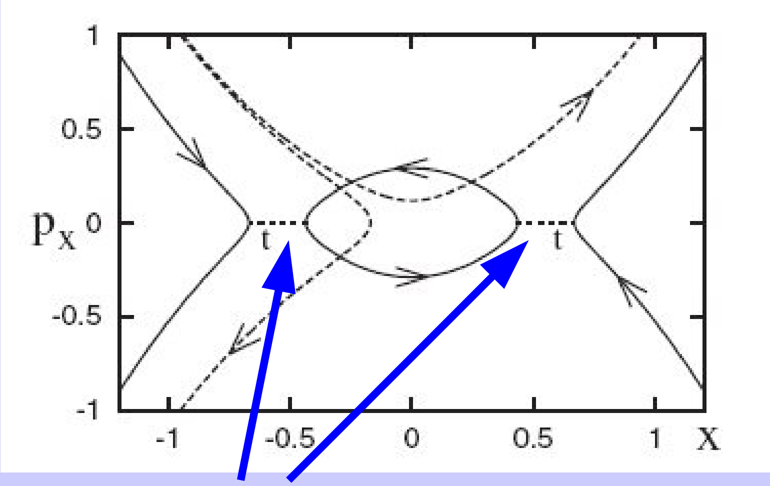

Tunneling

Turning points:

$$\frac{x_{\text{out}_\pm}}{x_0} = \pm\sqrt{2\frac{c|p_y| - \varepsilon}{U}}, \qquad \frac{x_{\text{in}_\pm}}{x_0} = \pm\sqrt{2\frac{-c|p_y| - \varepsilon}{U}}.$$

Degree of confinement can be tuned by gates

Geometric confinement in ribbons and dots

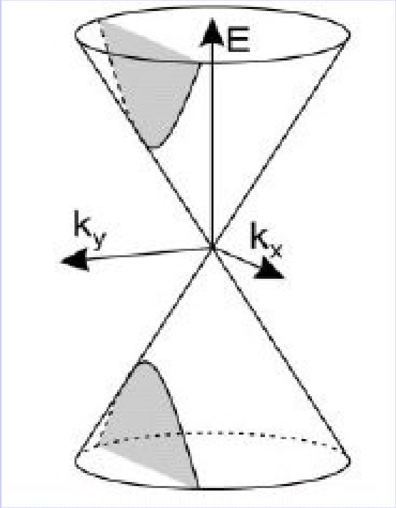

Nanoribbons: quantized $k_y = \pi$/width

Geometric energy gap $\Delta = hv_F$/width

Coulomb blockade in graphene

Geim, Novoselov

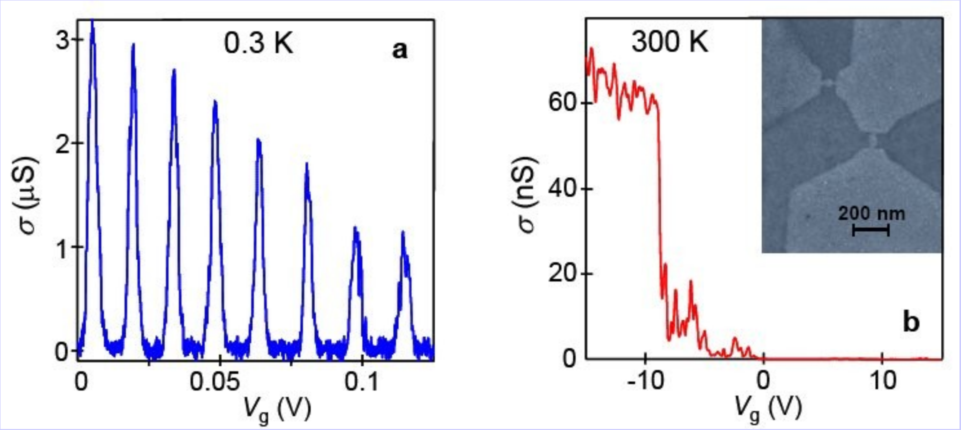

Electrons in a p-n junction

Potential step instead of a barrier (smooth or sharp)

Cheianov, Falko 2006

$$H = e\varphi(\mathbf{x}) + v_F \xi \begin{pmatrix} 0 & p_+ \\ p_- & 0 \end{pmatrix}, \quad p_\pm = p_1 \pm i p_2,$$

+1(-1) for points K(K')

p-n junction schematic:

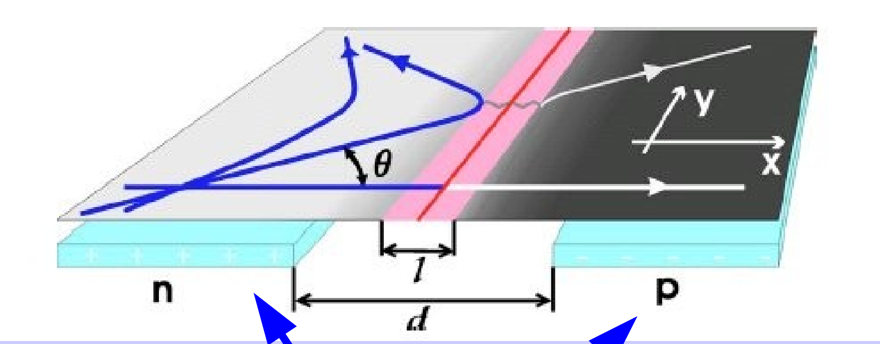

gates

smooth step:

$$w(\theta) = e^{-\pi(k_F d)\sin^2\theta}.$$

(nontrivial)

sharp step:

$$w_{\text{step}}(\theta) = \cos^2\theta$$

(straightforward)

In both cases, perfect transmission in the forward direction: manifestation of chiral dynamics

Exact solution in a uniform electric field

Use momentum representation (direct access to asymptotic plane wave scattering states)

Evolution in a fictitious time with a hermitian 2x2 Hamiltonian

$$-ieE\, d\psi/dp_2 = \tilde{H}\psi, \quad \tilde{H} = v_F(p_1\sigma_1 - p_2\sigma_2) - \varepsilon.$$

Equivalent to Landau-Zener transition at an avoided level crossing; Interpretation: interband tunneling for $p_2(t)=vt$

Transmission equals to the LZ probability of staying in the diabatic state:

$$T(p_1) = \exp(-\pi\hbar v_F p_1^2/|eE|),$$

Exact transmission matches the WKB result

Graphene p-n junctions: collimated transmission

- Ballistic transmission at normal incidence (cf. tunneling in conventional p-n junctions);
- Ohmic conduction (cf. direct/reverse bias asymmetry in conventional p-n junctions)
- No minority carriers

Signatures of collimated transmission in pnp structures

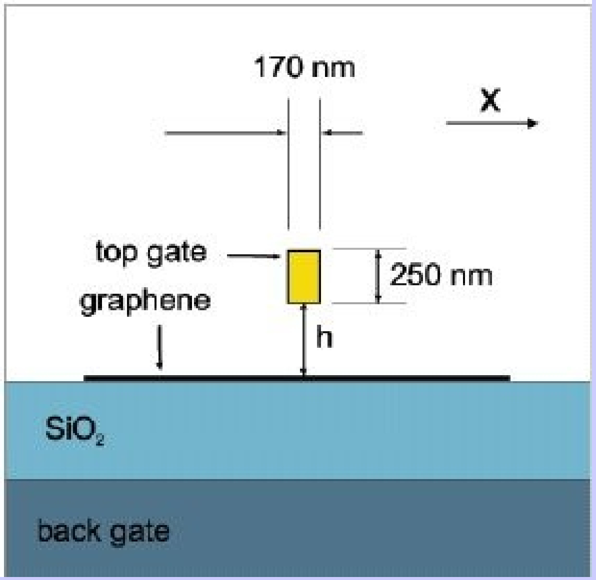

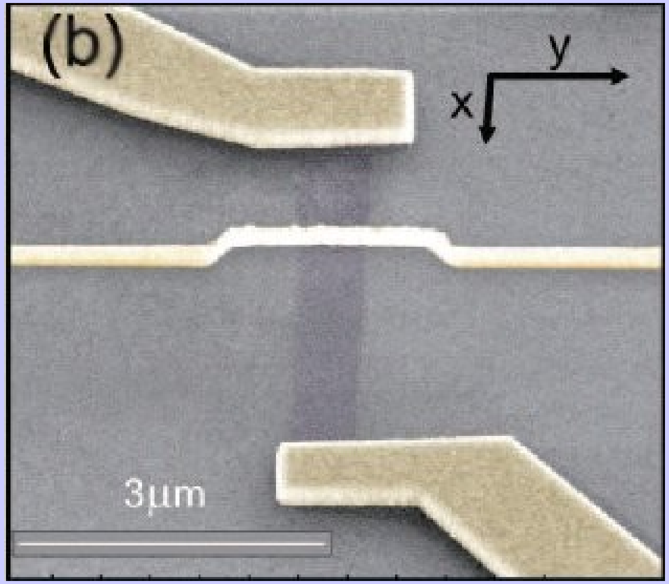

Exeter group:
narrow gate (air bridge)

simulated electrostatic potential, density profile

compare expected and measured resistance, find an excess part

Stanford group:
sharp confining potential (the top gate ~10 times closer)

analyze antisymmetric part of resistance

ΔR a small effect, model-sensitive

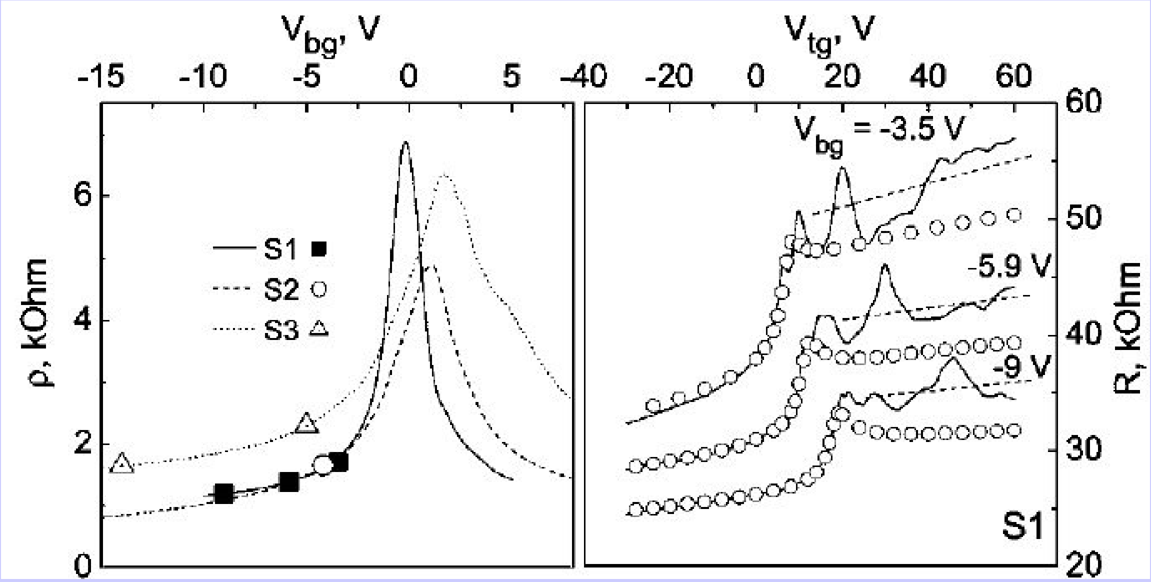

Homework Problem 3: Klein scattering

Consider scattering of a massless Dirac particle on a step-like potential

$$U(x<0) = -U_0; \quad U(x>0) = +U_0$$

By solving the Schroedinger equation $E\psi=[v\sigma.p+U(x)]\psi$,

(i) Find the transmission and reflection angles as a function of the incidence angle;

(ii) Find the transmission probability.

For simplicity, consider the case of particle energy E equal zero

Lecture I

Klein backscattering and Fabry-Perot resonances in p-n junctions

Klein backscattering and Fabry-Perot resonances

$$T(\varepsilon, p_y) = \frac{t_1 t_2}{\left|1 - \sqrt{r_1 r_2} e^{i\Delta\theta}\right|^2}$$

$r_{1(2)} = 1 - t_{1(2)}$ reflection coefficients,

$$\Delta\theta = 2\theta_{\rm WKB} + \Delta\theta_1 + \Delta\theta_2,$$

$$\theta_{\rm WKB} = \frac{1}{\hbar}\int_1^2 p_x(x')dx'$$

$\Delta\theta_{1(2)}$ the backreflection phases

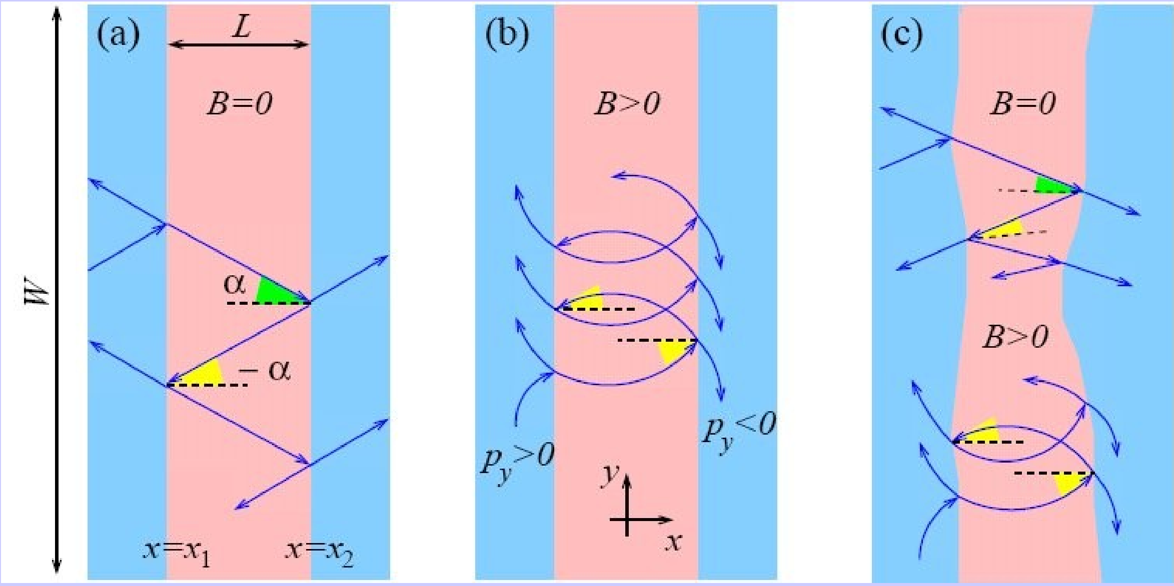

Phase of backreflection:

(i) phase jump by π at normal incidence shows up in FP interference;
(ii) the net FP phase depends on the sign of inner incidence angles;
(iii) can be controled by B field

$$p_y(x) = p_{y,0} - eBx,$$

$$-eBL/2 < p_{y,0} < eBL/2$$

$p_y(x_1) > 0$ and $p_y(x_2) < 0$

Transmission at B=0 and B>0

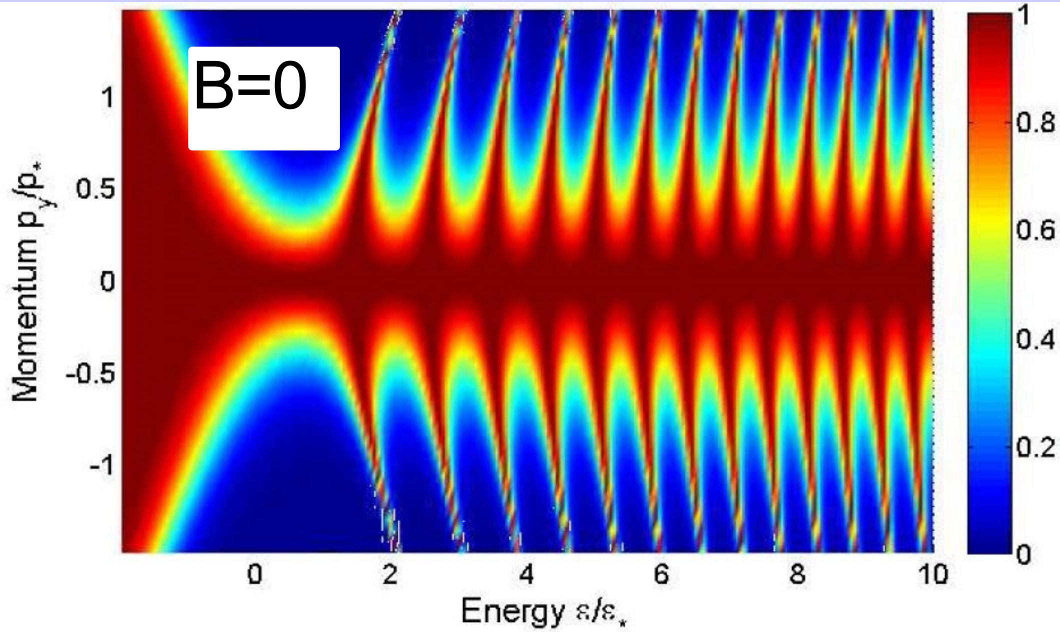

Top-gate potential;
Dirac hamiltonian

$$U(x) = ax^2 - \varepsilon,$$

$$\text{p-n interfaces at } x = \pm x_\varepsilon, \quad x_\varepsilon \equiv \sqrt{\varepsilon/a}$$

$$\mathcal{H} = v_F \sigma_3 p_x + v_F \sigma_2 (p_y - eBx) + U(x)$$

Lines of fringe
contrast reversal

$$p_y = \pm eB\sqrt{\varepsilon/a}$$

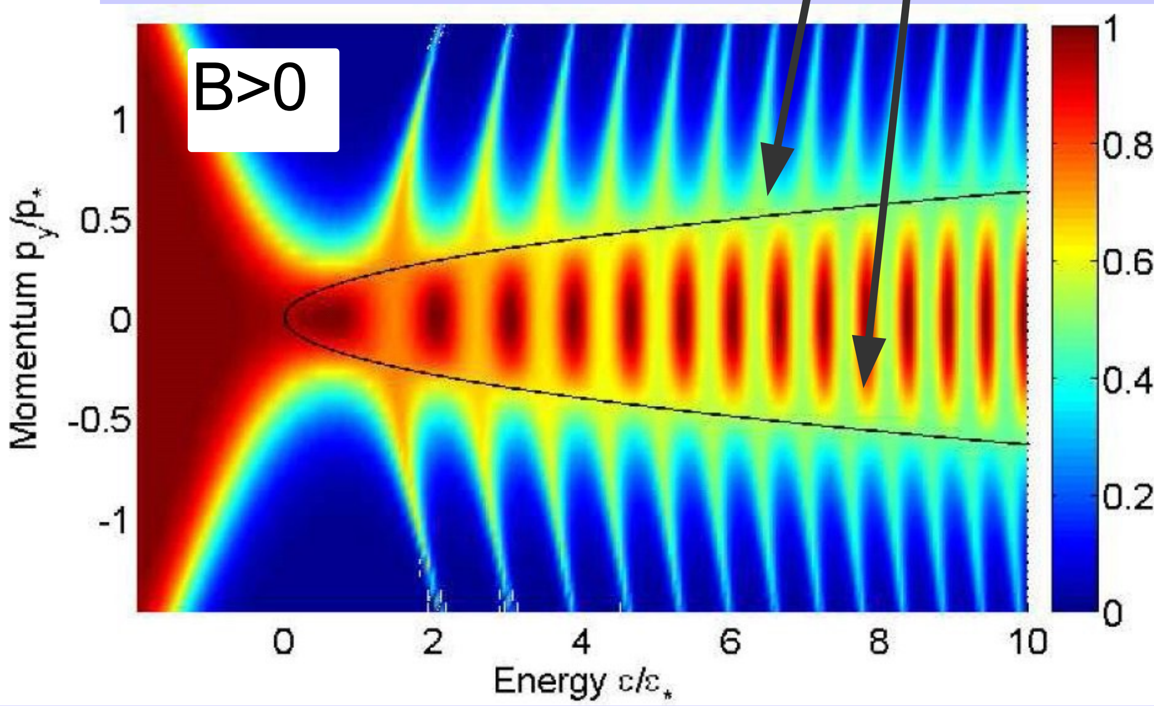

Interpretation of scattering problem: fictitious time t=x;
repeated Landau-Zener transitions;
Stuckelberg oscillations

$$i\partial_x \psi = (U(x)\sigma_3 - i(p_y - eBx)\sigma_1)\,\psi,$$

$$\Delta\theta = -2\int_{-x_\varepsilon}^{x_\varepsilon} U(x)dx = \tfrac{4}{3}\varepsilon x_\varepsilon$$

Quasiclassical analysis

Confining potential and Dirac hamiltonian

$$U(x) = ax^2 - \varepsilon,$$

$$\text{p-n interfaces at } x = \pm x_\varepsilon, \quad x_\varepsilon \equiv \sqrt{\varepsilon/a}$$

$$\mathcal{H} = v_F \sigma_3 p_x + v_F \sigma_2 (p_y - eBx) + U(x)$$

WKB wavefunction

$$\psi \sim \frac{e^{\pm i \int^x p_x(x')dx'}}{\sqrt{2}|U(x)|} \begin{pmatrix} -U(x) \\ \tilde{p}_y(x) \pm i p_x(x) \end{pmatrix}$$

$$p_x(x) = \sqrt{U^2(x) - \tilde{p}_y^2(x)}, \; \tilde{p}_y(x) \equiv p_y - eBx$$

Transmission and reflection amplitudes

$$t_1 = e^{-2\mathrm{Im} \int_{x_1}^{x_1'} p_x(x')dx'} \approx e^{-\lambda(p - eBx_\varepsilon)^2}, \quad \lambda = \frac{\pi}{2ax_\varepsilon}$$

Phase jump

$$\mathrm{sgn}(p \pm eBx_\varepsilon)\, e^{i\theta_{\mathrm{reg}}(p)} \sqrt{1 - e^{-\lambda(p \pm eBx_\varepsilon)^2}}$$

FP oscillations in conductance

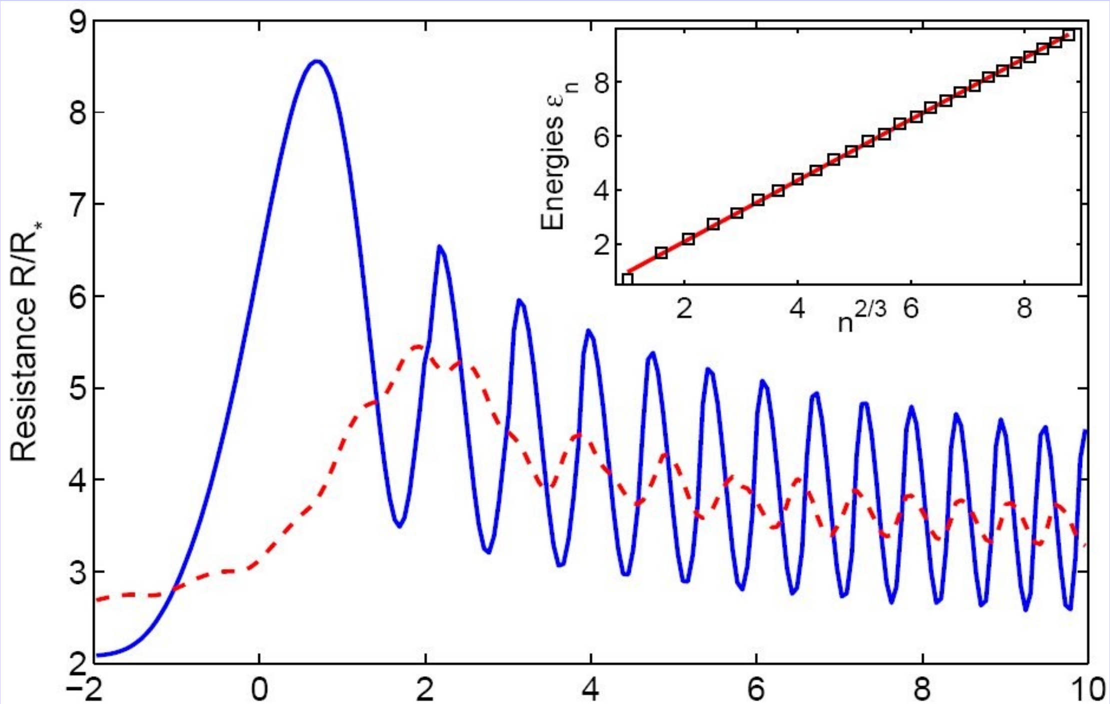

Landauer formula:

$$R(\varepsilon) = G^{-1}, \quad G = \frac{4e^2}{h} W \int_{-\infty}^{\infty} T(\varepsilon, p_y) \frac{dp_y}{2\pi}$$

Half-a-period phase shift induced by magnetic field

FP phase contrast not washed out after integration over p_y

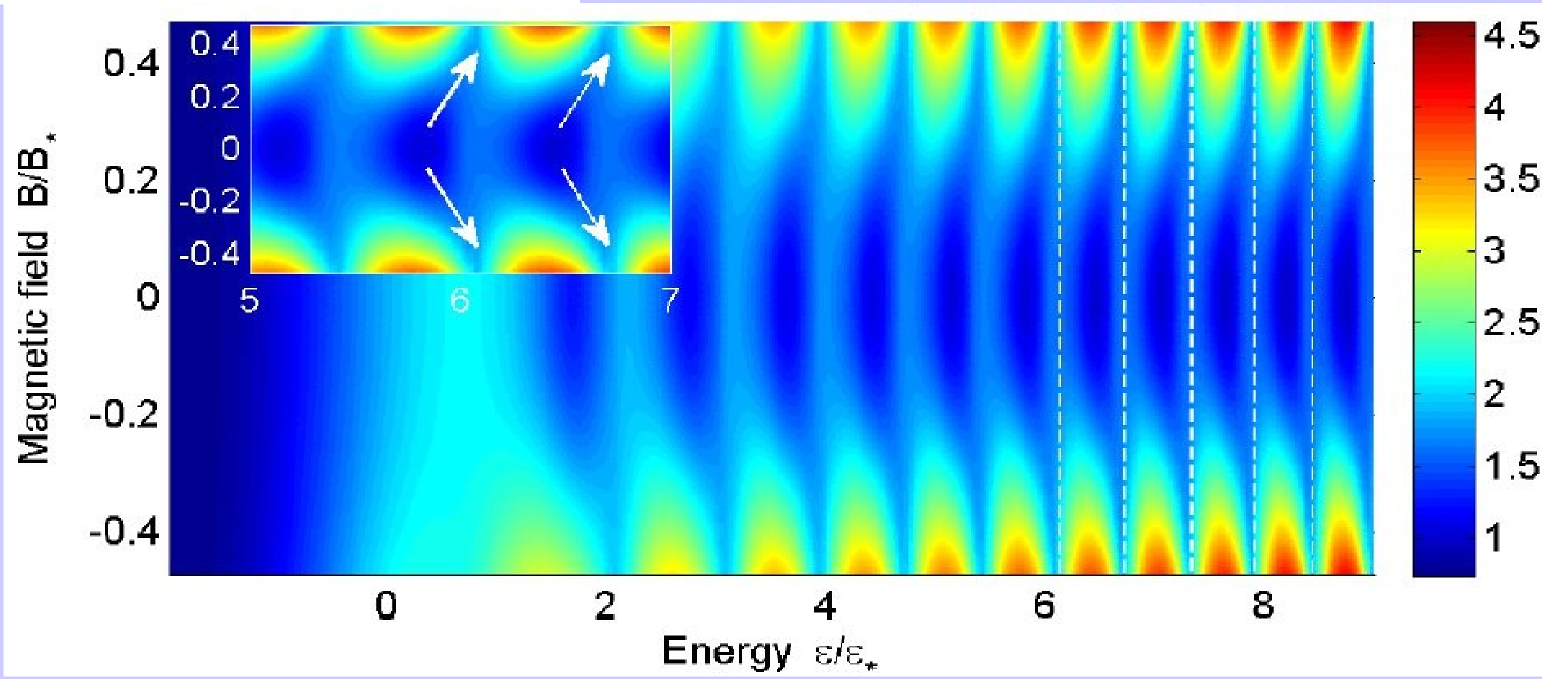

Berry phase interpretation of the π-shift

Trajectory in momentum space yields
an effective time-dependent "Zeeman" field

$$H = v\,\sigma.p(t)$$

Weak B:
zero not enclosed, $\Delta\theta = 0$

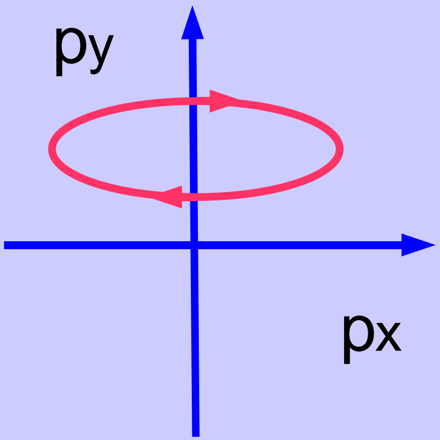

Strong B:
zero enclosed, $\Delta\theta = \pi$

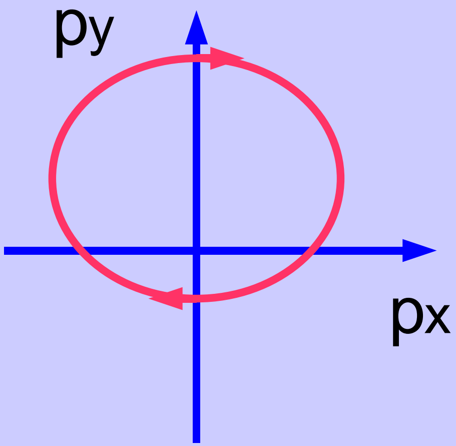

FP oscillations (experiment)

Columbia group (2008):

FP resonances in zero B; crossover to Shubnikov-deHaas oscillations at finite B

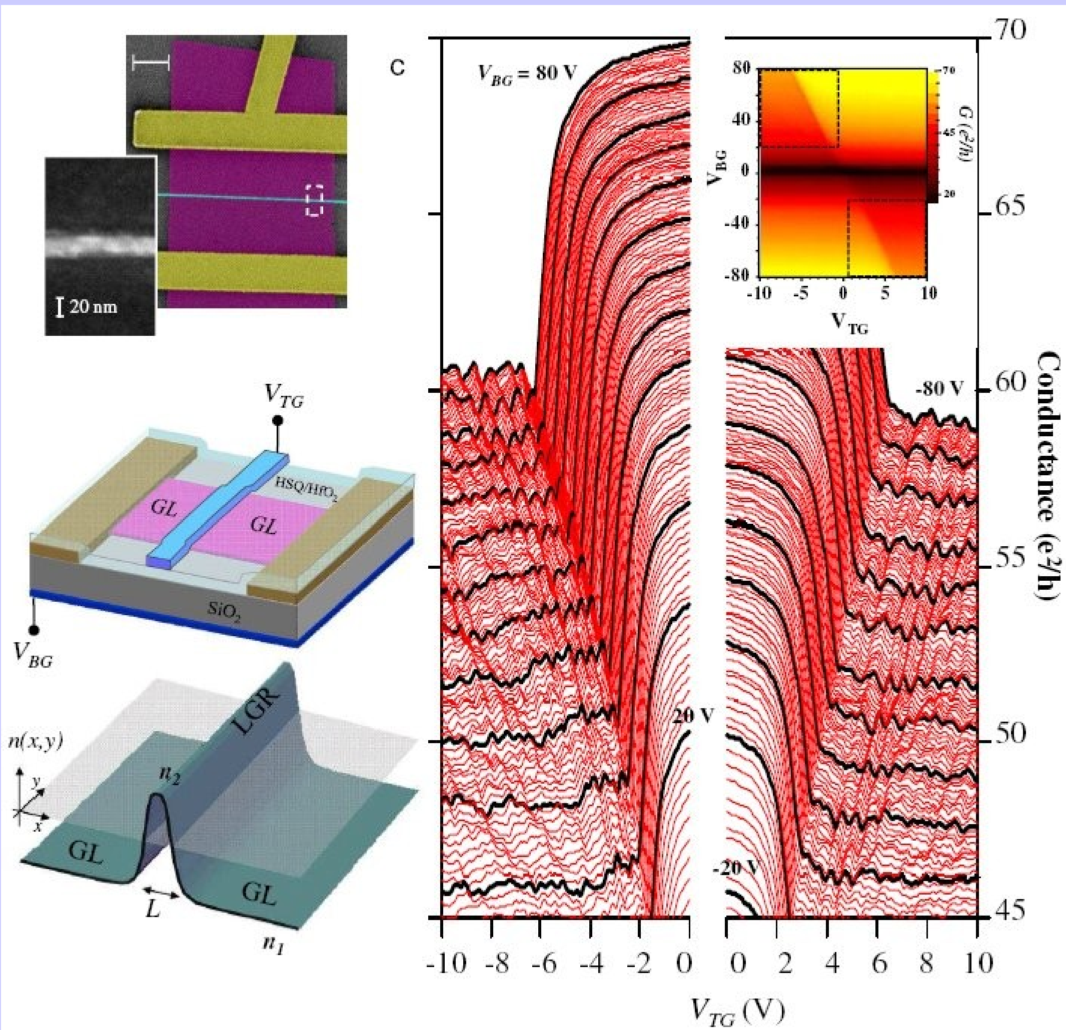

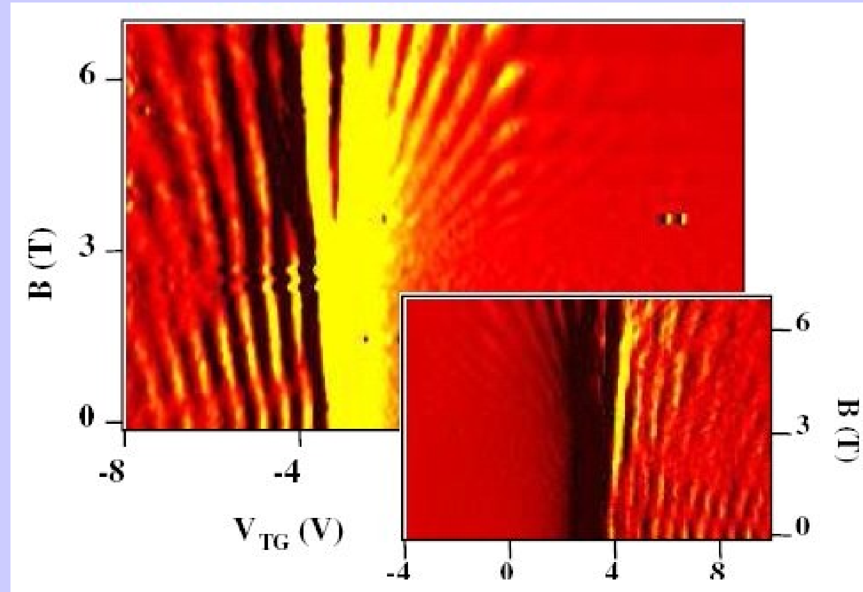

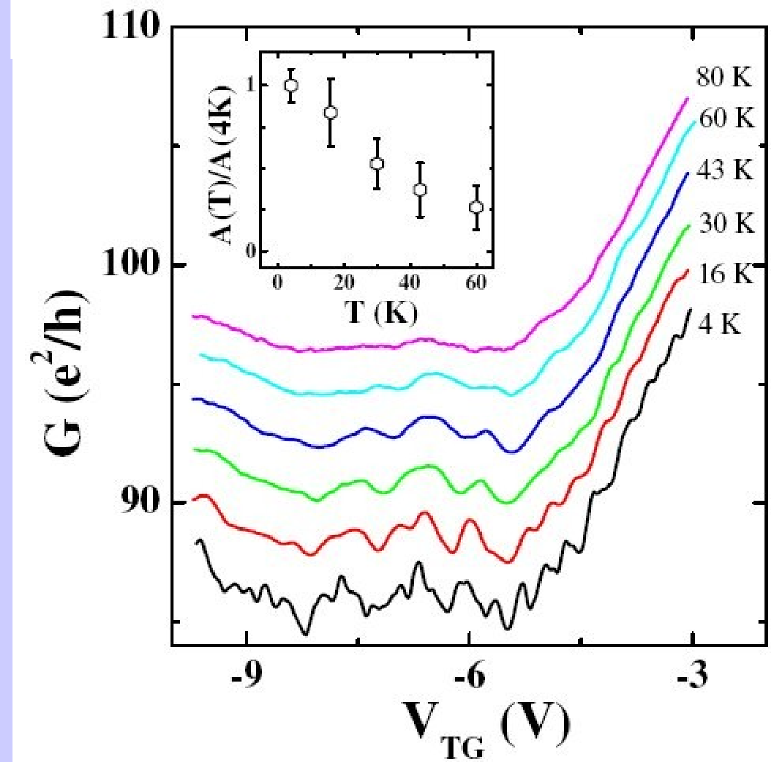

Lecture I

Lorentz boost and magnetoresistance of p-n junctions

Single p-n junction in B field

Recall relativistic motion in crossed E, B fields

Andrei Shytov, Nan Gu & LL

Two regimes:

Lorentz invariants $\mathbf{E}^2 - \mathbf{B}^2$, $\mathbf{E}.\mathbf{B}$

(i) electric case E>B ("parabolic" trajectories)
(ii) magnetic case B>E (cyclotron motion + drift)

Analogous regimes in graphene p-n junction:

Dirac equation (4) in a Lorentz-invariant form

$$\gamma^\mu (p_\mu - a_\mu)\psi = 0, \quad \{\gamma_\mu, \gamma_\nu\}_+ = 2g_{\mu\nu}, \qquad (7)$$

where γ^μ are Dirac gamma-matrices, $\gamma^0 = \sigma_3$, $\gamma^1 = -i\sigma_2$, $\gamma^2 = -i\sigma_1$, and ψ is a two-component wave function.

$$a_0 = -\frac{e}{v_F}Ey, \quad a_1 = -\frac{e}{c}By, \quad a_2 = 0.$$

c/v_F=300

Electric regime (scattering T-matrix, G>0) $\quad B < (c/v_F)E,$

Magnetic regime (Quantum Hall Effect, G=0) $\quad B > (c/v_F)E$

Lorentz transformation

Electric regime B<B$_*$, critical field $$B = B_* \equiv (c/v_F)E.$$

Eliminate B using Lorentz boost:

Aronov, Pikus 1967

$$\Lambda = \begin{pmatrix} \gamma & \gamma\beta & 0 \\ \gamma\beta & \gamma & 0 \\ 0 & 0 & 1 \end{pmatrix}, \quad \gamma = \frac{1}{\sqrt{1-\beta^2}}$$

Transmission coefficient is Lorentz invariant:

$$T(p_1) = e^{-\pi\gamma^3 d^2 (p_1+\beta\xi)^2}, \quad d = (\hbar v_F/|eE|)^{1/2}.$$

experiment in Stanford:

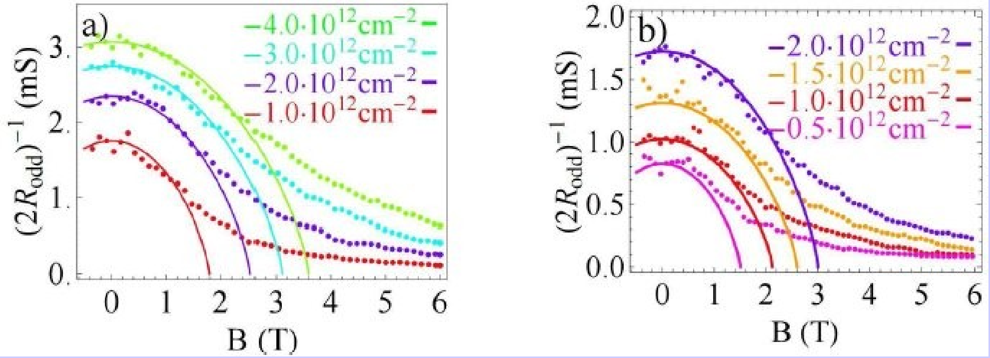

Net conductance (Landauer formula):

$$G = \frac{e^2}{h} \sum_{-k_F < p_1 < k_F} T(p_1) = \frac{we^2}{2\pi h} \int_{-k_F}^{k_F} T(p_1) dp_1$$

$$G(B \le B_*) = \frac{e^2}{2\pi h} \frac{w}{d} \left(1 - (B/B_*)^2\right)^{3/4}$$

Suppression of G in the electric regime precedes formation of Landau levels and edge states at p-n interface

At larger *B*: no bulk transport, only edge transport

Collimated transmission for subcritical B

Electric regime B<B*

Perfect transmission at a finite angle $\theta_B = \arcsin B/B_*$

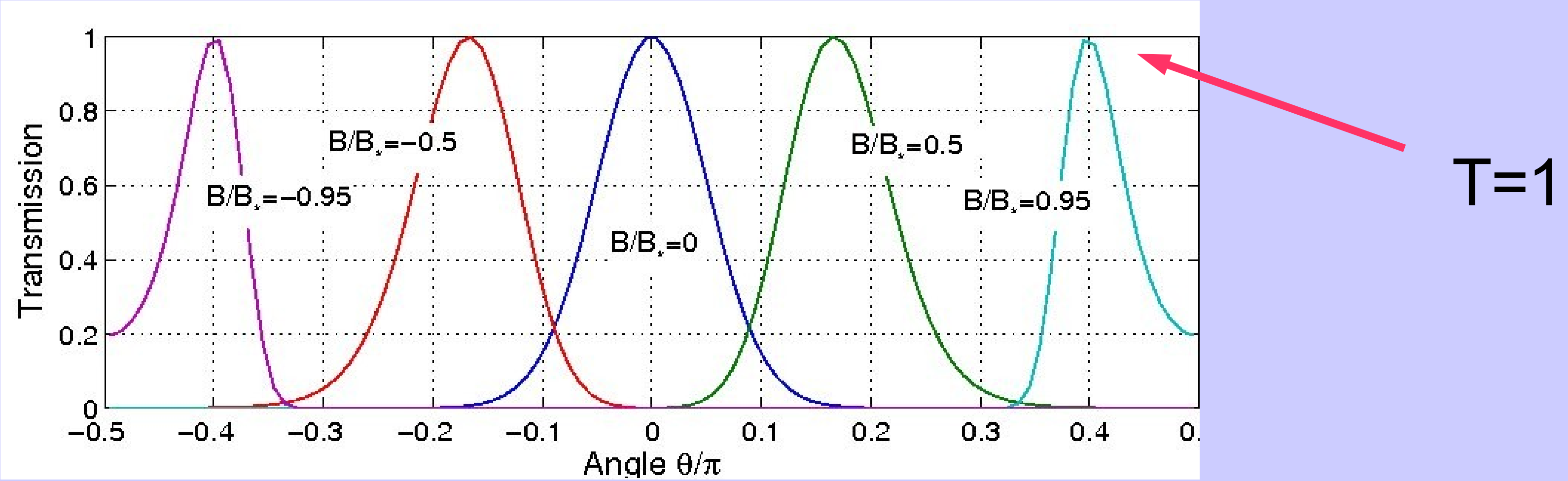

Collimation angle reduced by Lorentz contraction

Current switch controled by B

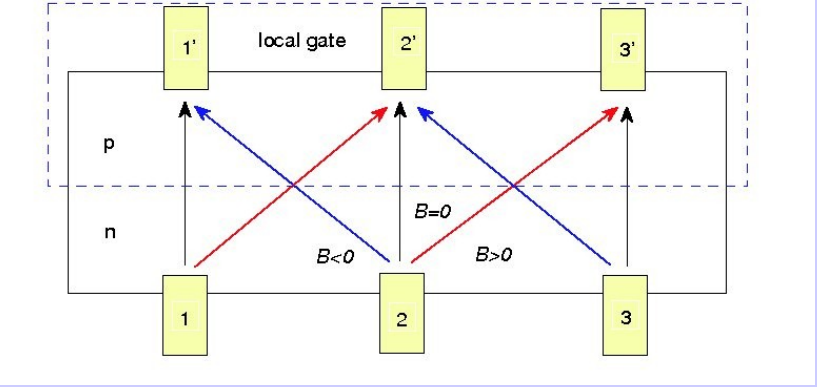

Mapping to the Landau-Zener transition problem

Quasiclassical WKB analysis

Evolution with a non-hermitian Hamiltonian

$$i\partial_x\psi(x) = ((\varepsilon + ax)\sigma_2 + i(p_1 + bx)\sigma_3)\,\psi(x).$$

Eigenvalues:

$$\kappa(x) \;=\; \sqrt{(\varepsilon + ax)^2 - (p_1 + bx)^2}$$

$$S = 2\int_{x_1}^{x_2} \operatorname{Im}\kappa(x)dx = \pi\frac{(p_1 a - \varepsilon b)^2}{(a^2 - b^2)^{3/2}}.$$

$$T(p_1) = \exp(-\pi\hbar v_F p_1^2/|eE|),$$

Exact solution: use momentum representation (gives direct access to asymptotic plane wave scattering states)

$$-ieE\,d\psi/dp_2 = \tilde{H}\psi, \quad \tilde{H} = v_F(p_1\sigma_1 - p_2\sigma_2) - \varepsilon.$$

Equivalent to the Landau-Zener transition
Interpretation: interband tunneling for $p_2(t)=vt$
L-Z result agrees with WKB

Classical trajectories

a comment by Haldane, 2007

Electron ("comet") orbits the Dirac point ("Sun")

$$\mathcal{H}(p,r) = \epsilon(\mathbf{p}) - eEx, \quad \mathbf{p} = \tilde{\mathbf{p}} - e\mathbf{A}, \quad \mathbf{A} = (0, Bx)$$

$$\text{Energy integral}: \ \epsilon(\mathbf{p}) - \mathbf{v}_D.\mathbf{p} = \epsilon_0, \quad \mathbf{v}_D = \mathbf{E} \times \mathbf{B}/B^2$$

$$\text{Poisson brackets}: [p_1, p_2] = e\hbar B$$

$$\text{Graphene}: \ \epsilon(\mathbf{p}) = v_F|\mathbf{p}|, \quad p(\theta) = \frac{\epsilon_0}{v_F - v_D \cos\theta}$$

Two cases, open and closed orbits:

$$v_D > v_F: \ \text{hyperbola}; \quad v_D < v_F: \ \text{ellipse}$$

Graphene bilayer: electronic structure and QHE

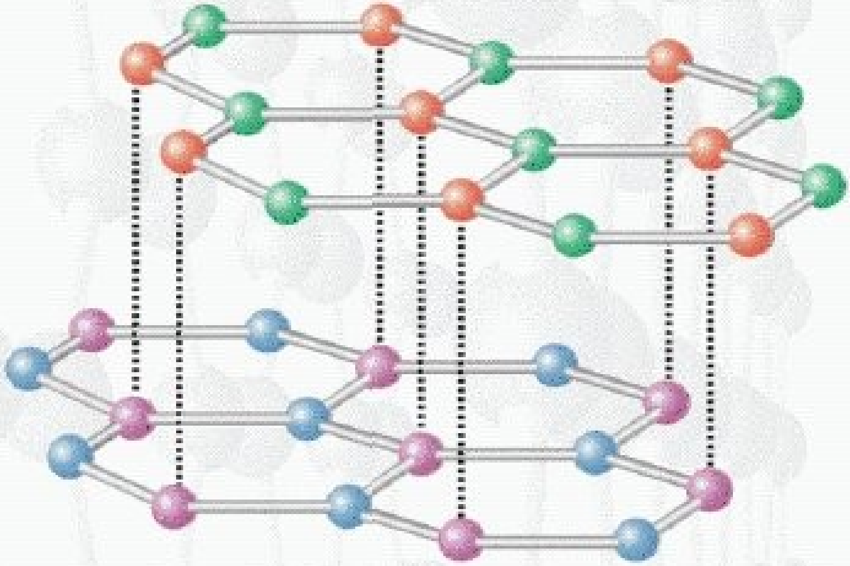

$$E(p) = \pm \tfrac{1}{2}\gamma_1 \pm \sqrt{\tfrac{1}{4}\gamma_1^2 + v_F^2 p^2}$$

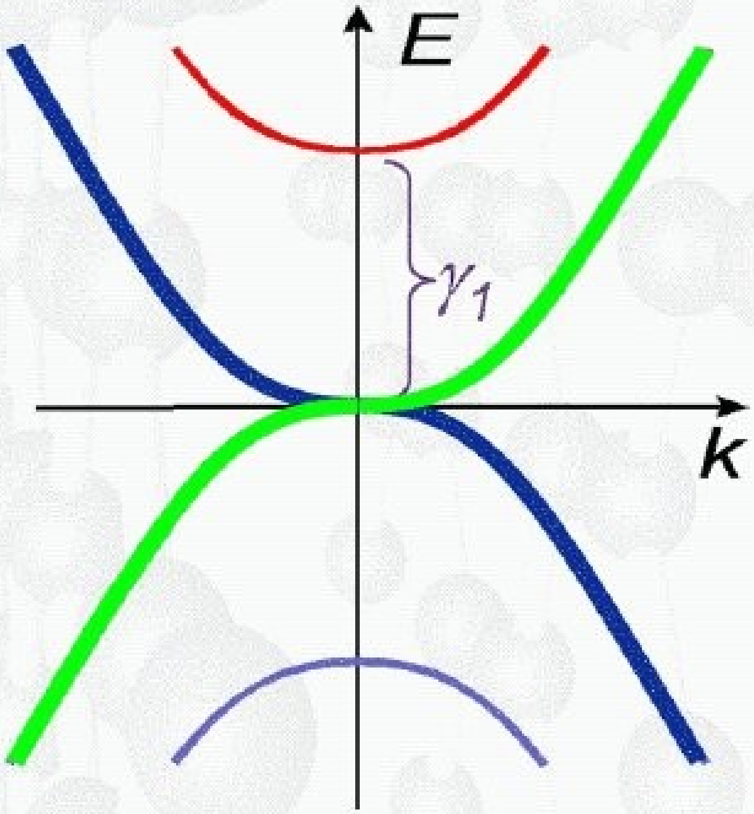

$$\hat{H} = -\frac{1}{2m}\begin{pmatrix} 0 & (\hat{p}_x + i\hat{p}_y)^2 \\ (\hat{p}_x - i\hat{p}_y)^2 & 0 \end{pmatrix}$$

$$E_N = \pm\hbar\omega_c\sqrt{N(N-1)}$$

McCann & Falko 2006

p-n junction in graphene bilayer

Bilayer Dirac Hamiltonian with vertical field and interlayer coupling

$$H = v_F p_1 \sigma_1 - v_F p_2 \sigma_2 + \frac{1}{2} u \tau_3 + \frac{\Delta}{2} (\tau_1 \sigma_1 + \tau_2 \sigma_2)$$

Dirac eqn with fictitios pseudospin-dependent gauge field:

$$\gamma^\mu (p_\mu - a_\mu - g_\mu)\psi = 0, \quad g_\mu = \left(\tilde{u}\tau_3, -\tilde{\Delta}\tau_1, \tilde{\Delta}\tau_2\right)$$

After Lorentz boost (B eliminated):

$$H_k(p_1', p_2') = \frac{1}{2}\gamma \left(u\tau_3 - \beta\Delta\tau_1\right) +$$
$$\left(v_F p_1' - \frac{1}{2}\gamma(\beta u \tau_3 - \Delta\tau_1)\right)\sigma_1 - \left(v_F p_2' - \frac{1}{2}\Delta\tau_2\right)\sigma_2.$$

Transmission characteristics

4x4 transfer matrix in momentum space (effectively 2x2)

$$ieE'\, d\psi/dp_2' = (H_k(p_1', p_2') - \varepsilon')\,\psi$$

Gapped spectrum at finite vertical field

Zero transmission near *u*=0 --- tunable!

Perfect transmission for certain *u* and *p*

Tunneling at small *p* suppressed by *B* field

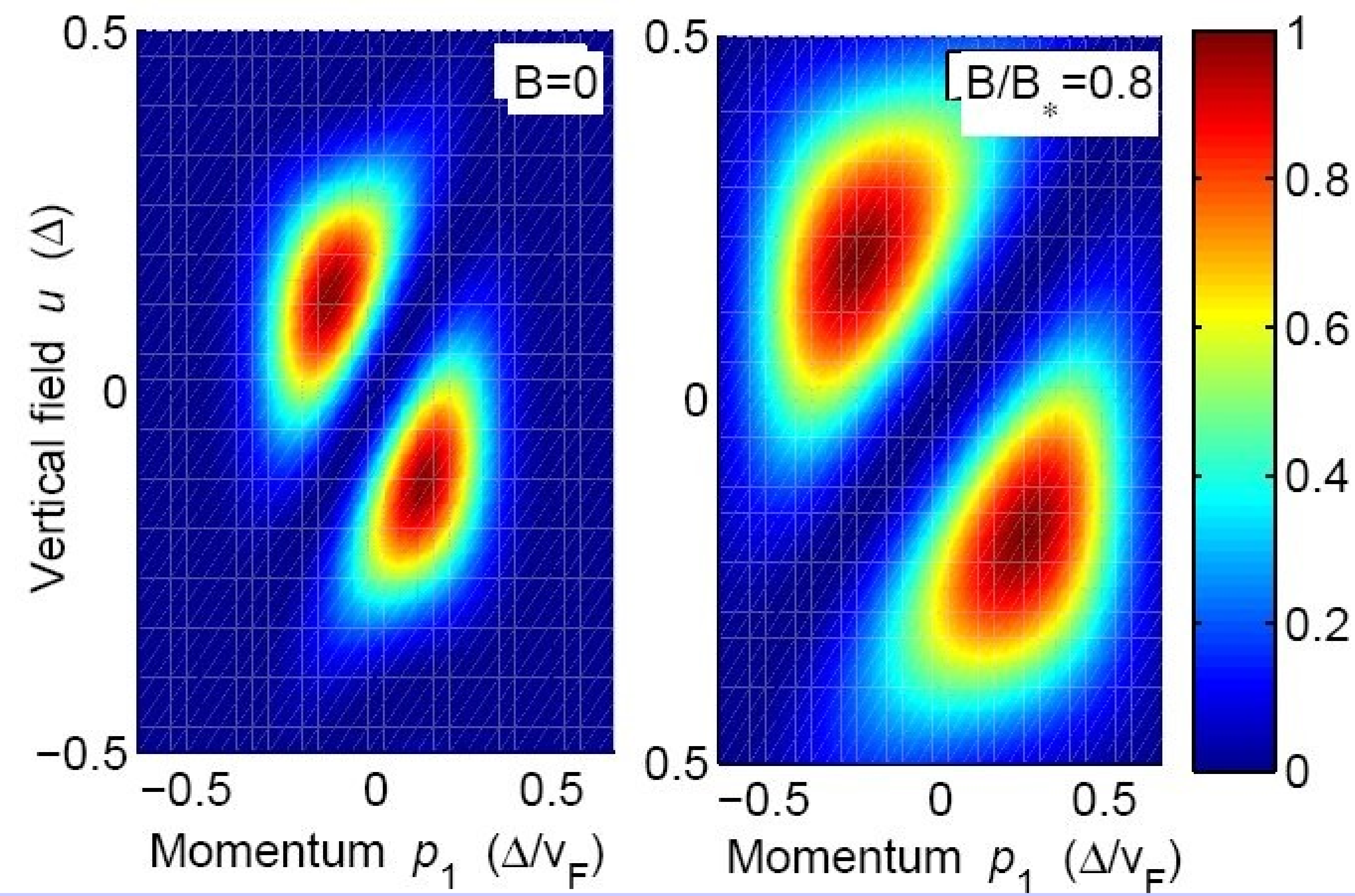

Transport in E and B fields, Manifestations of relativistic Dirac physics:

- Klein tunneling via Dirac sea of states with opposite polarity;
- chiral dynamics (perfect transmission at normal incidence);
- Half a period phase shift a hallmark of Klein scattering
- electric and magnetic regimes B<300E and B>300E (300=c/v_F)
- Consistent with FP oscillations and magnetoresistance of existing p-n junctions

Lecture II

recall Quantum Hall effect

Background on QHE

General 2D physics

Parabolic spectrum E(p)=p^2/2m

Bob Willett's lecture notes

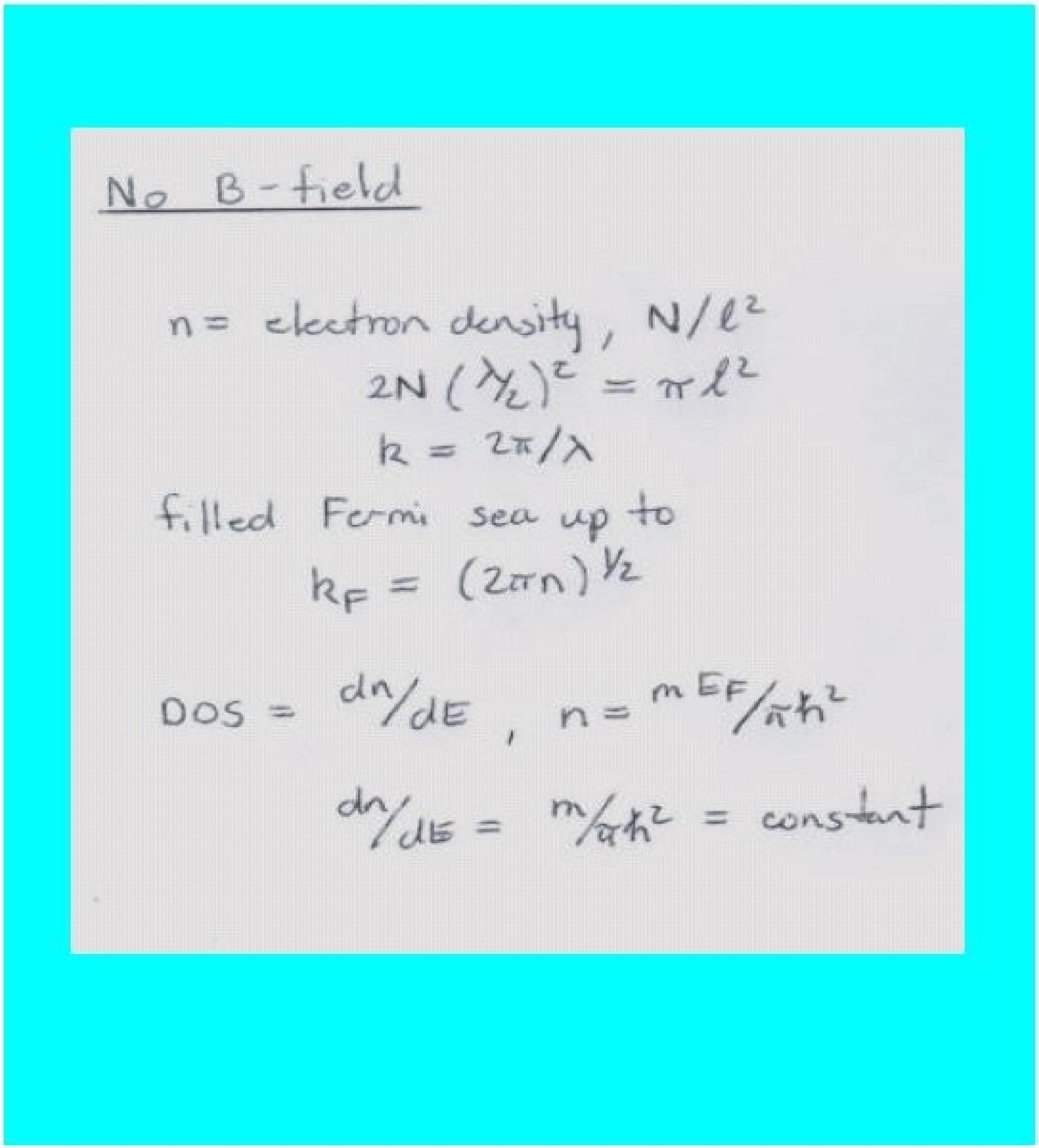

No B-field

n = electron density, N/ℓ^2

$$2N\,(\lambda/2)^2 = \pi \ell^2$$

$$k = 2\pi/\lambda$$

filled Fermi sea up to

$$k_F = (2\pi n)^{1/2}$$

$$\mathrm{DOS} = dn/dE, \quad n = m E_F/\pi\hbar^2$$

$$dn/dE = m/\pi\hbar^2 = \text{constant}$$

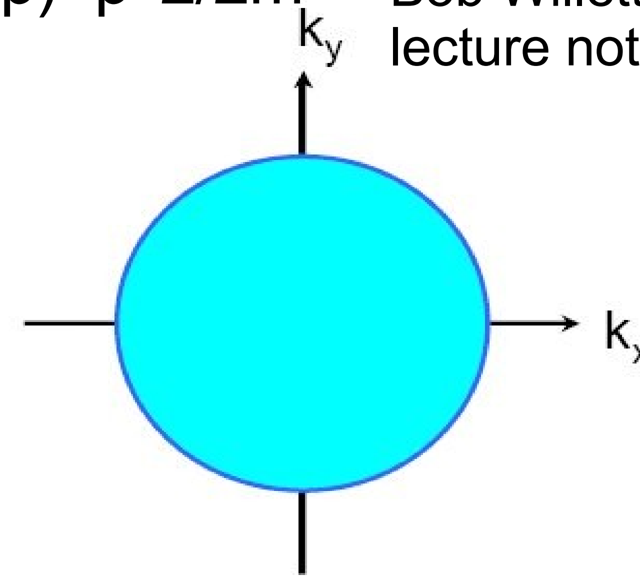

$$k_F = (2\pi n)^{1/2}$$

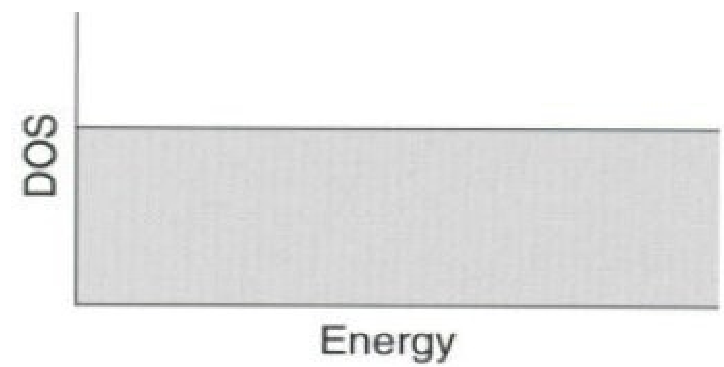

Quantum Hall effect

General 2D physics

With B-field

Hamiltonian

$$H = \frac{(\vec{p} + e\vec{A})^2}{2m^*} + \frac{1}{2} g \mu_B \vec{\sigma} \cdot \vec{B} + V(z)$$

energy eigenvalues

$$E_n = (N + 1/2)\hbar\omega_c + \frac{1}{2} g \mu_B B + E_0$$

$m^*/m_0 = 0.067$, $g = -0.44$

cyclotron frequency $\omega_c = eB/m^*$

density of states $D = eB/h$

Bohr magneton $\mu_B = e\hbar/2m_0$

$\hbar\omega_c = 20K$ at $B = 1T$; $g\mu_B B \sim \hbar\omega_c/70$

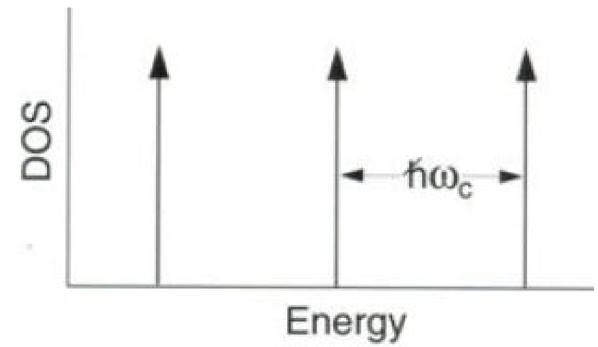

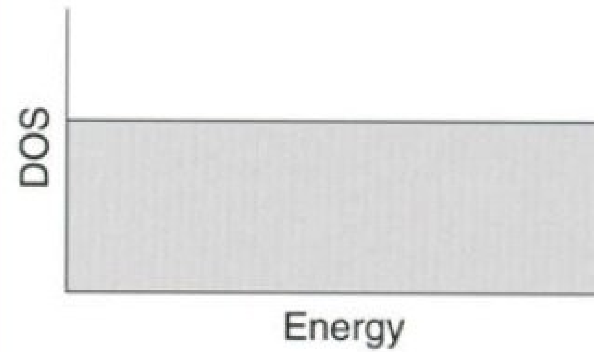

Quantum Hall effect

General 2D physics

With B-field (cont.)

$$H = \frac{(\bar{p} + e\bar{A})^2}{2m^*}$$

symmetric gauge: $\vec{A} = \frac{1}{2}(\bar{r} \times \bar{B})$

$$\psi_{0,j} = z^j e^{-|z|^2/4} u(j), \quad j = 0, 1, 2 \ldots$$

$N=0$

$$z = (x + iy)$$

Landau gauge: $\vec{A} = -yB\hat{x}$

$$\psi_{N,k} = e^{ikx} v_N(y - y_k)$$

Guiding center of cycl. orb.

$$v_N(\alpha) = e^{-\alpha^2/2\ell^2} H_N(\alpha)$$

note nodal structure for $N > 0$

p-x duality

$$y_k = k\ell^2$$

$\ell^2 = \hbar/eB$, magnetic length

Higher Landau levels have more nodes

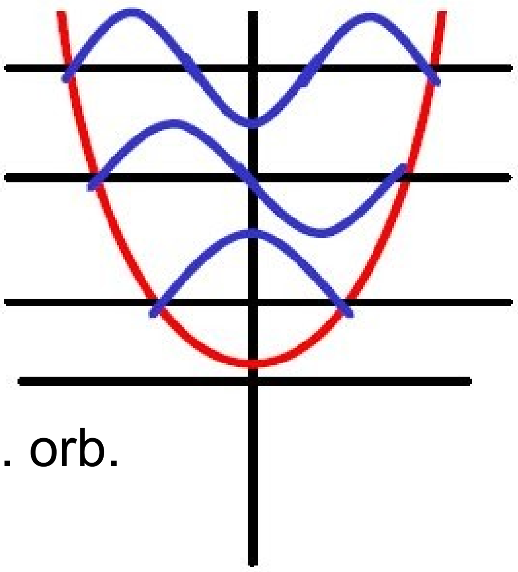

Magnetic length l_0

Quantum Hall effect

General 2D physics

With B-field and disorder

scattering times

a) level broadening $\Gamma = \hbar/\tau$
relaxation time $\tau \equiv$
time to be scattered into a different state
$\omega_c \tau \gg 1 \Rightarrow$ resolved Landau levels

b) transport scattering time
mean-free-path $\ell_{mfp} = v_F \tau_{tr}$

mobility $\mu \equiv v/E$; $\mu = \frac{1}{ne\rho}$
ρ = resistivity , n = areal density

$\sigma = ne\mu = ne^2 \tau_{tr}/m$

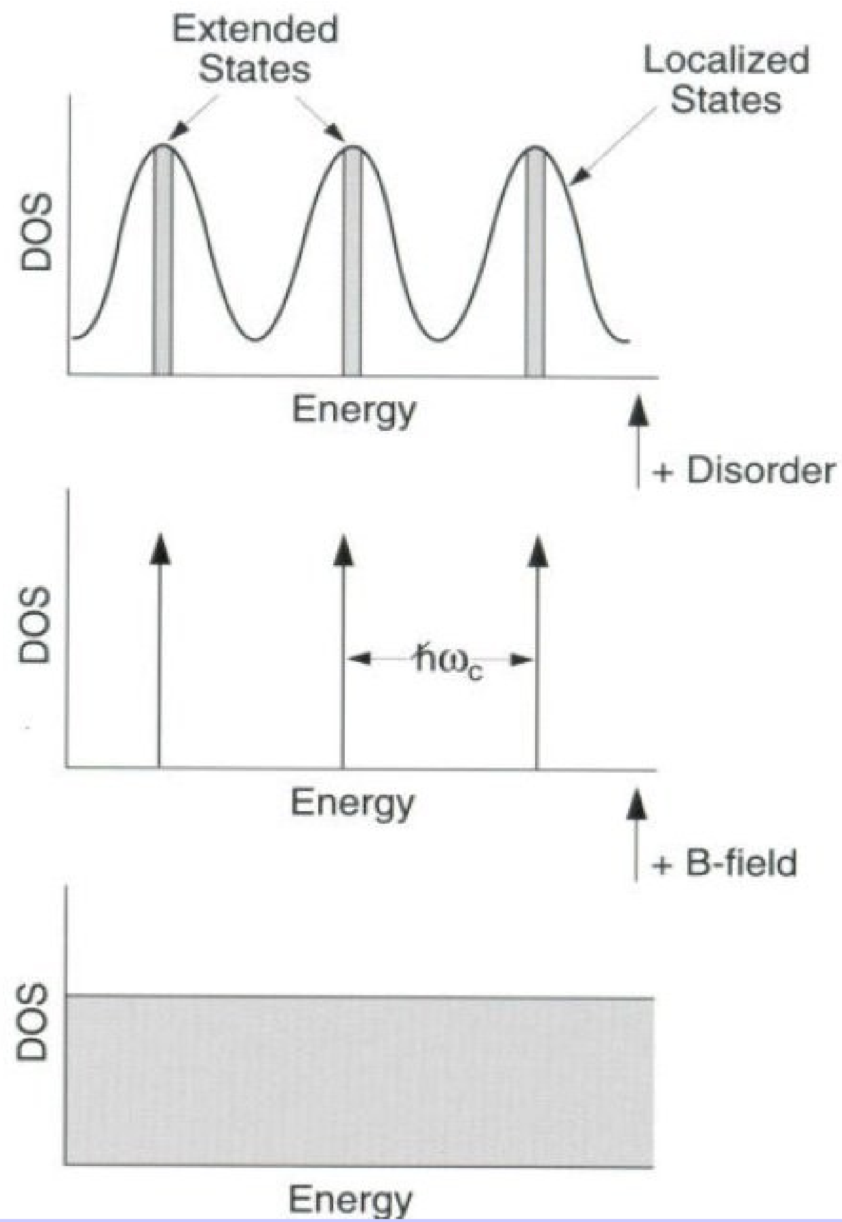

QHE measurement I

Measurements – Hall effect

Measured quantities are R_{xx}, R_{xy},
find σ_{xx}, σ_{xy} by inverting a 2x2 matrix

With increasing B, degeneracy of LL increases and Fermi level is swept through spectrum (constant density n)

Landau levels resolved

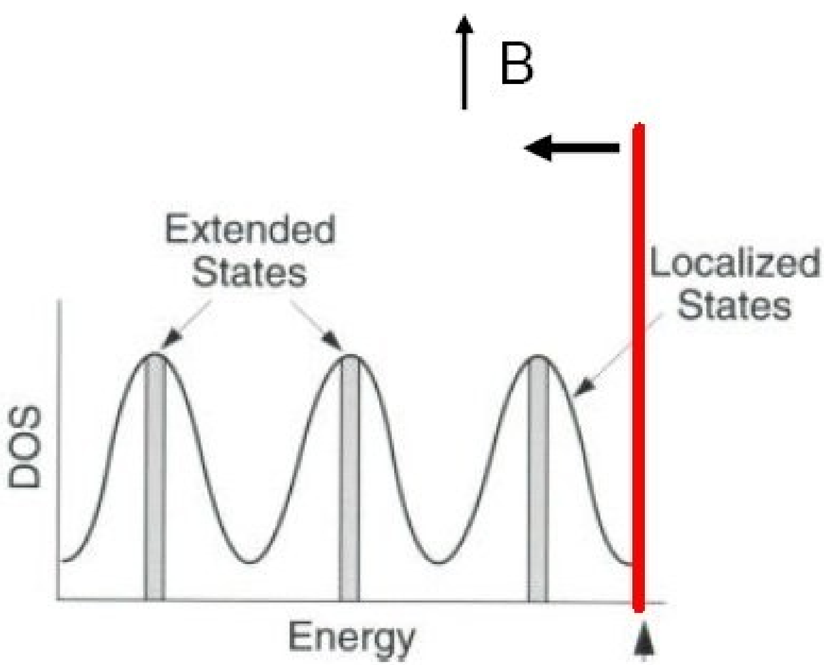

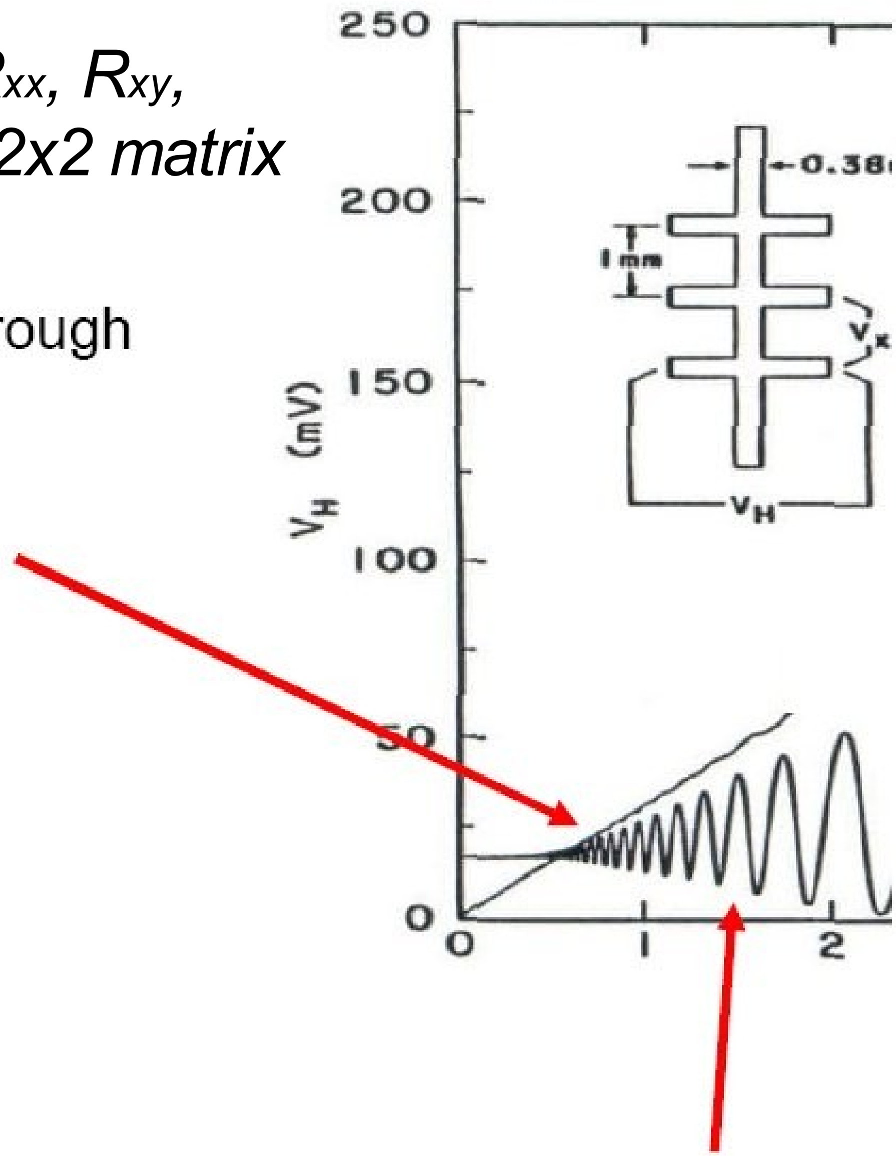

Shubnikov-deHaas oscillations

QHE measurement II

Measurements – **quantum Hall effect**

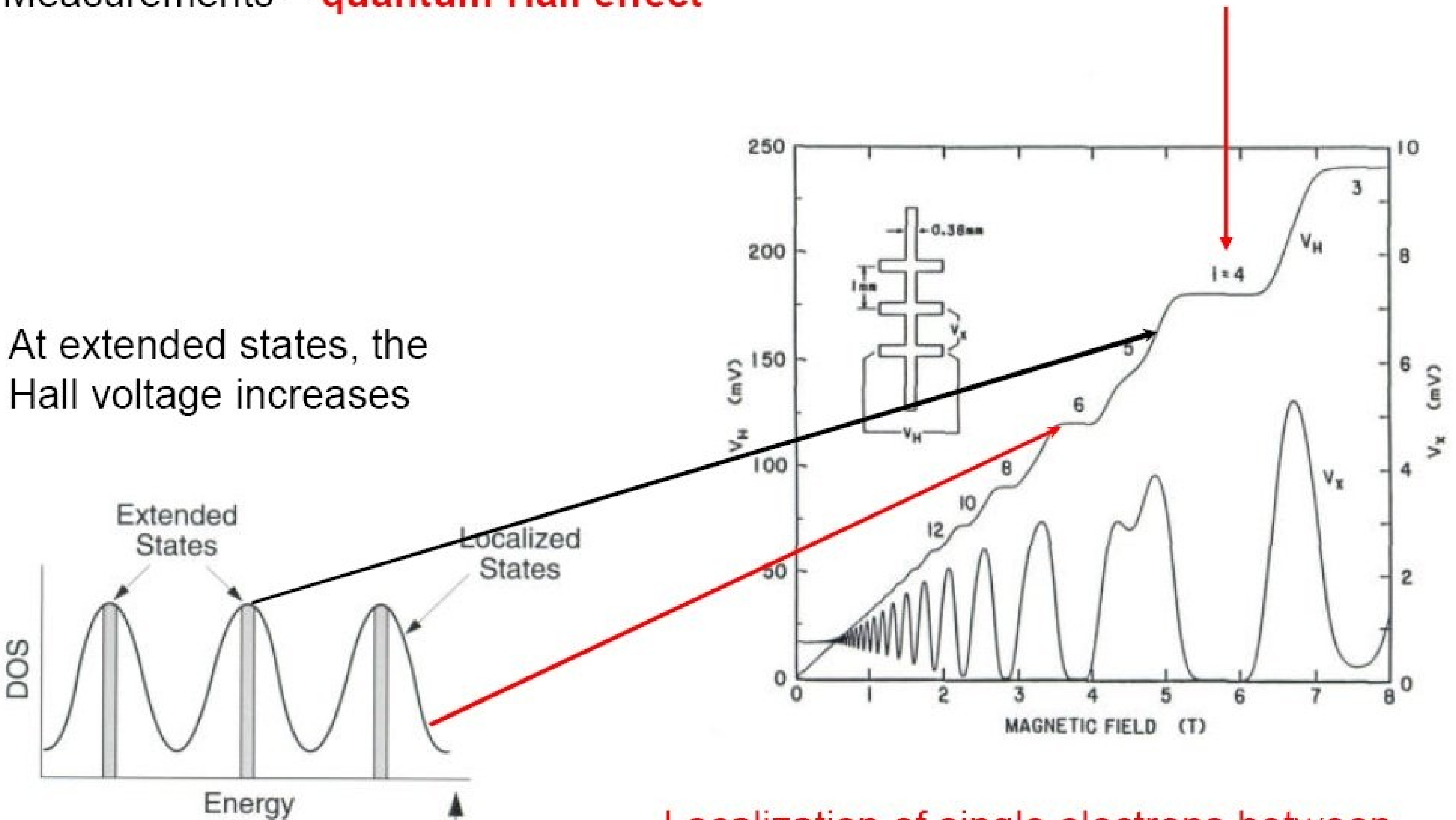

Localization of single electrons between extended states produces plateaus in Hall resistance

QHE: edge transport

Measurements – quantum Hall effect

Integer QHE and Edge States

Chiral dynamics along edge (unidirectional)

Edge conduction

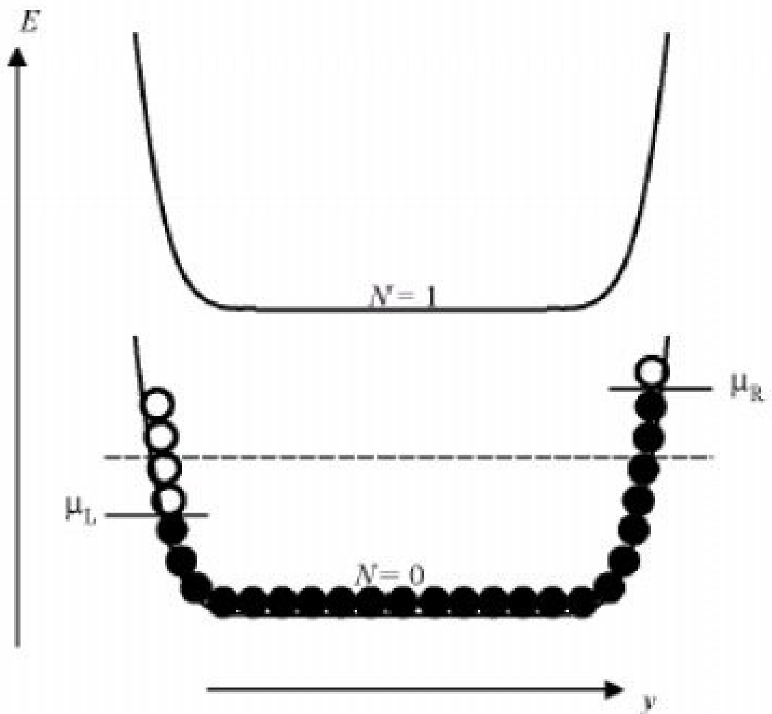

No backscattering along same edge

$$I = \sum_{occ.} i_k = \int \frac{L_x dy_k}{2\pi \ell^2}\left(\frac{\partial \varepsilon_N}{\partial y_k}\frac{e\ell^2}{\hbar L_x}\right) = \frac{e}{h}(\mu_R - \mu_L) = \frac{e^2}{h} V_H$$

Lecture II

The half-integer QHE:

Berry's phase,
edge states in graphene,
QHE as an axial anomaly

Quantum Oscillations in Graphene

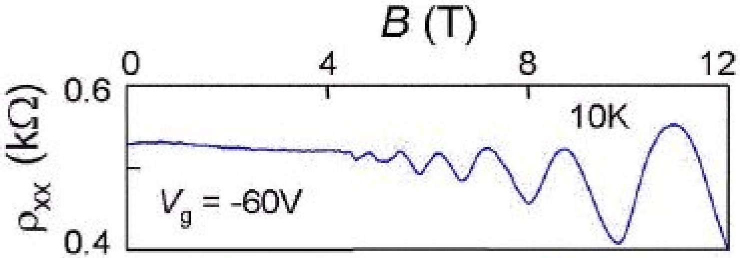

degeneracy f=4
two spins & two valleys

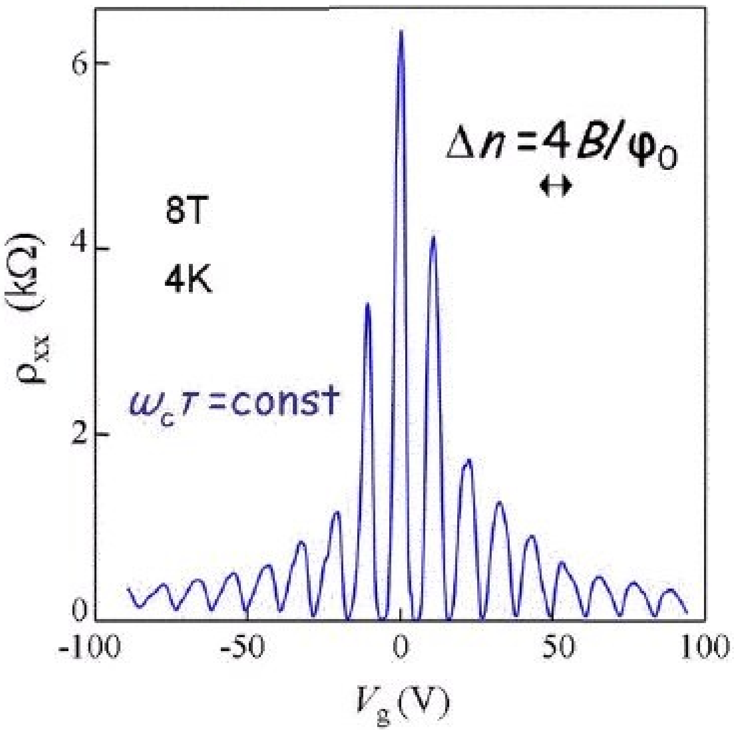

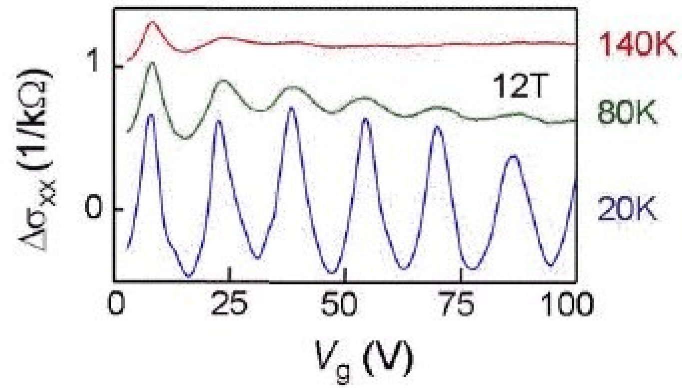

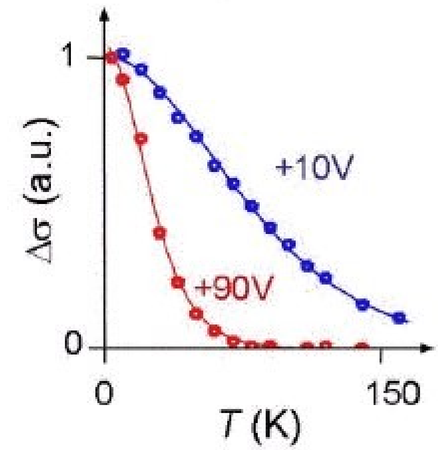

$$\Delta\sigma_{xx} \propto T / \sinh\left(\frac{2\pi^2 k_B T m_c}{\hbar e B}\right)$$

The "half-integer" QHE in graphene

Single-layer graphene:
QHE plateaus observed at

$$\nu = 4 \times (0, \pm 1/2, \pm 3/2 \ldots)$$

4=2x2 spin and valley degeneracy

double layer: single layer:

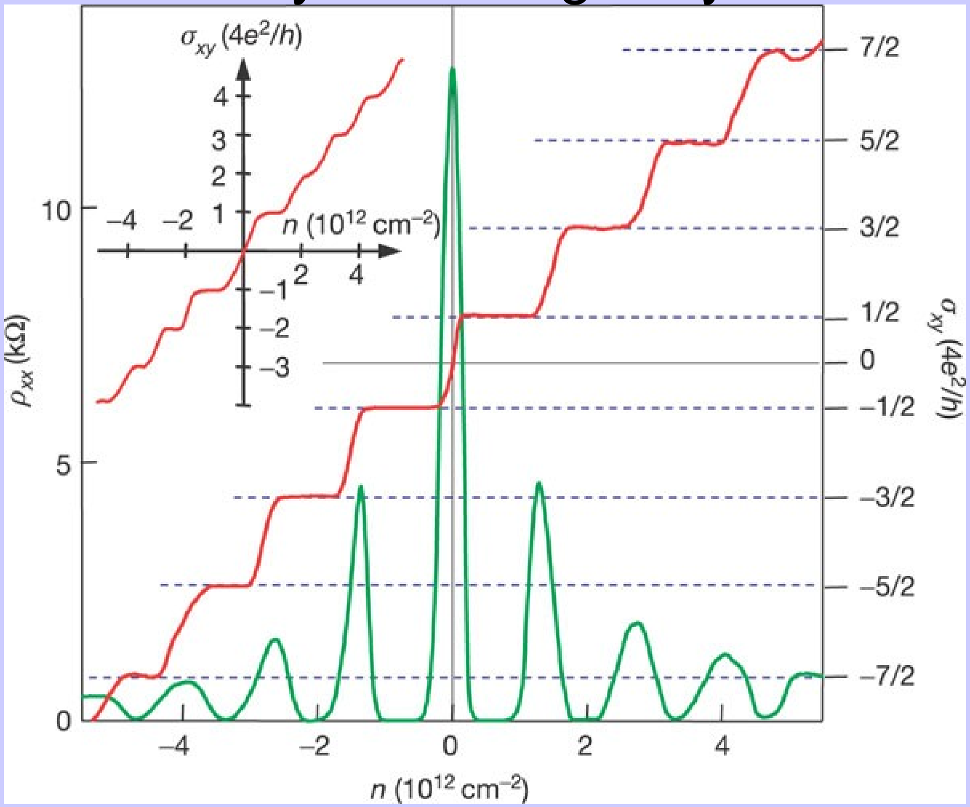

Explanations of half-integer QHE:

(i) anomaly of Dirac fermions;
(ii) Berry phase;
(iii) counter-propagating edge states

Novoselov et al, 2005, Zhang et al, 2005

room-temperature QHE

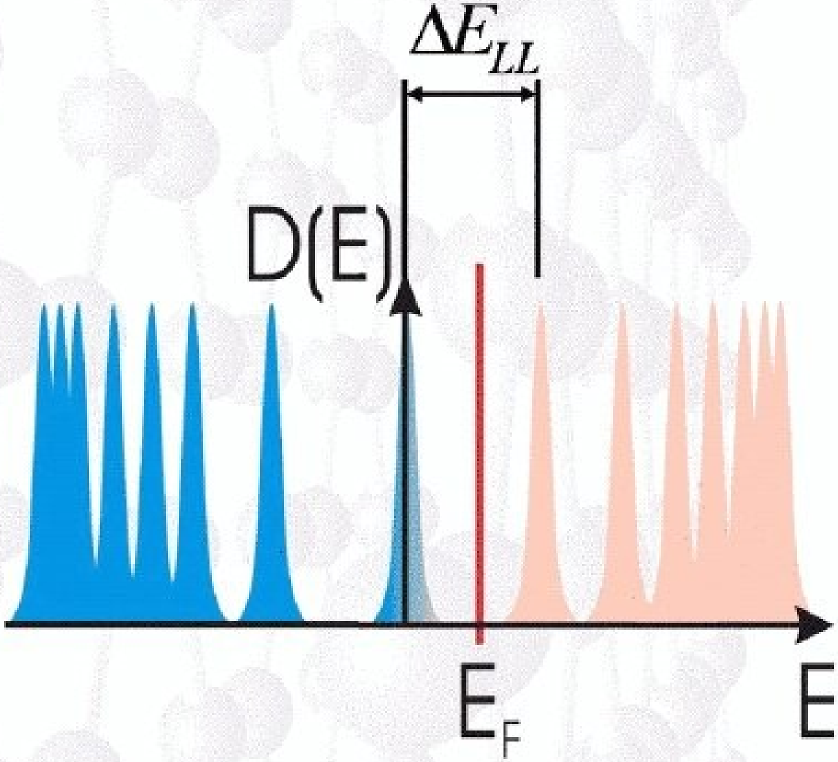

$$\Delta E_{LL} = v_F \sqrt{2e\hbar B}$$

$$\Delta E_{LL}(K) = 420\sqrt{B(T)}$$

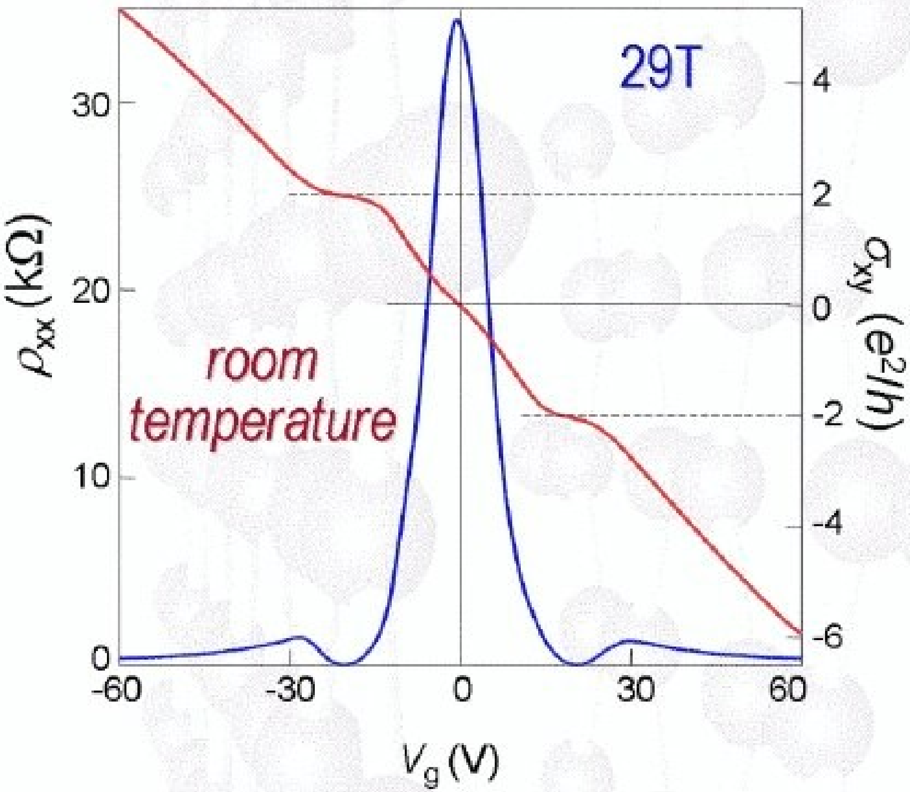

previously, only below 30K

The half-integer quantization from Berry's phase

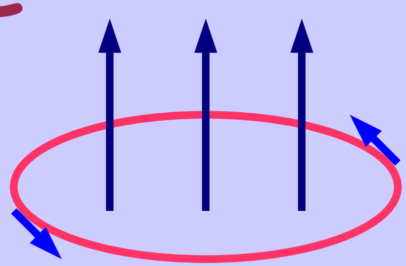

Quasiclassical Landau levels (nonrelativistic):
Bohr-Sommerfeld quantization for electron energy
in terms of integer flux $\Phi = n\Phi_0$ enclosed by a cyclotron orbit

For massless relativistic particles (pseudo)spin $\sigma \parallel p$,
subtends solid angle 2π per one revolution:
quantization condition modified as $\Phi = (n+1/2)\Phi_0$

Prediction of half a period shift of Shubnikov-deHaas oscillation

Evolves into half-integer QHE in quantizing fields

Edge states for graphene QHE

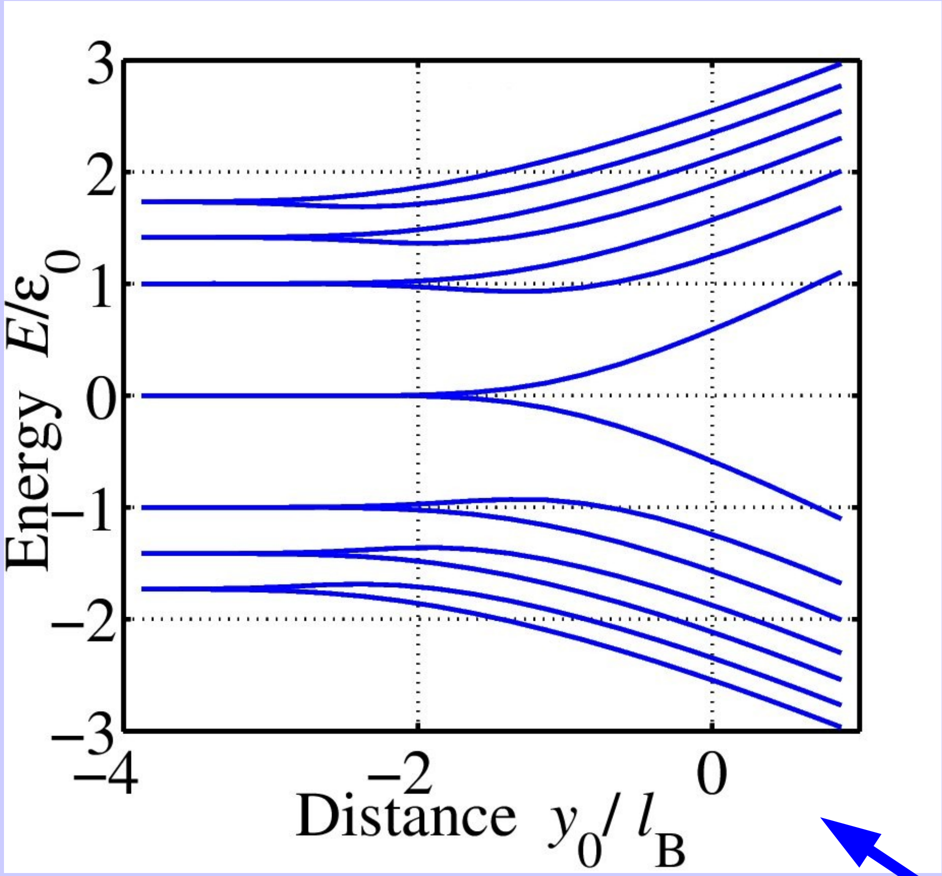

Properties of the edge states:

(i) KK' splitting due to mixing at the boundary;

(ii) Counter-circulating electron & hole states;

(iii) Symmetric splitting of n=0 Landau level

(iv) Universality, same for other edge types;

(v) The odd numbers of edge modes result in half-integer QHE

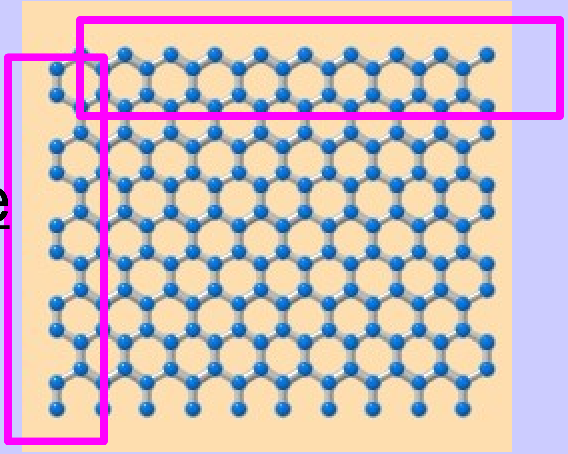

armchair edge

zigzag edge (similar, +surface states)

Edge states from 2d Dirac model

Abanin, Lee, LL, PRL 96, 176803 (2006)

Also: Peres, Guinea, Castro-Neto, 2005, Brey and Fertig, 2006

The half-integer QHE: Field-Theoretic Parity Anomaly

R. Jackiw, Phys.Rev D29, 2377 (1984)

A novel axial anomaly has been found in gauge theories defined on three-dimensional space-time, which describe dynamics confined to a plane: fermions moving in an external gauge field and governed by the 2×2 matrix equation (massless Dirac equation)

$$\gamma^\mu(i\partial_\mu - eA_\mu)\Psi = 0 \quad (1)$$

induce a topologically nontrivial vacuum current of abnormal parity,

$$\langle j^\mu \rangle = \pm c \frac{e}{8\pi} \epsilon^{\mu\alpha\beta} F_{\alpha\beta} + \cdots \quad (2)$$

Recognize Lorentz-invariant QHE relation $j = \sigma_{xy} E$, where $\sigma_{xy} = 1/2$

Here γ^μ are three 2×2 "Dirac" matrices (Pauli matrices) and A_μ is the external vector potential, leading to the field strength $F_{\alpha\beta}$.

c=1 for Abelian gauge field

Anomaly: relation to fractional quantum numbers

The purpose of this paper is to derive similar results in the three-dimensional case under present discussion. We show that for static background fields in the $A_0=0$ Weyl gauge, the Dirac Hamiltonian corresponding to (1) possesses a conjugation-symmetric spectrum with zero modes, if the background field satisfies certain requirements. Although the topological interest is mainly in the non-Abelian theory, we shall concern ourselves with the Abelian Maxwell theory, which is of greater physical relevance, since it can describe the motion of charged fermions on a plane perpendicular to an external magnetic B field.

The demonstration is very simple. The Hamiltonian corresponding to (1) is

$$H=\vec{\alpha}\cdot(\vec{\mathrm{p}}-e\vec{\mathrm{A}}) , \quad (3)$$

where the "Dirac" $\vec{\alpha}$ matrices are the two Pauli matrices: $\alpha^1=-\sigma^2$, $\alpha^2=\sigma^1$. The β matrix, which would be present if there were a mass term, is taken to be σ^3. Since $\beta=\sigma^3$ anticommutes with H, it serves as a conjugation matrix, and the energy eigenmodes are symmetric about $E=0$,

$$\vec{\alpha}\cdot(\vec{\mathrm{p}}-e\vec{\mathrm{A}})\psi_E=E\psi_E , \qquad \sigma^3\psi_E=\psi_{-E} . \quad (4)$$

Of course in the presence of the mass term, the conjugation symmetry is broken.

To find the zero-energy modes we write the wave function as $\psi_0=\binom{u}{v}$, and choose the Coulomb gauge for $\vec{\mathrm{A}}$, which we assume to be single valued and well behaved at the origin,

$$A^i=\epsilon^{ij}\partial_j a , \quad (5)$$

$$B=-\nabla^2 a . \quad (6)$$

Then Eq. (4) reduces to the pair

$$(\partial_x+i\partial_y)u-e(\partial_x+i\partial_y)au=0 , \qquad (\partial_x-i\partial_y)v+e(\partial_x-i\partial_y)av=0 , \quad (7)$$

with the obvious solution

$$u=\exp(ea)f(x+iy) , \qquad v=\exp(-ea)g(x-iy) , \quad (8)$$

where f and g are arbitrary entire functions. Thus we can form self-conjugate solutions $\binom{u}{0}$ and $\binom{0}{v}$. Whether these are acceptable wave functions depends on the large-r behavior of a. If a grows sufficiently rapidly at large distance, then either u or v will be normalizable, and there exist one or more isolated zero-energy bound states, the multiplicity depending on how many different forms for f or g may be taken.

It is useful to classify the various possibilities in terms of the total flux, which is also proportional to the total induced charge:

$$\langle j^0\rangle=\pm\frac{e}{4\pi}B , \qquad Q=\int d^2\vec{\mathrm{r}}\langle j^0\rangle=\pm\frac{e}{4\pi}\int d^2\vec{\mathrm{r}}B=\pm\frac{e}{2}\Phi , \quad (9)$$

Each zero-energy state filled (unfilled) contributes +1/2(-1/2) of an electron macroscopically: (1/2)*LL density

Lecture II

valley-split and spin-split QHE states;

QHE in graphene bilayers;

Pseudospin K-K' valley states

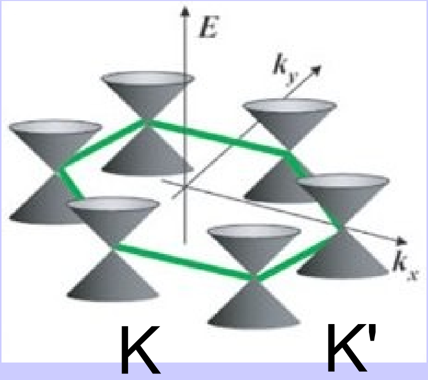

(i) Spin and valley n=0 Landau level degeneracy:

2x2=4;

(ii) SU(4) symmetry, partially lifted by Zeeman interaction:

SU(4) lowered to SU(2), associated with KK' mixing;

(iii) Assume that the ν=1 QHE plateau is described by KK' splitting of spin-polarized n=0 Landau level

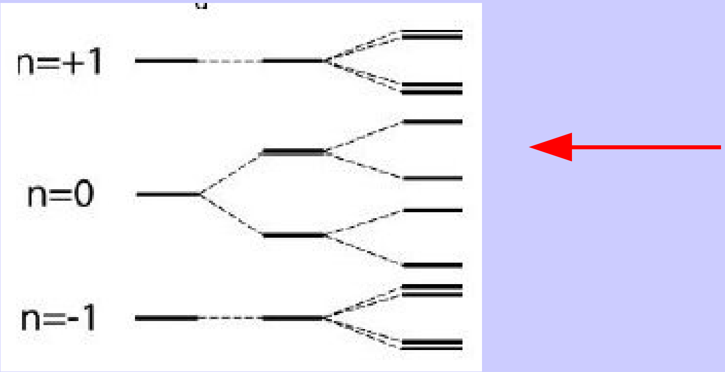

Many aspects similar to quantum Hall bi-layers (here KK')
Girvin, MacDonald 1995, and others

Observation of valley-split QHE states

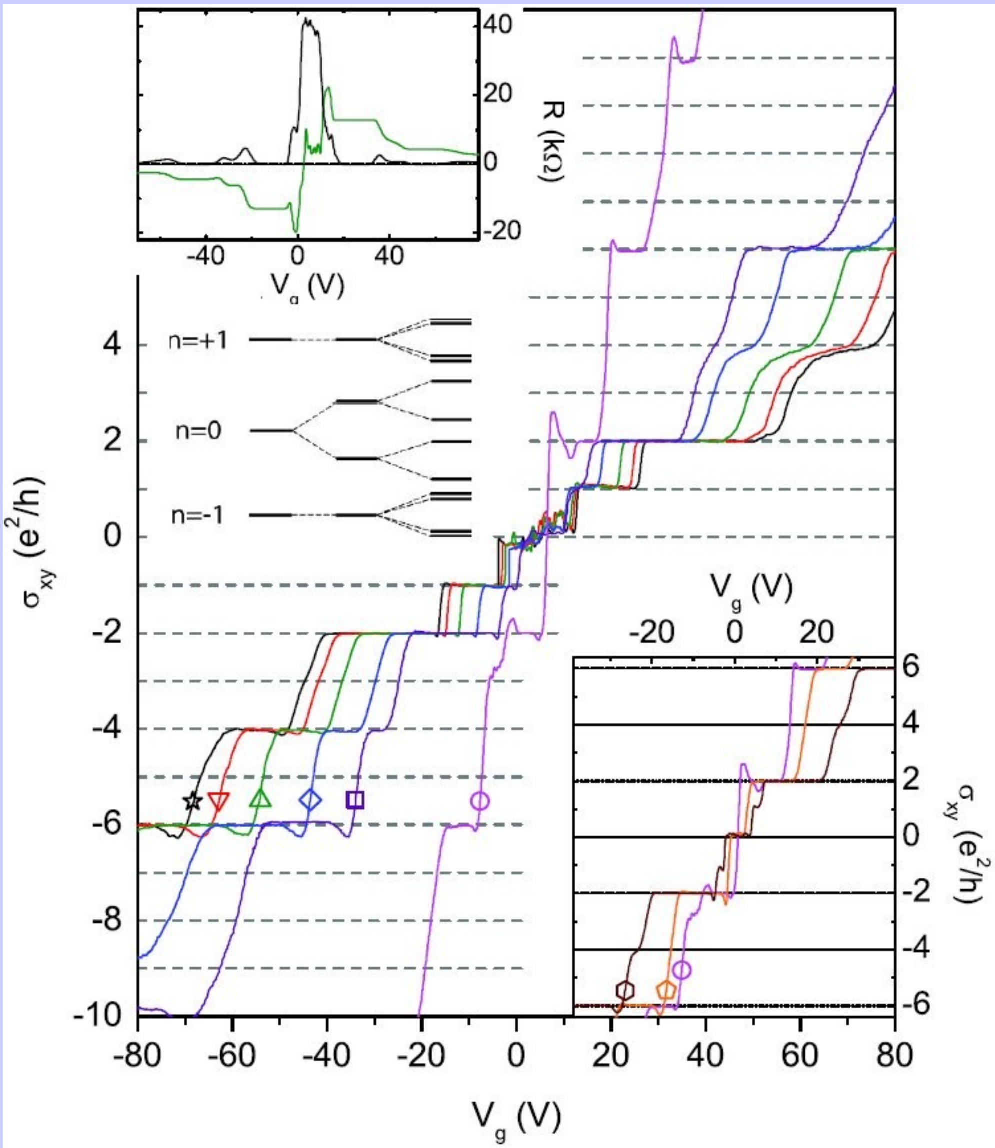

Four-fold degenerate n=0 LL splits into sub-levels at ultra high magnetic field:

spin (n=0,+1,-1), KK' (n=0)

confirmed by exp in tilted field ☺

B=9,25,30,37,42,45 Tesla, T=1.4K

(Zhang et al, 2006)

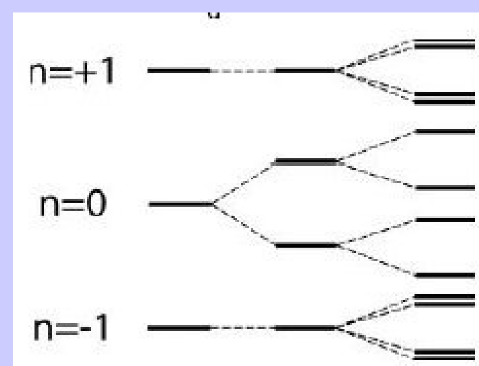

Recent transport measurments

Checkelsky, Ong (Princeton): unusual behavior of resistance near Dirac point

(i) dramatic icrease of resistance under applied B field;

(ii) same upon lowering T

(iii) unremarkable at other densities

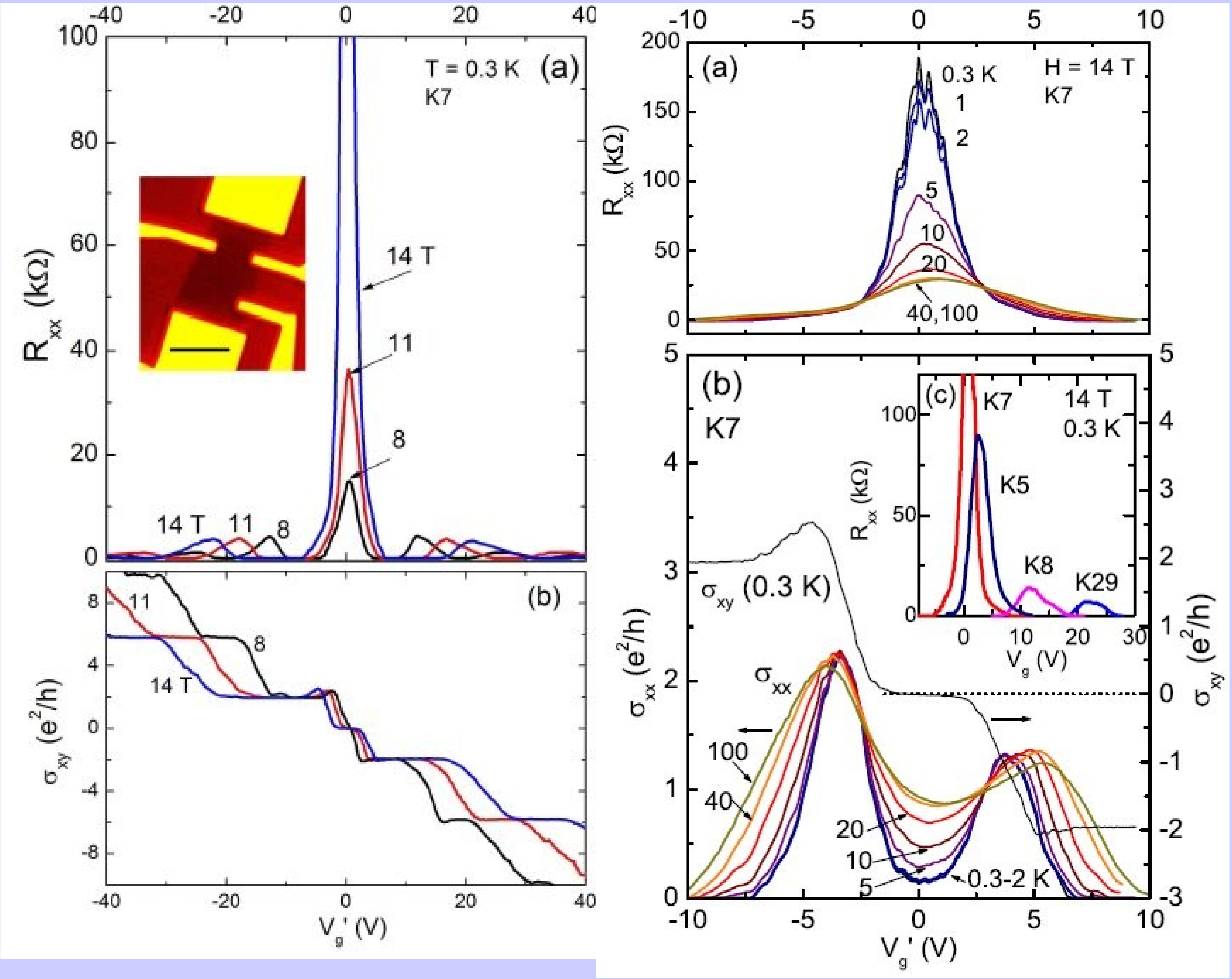

Evidence for critical behavior of resistance

Data fitted to a model surmised from Berezinskii-Kosterlitz-Thouless theory: R ~ ξ^2, diverging at a critical B field

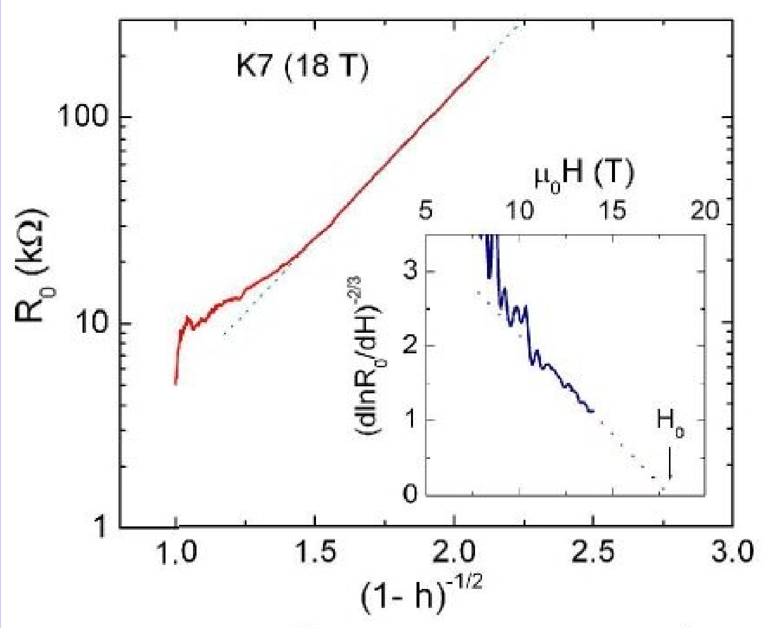

$R_0(h) \sim \exp[2b/\sqrt{1-h}]$ with $b \sim 0.7$

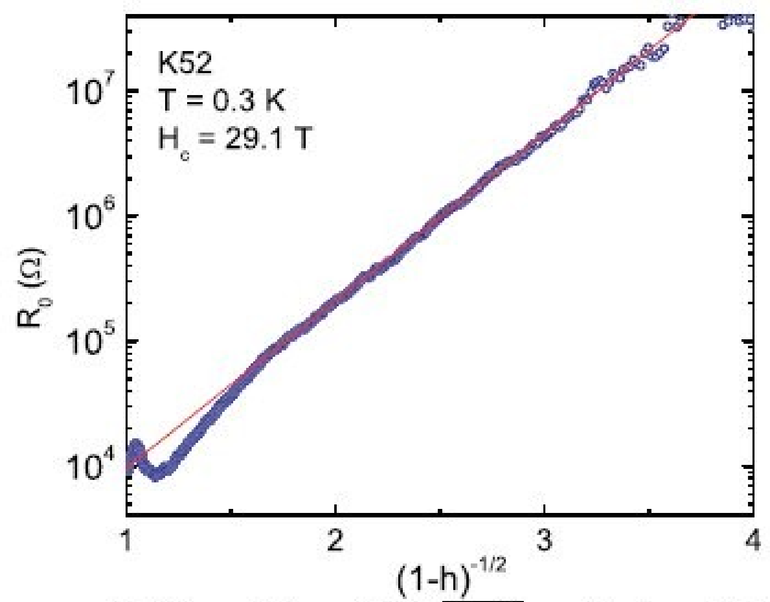

$R_\xi(h) = 440\exp[2b/\sqrt{1-h}]$, with $b = 1.54$.

Graphene bilayer: electronic structure and QHE

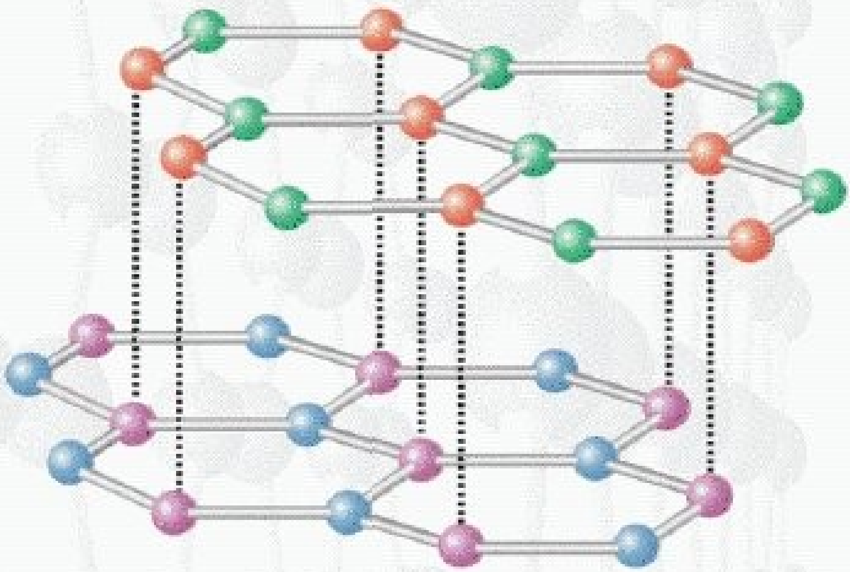

$$E(p) = \pm \tfrac{1}{2}\gamma_1 \pm \sqrt{\tfrac{1}{4}\gamma_1^2 + v_F^2 p^2}$$

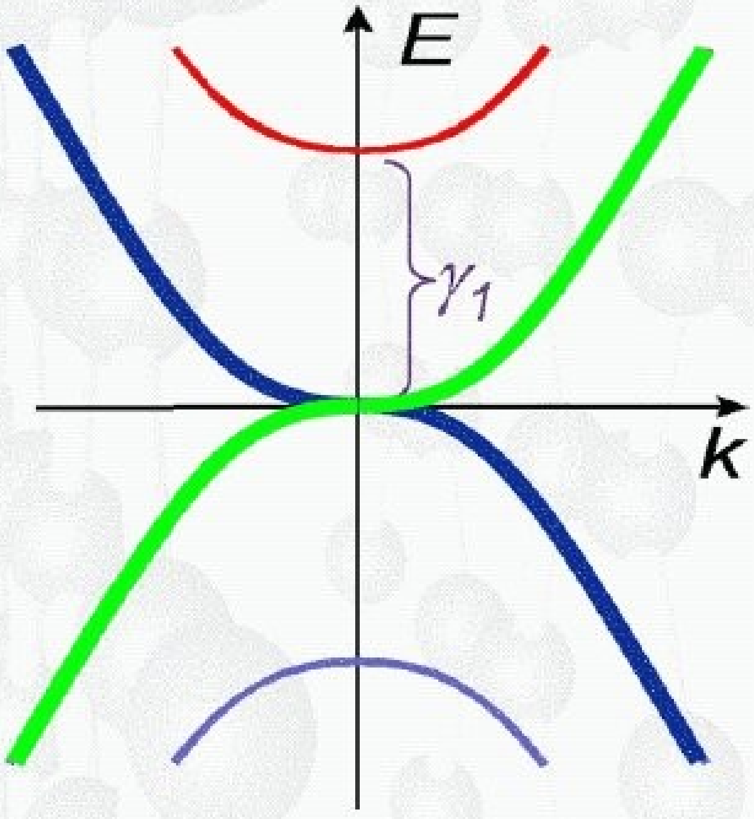

$$\hat{H} = -\frac{1}{2m}\begin{pmatrix} 0 & (\hat{p}_x + i\hat{p}_y)^2 \\ (\hat{p}_x - i\hat{p}_y)^2 & 0 \end{pmatrix}$$

$$E_N = \pm\hbar\omega_c\sqrt{N(N-1)}$$

McCann & Falko 2006

Bilayer: field-tunable semiconducting energy gap

monolayer

bilayer

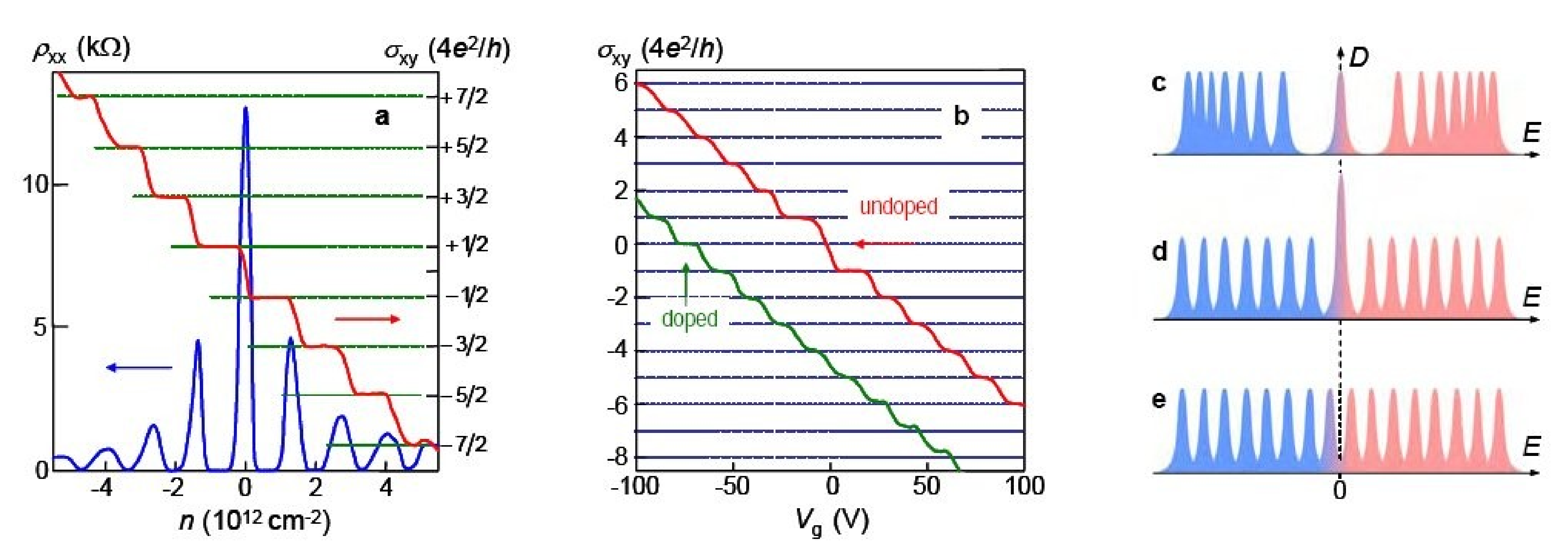

HW?

Lecture III

QHE in p-n and p-n-p lateral junctions:

Edge state mixing; Fractionally-quantized QHE

QHE in p-n junctions I

Local density control (gating): p-n and p-n-p junctions

(Stanford, Harvard, Columbia)

QHE in p-n junctions, integer and fractional conductance quantization:
(i) g=2,6,10..., unipolar regime, (ii) g=1,3/2..., bipolar regime

Williams, DiCarlo, Marcus, Science 28 June 2007

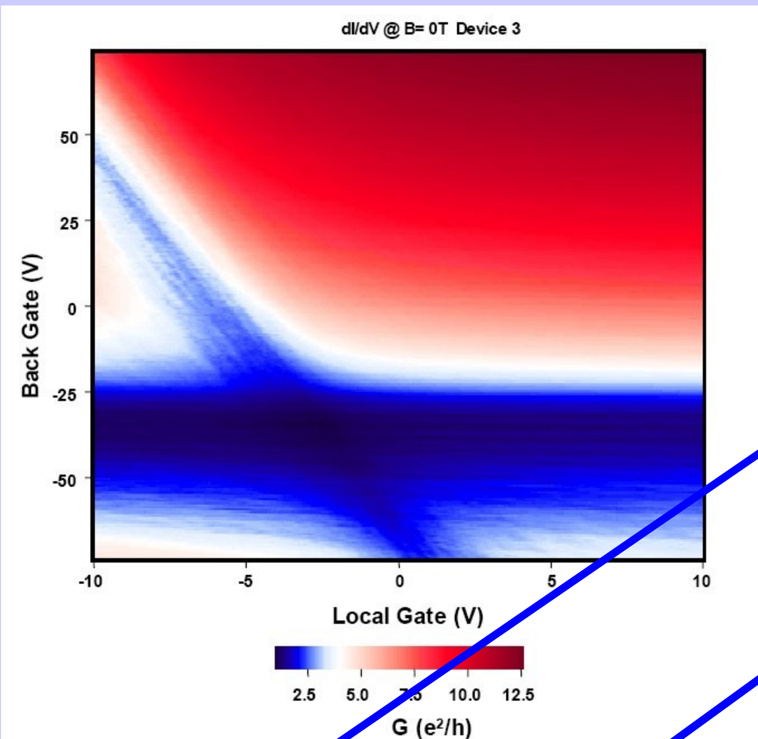

B>0

B=0

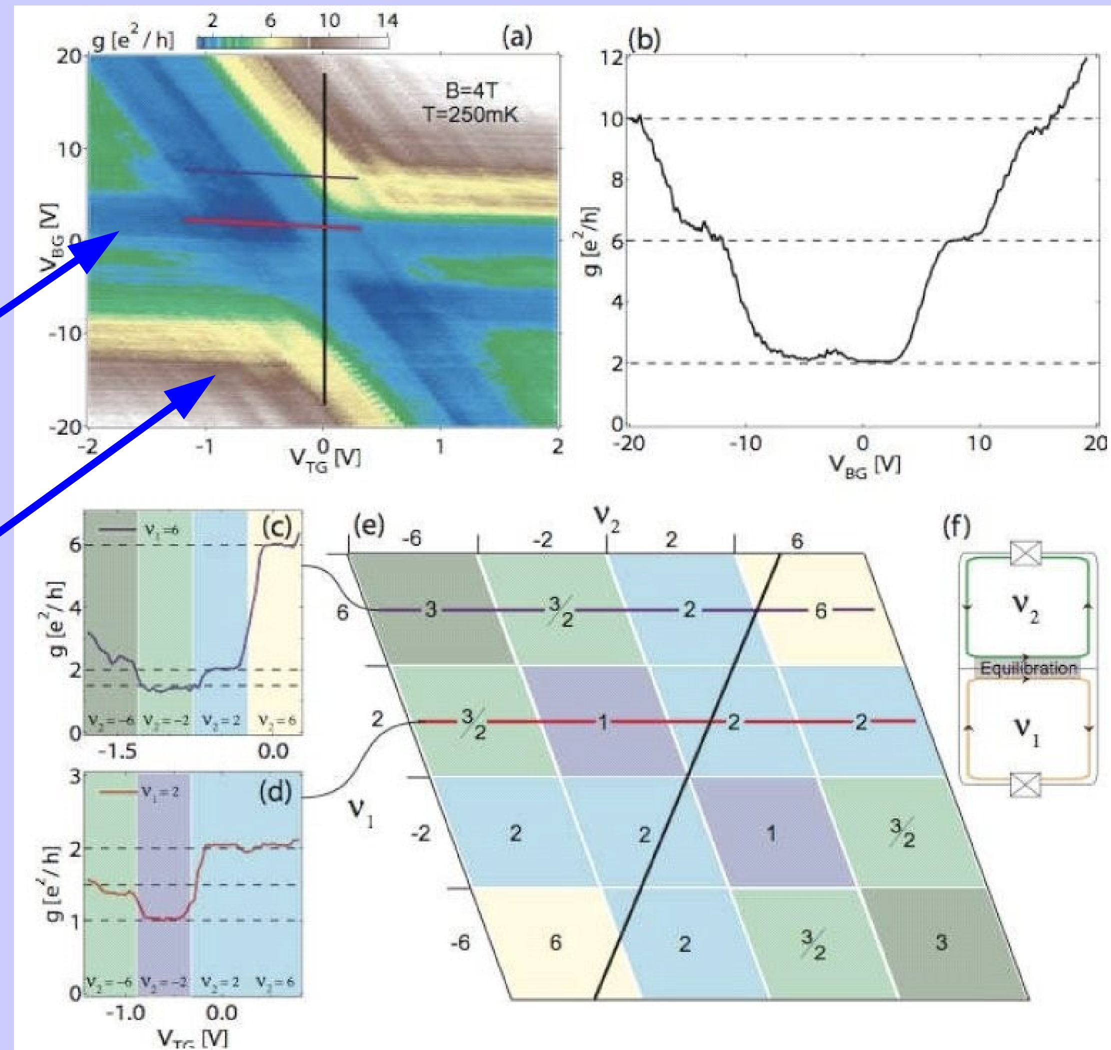

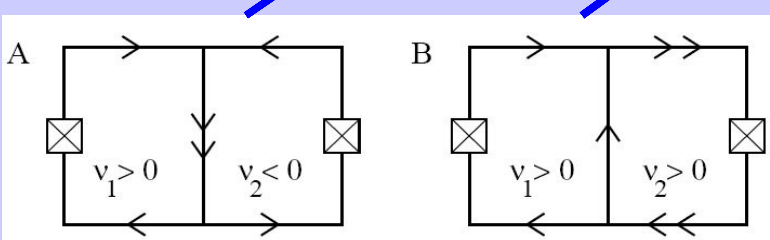

QHE in p-n junctions II

p-n

n-n, p-p

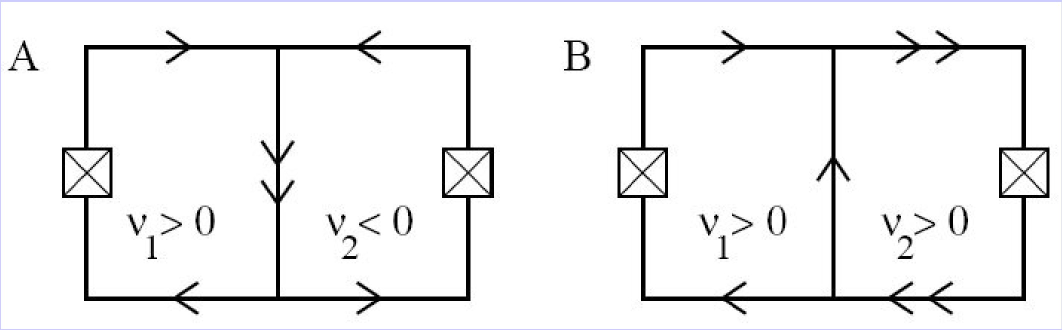

No mixing

$$g_{\rm nn} = g_{\rm pp} = \min(|\nu_1|, |\nu_2|) = 2, 6, 10\ldots$$

Noiseless transport

Quantized conductance

Mode mixing, but UCF suppressed

$$g_{\rm pn} = \frac{|\nu_1||\nu_2|}{|\nu_1| + |\nu_2|} = 1,\ \frac{3}{2},\ 3,\ \frac{5}{3}\ldots$$

Current partition, noise

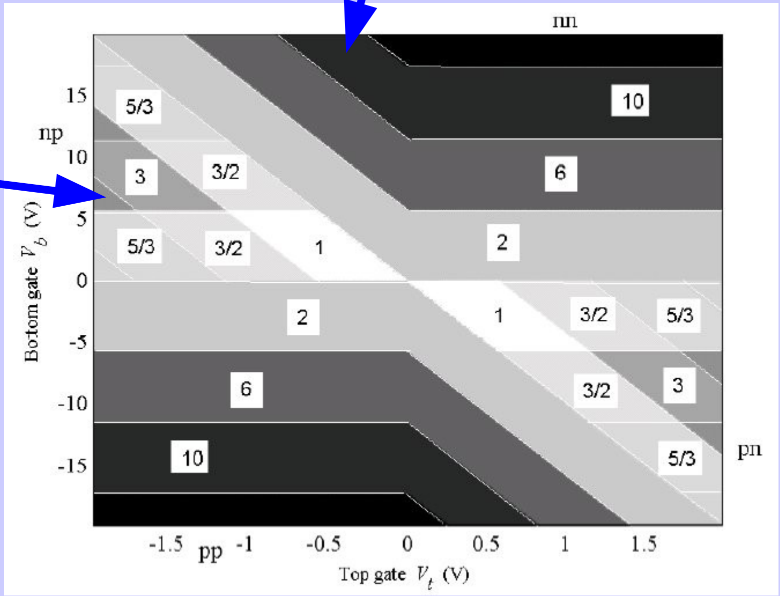

F>0

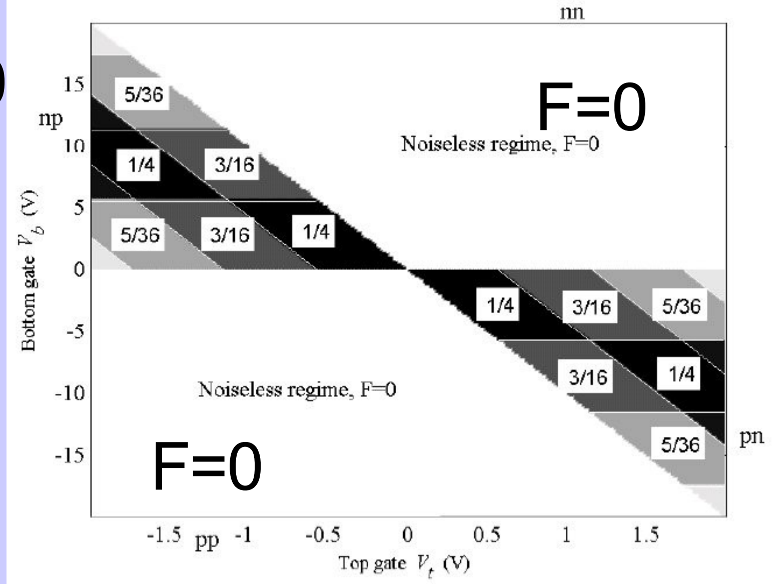

F>0

Quantized shot noise (fractional F=S/I)

Abanin & LL, Science 28 June 2007

Edge states mixing and fractional QHE in p-n-p juntions

Ozyilmaz et al 2007

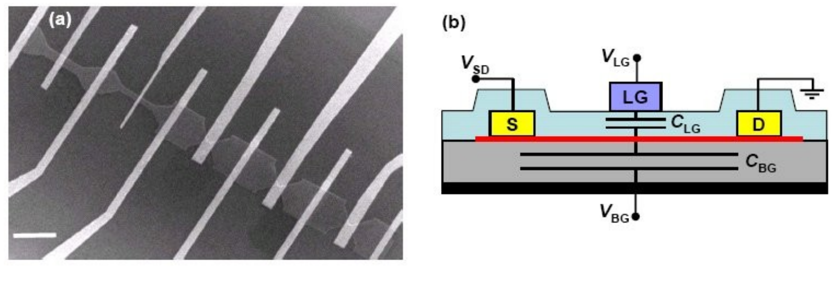

FIG. 1: (a) Scanning electron microscopy (SEM) picture showing several complete two-probe devices with local gates.

B=0

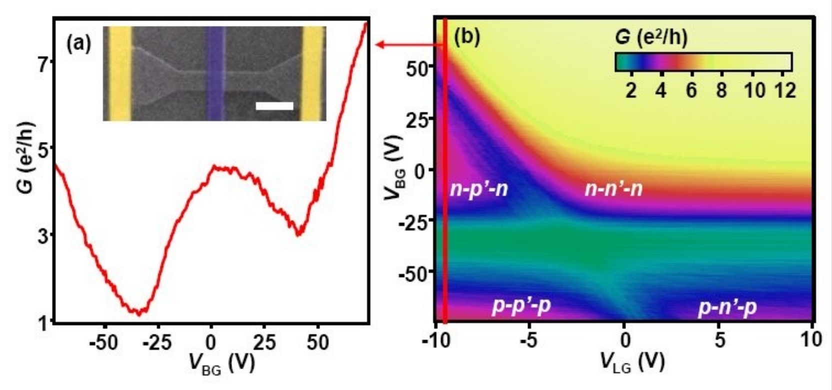

B>0

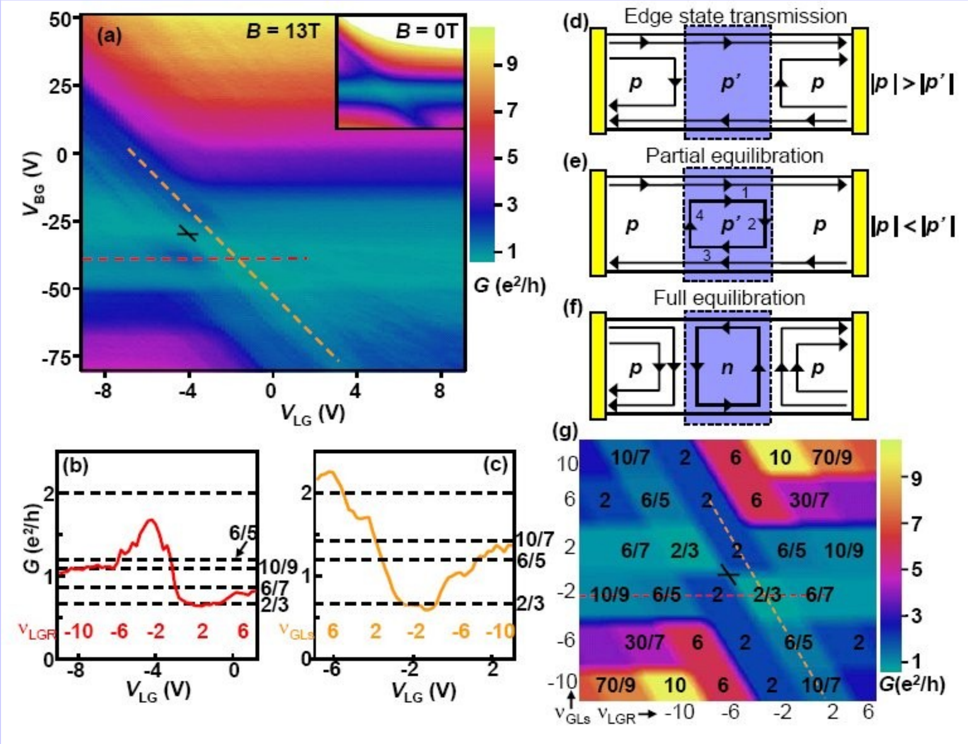

$$G = (e^2/h)|\nu'|. \quad |\nu'| \leq |\nu|$$

$$G = \frac{e^2}{h}\frac{|\nu'||\nu|}{2|\nu'| - |\nu|} = \frac{6}{5}, \frac{10}{9}, \frac{30}{7}, \ldots \quad (|\nu'| \geq |\nu|)$$

$$G = \frac{e^2}{h}\frac{|\nu'||\nu|}{2|\nu'| + |\nu|} = \frac{2}{3}, \frac{6}{5}, \frac{6}{7}, \ldots \quad (\nu\nu' < 0),$$

Little or no mesoscopic fluctuations

Stability of different fractional plateaus

2D transport vs 1D edge transport: results are identical at $\sigma_{xx}=0$

Model exactly solved by conformal mapping:
by generalizing the method of Rendell, Girvin, PRB 23, 6610 (1981)

Plateaus with $\nu=\nu'$ less stable w.r.p.t. finite σ_{xx} than other plateaus

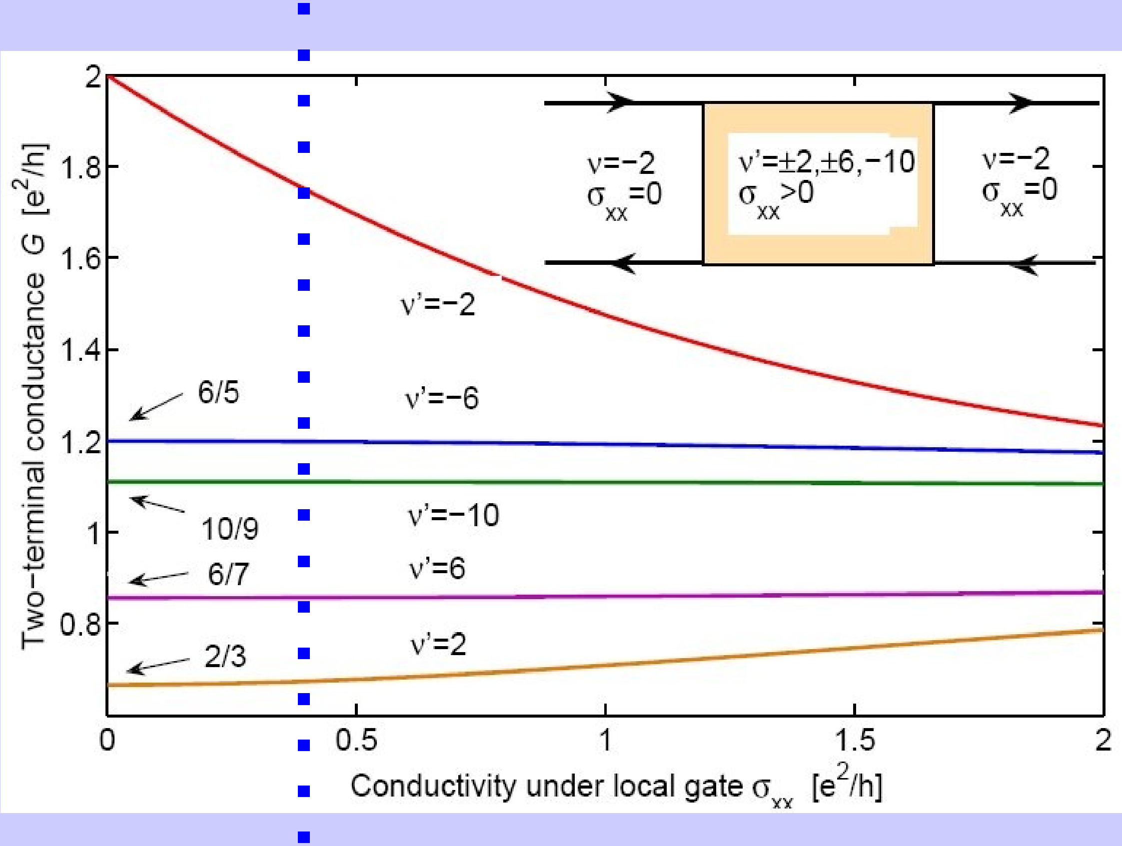

Lecture III

Spin transport at graphene edge

Spin-polarized edge states for Zeeman-split Landau levels

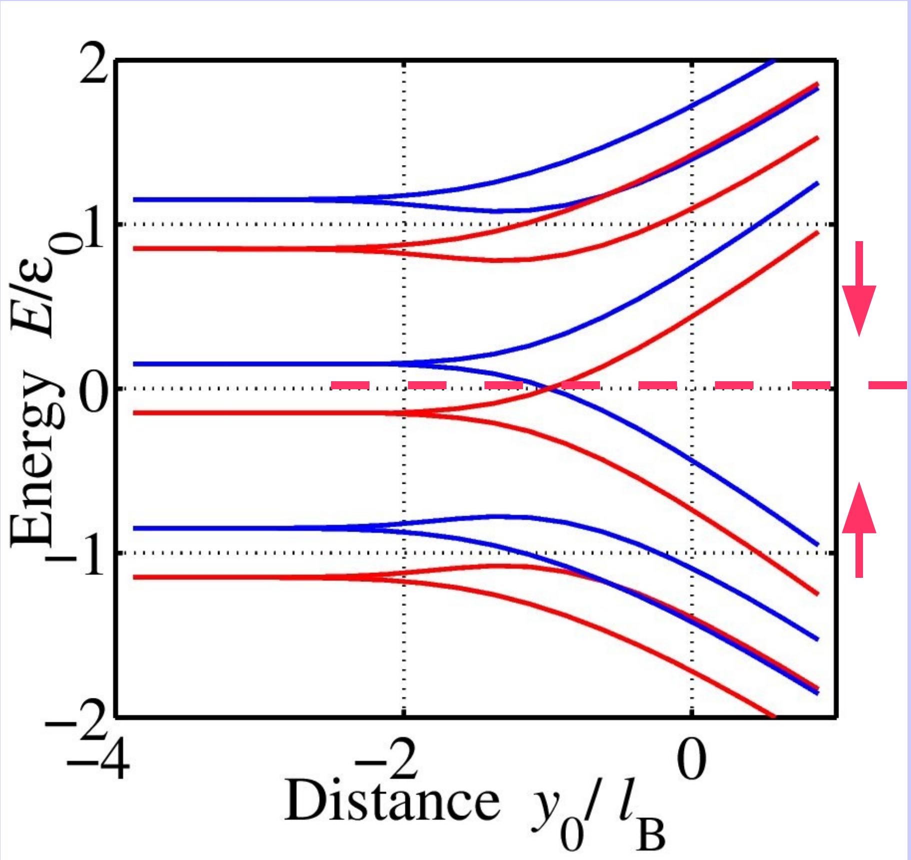

Near $\nu=0$, E=0:
(i) Two chiral counter-propagating edge states;
(ii) Opposite spin polarizations;
(iii) No charge current, but finite spin current.

Quantized spin Hall effect (charge Hall vanishes)

Edge transport as spin filter

Applications for spintronics

Similar to QSHE predicted by Kane and Mele (2005) in graphene with spin-orbital interaction (B=0, weak SO gap). Here a large gap!

What symmetry protects gapless edge states?

Gapless states, e.g. spin-split   Gapped states, e.g. valley-split

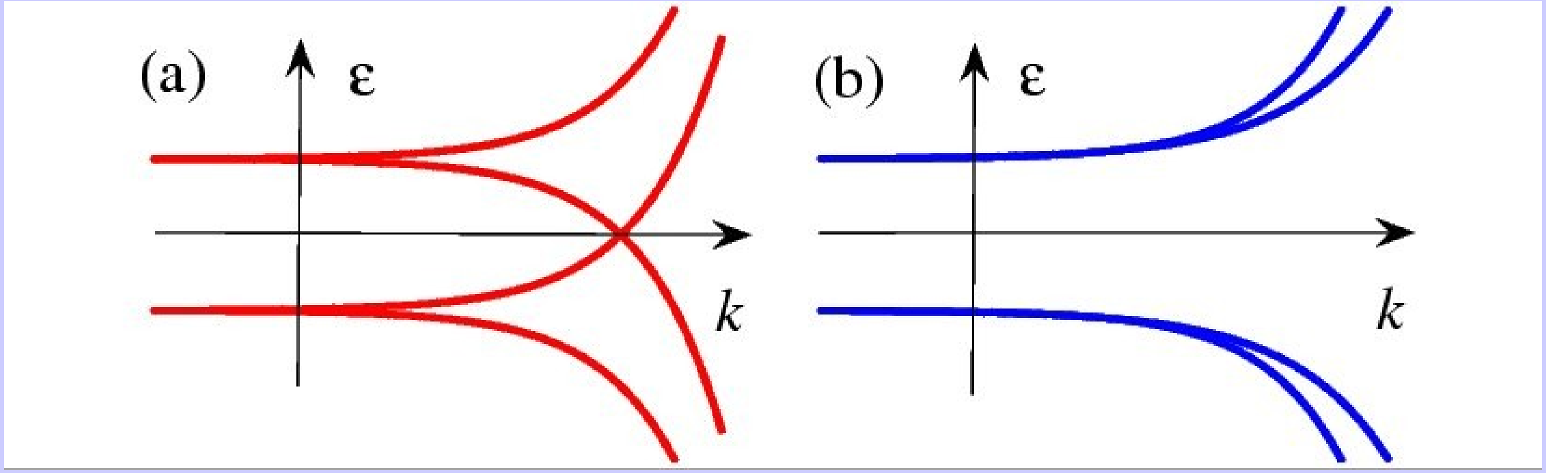

Special Z_2 symmetry requirements (Fu, Kane, Mele, 2006): in our case, the Z_2 invariant is S_z that commutes with H

Resembles massless Dirac excitations in band-inverted heterojunctions, such as PbTe, protected by supersymmetry (Volkov and Pankratov, 1985)

Manifestations in transport near the neutrality point

Gapless spin-polarized states:

a) Longitudinal transport of 1d character;
b) Conductance of order unity, e^2/h,
at weak backscattering (SO-induced spin flips);
c) No Hall effect at $\nu=0$

Gapped states:

a) Transport dominated by bulk resistivity;
b) Gap-activated temperature dependent resistivity;
c) Hopping transport, insulator-like T-dependence
d) Zero Hall plateau

Spintronics in grapene: chiral spin edge transport

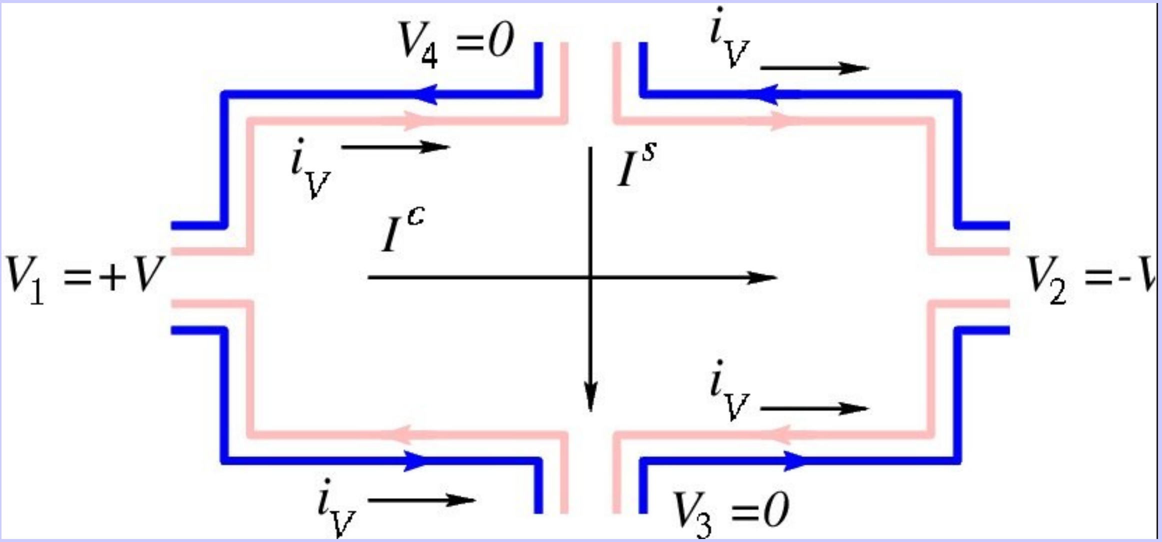

Charge current

$$I_k^c = \sum_{k'} g_{kk'} (V_k - V_{k'})$$

(Landauer-Buttiker)

A 4-terminal device,
full spin mixing in contacts

Spin current $$I_k^s = \sum_{k'} I_{kk'}^s = \sum_{k'} \epsilon_{kk'} g_{kk'} (V_k - V_{k'})$$

where $\epsilon_{kk'} = -\epsilon_{k'k}$ equals $+1$ (-1) when the current from k to k' is carried by spin up (spin down) electrons.

In an ideal clean system (no inter-edge spin-flip scattering):
charge current along V, spin current transverse to V:

$$\rho_{xx} = h/2e^2.$$

Quantized spin Hall conductance

Spin-filtered transport

Asymmetric backscattering filters one spin polarization, creates longitudinal spin current:

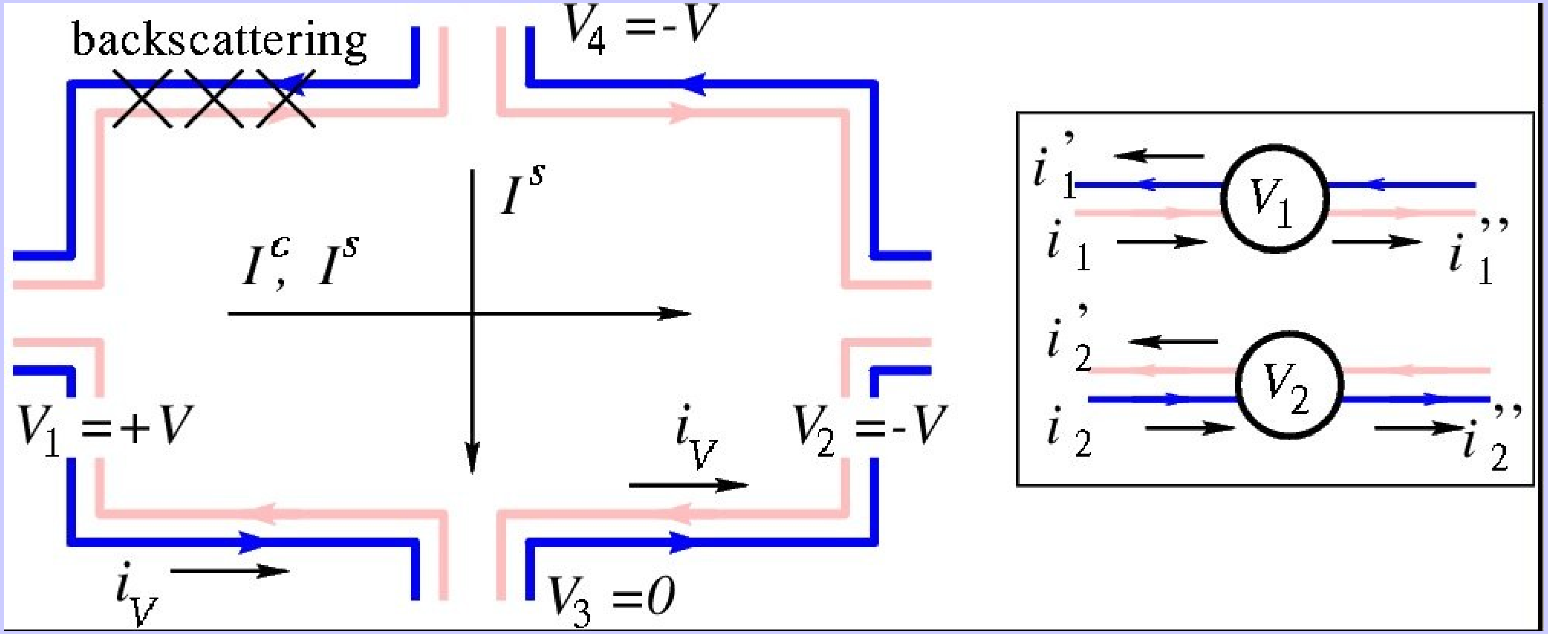

Hall voltage measures spin not charge current!

Applications: (i) spin injection; (ii) spin current detection.

Spin current without ferromagnetic contacts

Control spin-flip scattering?

- Rashba term very small, 0.5 mK;
- Intrinsic spin-orbit very small and also ineffective when spins are perpendicular to 2d plane;
- In-plane magnetic field tips the spins and allows to tune the spin-flip scattering, induce backscattering
- Magnetic impurities? Oxygen?

Applications for spintronics:

1) Quantized spin Hall effect (charge Hall effect vanishes);

2) Edge transport as spin filter or spin source;

3) Detection of spin current

Estimate of the spin gap

Exchange in spin-degenerate LL's at $\nu=0$, E=0:

- Coulomb interaction favors spin polarization;
- Fully antisymmetric spatial many-electron wavefunction;
- Spin gap dominated by the exchange somewhat reduced by correlation energy:

correlation

$$\Delta = \frac{n}{2}\int \frac{e^2}{\epsilon r}\left(1 - e^{-r^2/2l_B^2}\right) d^2 r = \left(\frac{\pi}{2}\right)^{1/2} \frac{e^2}{\epsilon l_B}(1-\alpha)$$

Gives spin gap ~100K much larger than Zeeman energy (10K)

Chiral spin edge states summary

PRL 96, 176803 (2006) and PRL 98, 196806 (2007)

- Counter-propagating states with opposite spin polarization at ν=0, E=0;
- Large spin gap dominated by Coulomb correlations and exchange
- Experimental evidence for edge transport: dissipative QHE near ν=0 (see below)
- Gapless edge states at ν=0 present a constraint for theoretical models
- Novel spin transport regimes at the edge (no experimental evidence yet)

Dissipative Quantum Hall effect

Abanin, Novoselov, Zeitler, P.A. Lee, Geim & LL,
PRL 98, 196806 (2007)

Dissipative QHE near $\nu=0$

Longitudinal and Hall resistance, T=4K, B=30T

Features:

a) Peak in ρ_{xx} with metallic T-dependence;

b) Resistance at peak ~h/e^2

c) Smooth sign-changing ρ_{xy} no plateau;

d) Quasi-plateau in calculated Hall conductivity, double peak in longitudinal conductivity

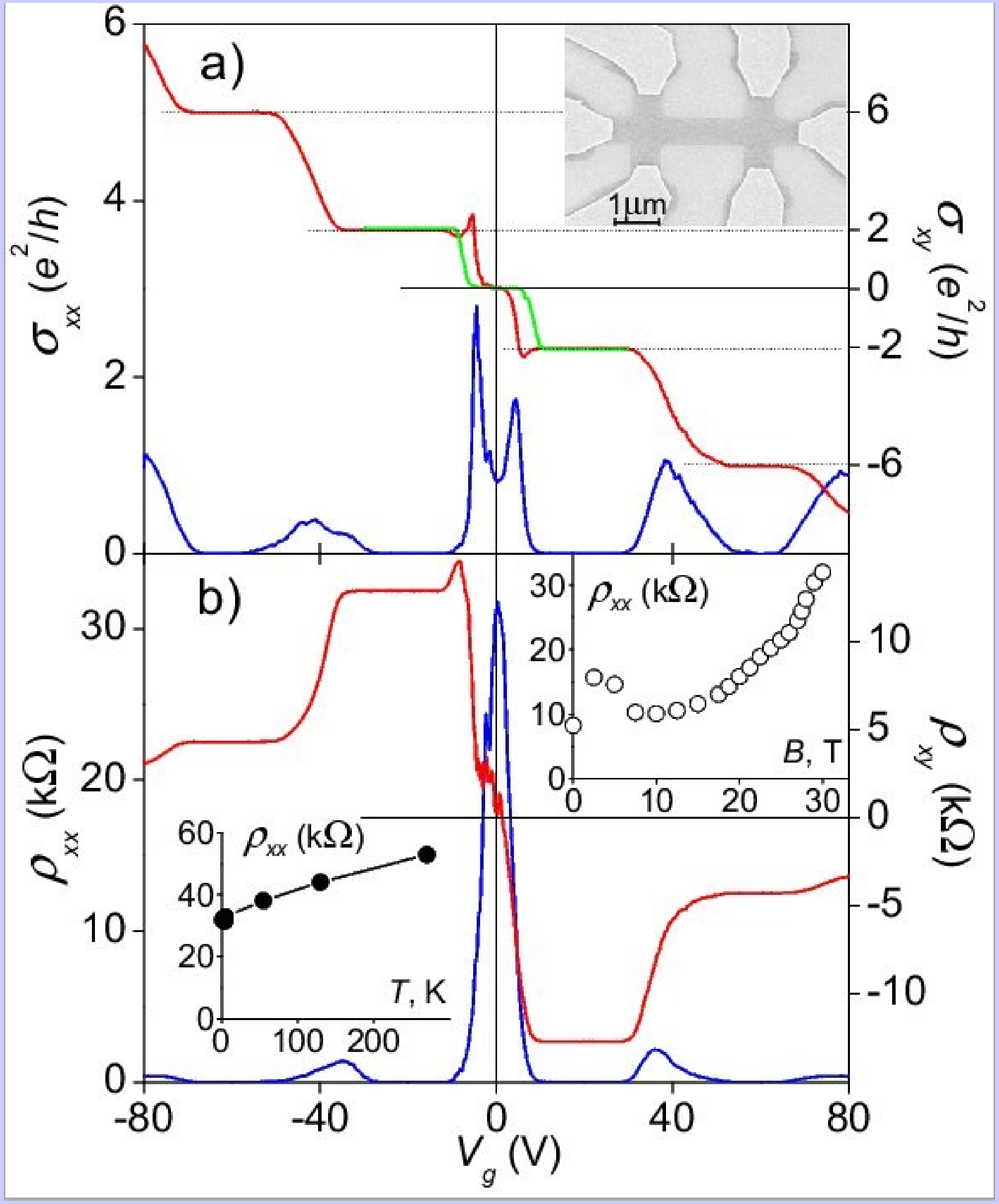

Novoselov, Geim et al, 2006

Edge transport model

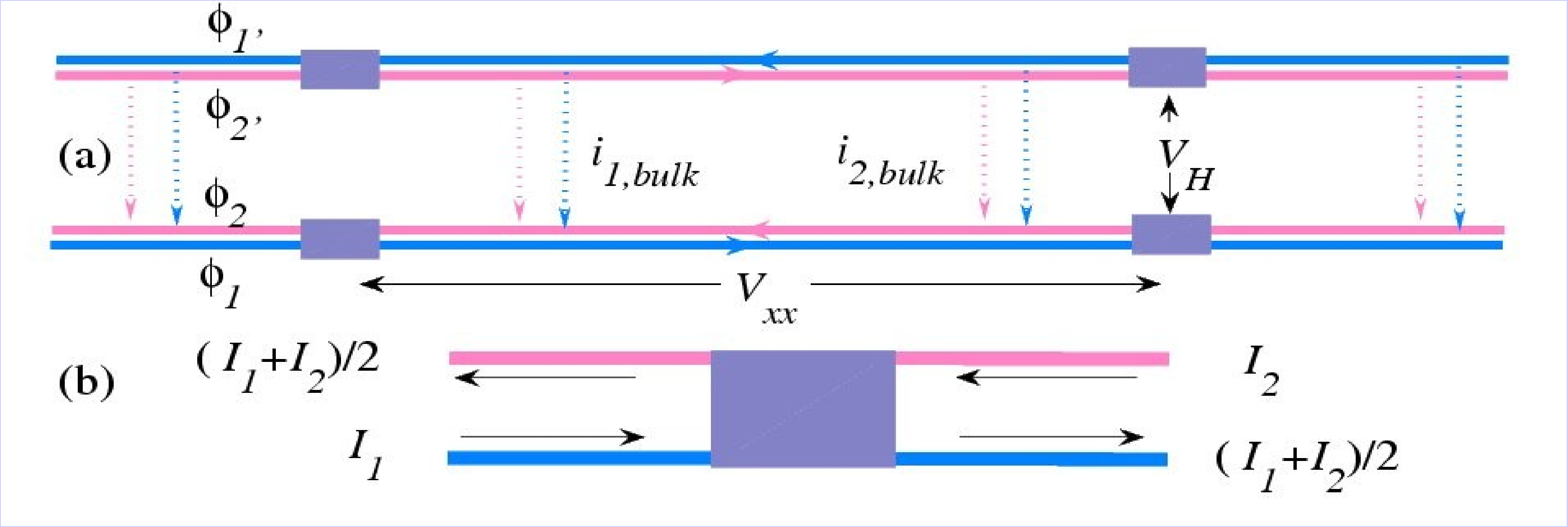

$$I_1 = \frac{e^2}{h}\varphi_1, \quad I_2 = \frac{e^2}{h}\varphi_2, \quad I = I_1 - I_2$$

$$I_{1,2}^{(\mathrm{out})} = \frac{1}{2}(I_1 + I_2)$$

$$V_{\mathrm{probe}} = \frac{h}{e^2} I_{1,2}^{(\mathrm{out})}$$

Ideal edge states, contacts with full spin mixing:
voltage drop along the edge across each contact
universal resistance value

$$\Delta\varphi = \frac{h}{2e^2}(I_1 - I_2)$$

Dissipative edge, unlike conventional QHE!

Backscattering (spin-flips), nonuniversal resistance
Estimate mean free path ~0.5 μm

$$R_{xx} = (\gamma L + 1)\frac{h}{2e^2}$$

Transport coefficients versus filling factor

Broadened, spin-split Landau levels

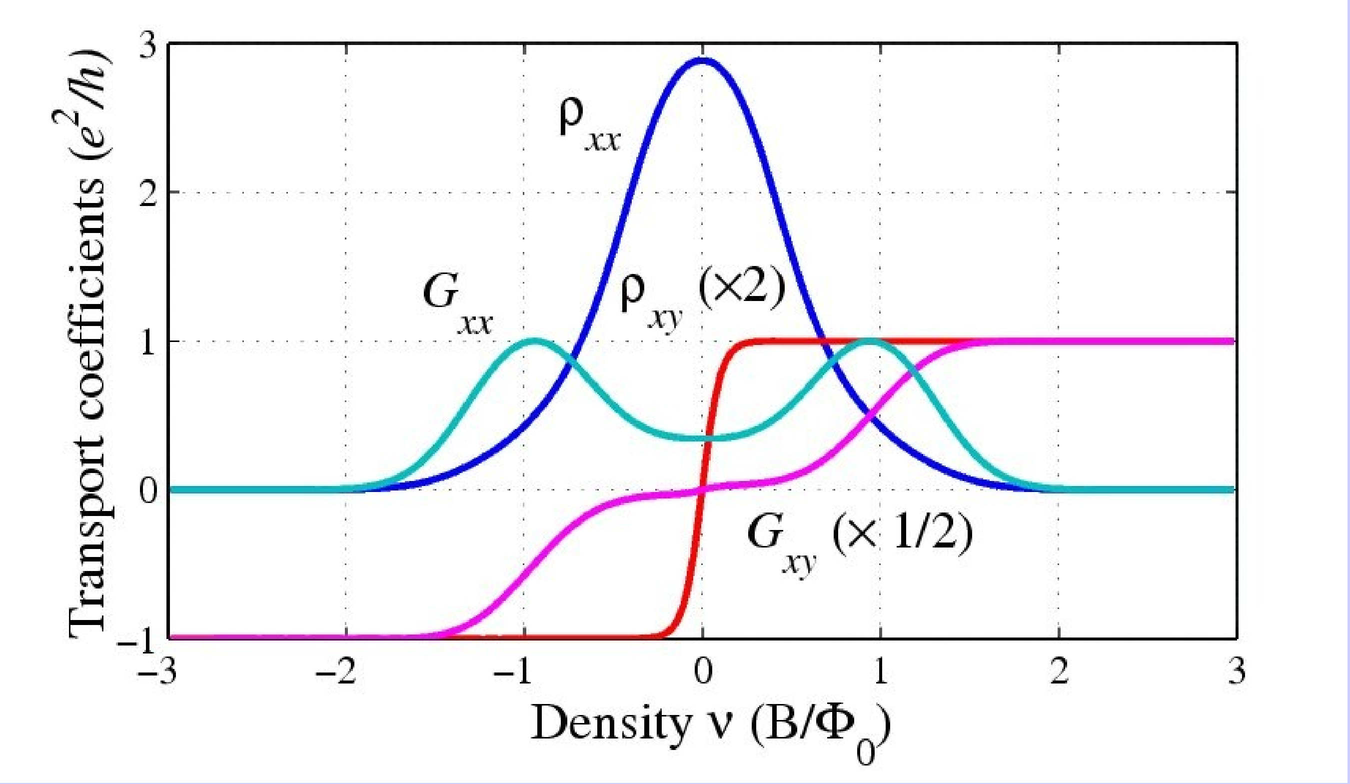

Bulk conductivity short-circuits edge:

a) peak in ρ_{xx} at $\nu=0$;

b) smooth ρ_{xy}, sign change, no plateau

c) quasi-plateau in $G_{xy}=\rho_{xy}/(\rho_{xy}^2+\rho_{xx}^2)$;

d) double peak in $G_{xx}=\rho_{xx}/(\rho_{xy}^2+\rho_{xx}^2)$

Model explains all general features of the data near $\nu=0$

The roles of bulk and edge transport interchange (cf. usual QHE): longitudinal resistivity due to edge transport, Hall resistivity due to bulk.

Charge impurities in graphene:

Atomic Collapse, Dirac-Kepler scattering, quasi-Rydberg states,

vacuum polarization, screening

Shytov, Katsnelson & LL (2007)

Transport theory

Facts:

- linear dependence of conductivity vs. electron density;
- minimal conductivity 4e^2/h

Born approximation:

$$\sigma = \frac{e^2}{\hbar} 2k_F \ell = \frac{e^2}{\hbar} 2E_F \tau_0/\hbar, \quad \hbar/\tau_0 = 2\pi\nu_F \bar{V}^2$$

Charge impurities: dominant scattering mechanism (MacDonald, Ando)

$$V(q) = \frac{2\pi e^2}{\kappa(q + 4\alpha k_F)} \approx \frac{\hbar v \pi}{2k_F}, \quad \alpha = e^2/\kappa\hbar v \approx 2.5$$

$$\sigma \propto (4e^2/h) n_{el}/n_{imp}$$

Screening of impurity potential: no difference on the RPA level

Effects outside Born and RPA approximation?

Anomaly in the Dirac theory of heavy atoms, Z>137

Textbook solution for hydrogenic spectrum fails at Z>137:

$$E_{n,j} = mc^2 \left[1 + \frac{(Z\alpha)^2}{\left(n - |\kappa| + \sqrt{\kappa^2 - (Z\alpha)^2}\right)^2} \right]^{-1/2}, \quad \alpha \equiv \frac{e^2}{\hbar c} = \frac{1}{137}, \quad n, \kappa = 1, 2, 3 \ldots$$

Finite nuclear radius important at Z>137 (Pomeranchuk, Smorodinsky)

New spectrum at 137<Z<170;
Levels diving one by one into the Dirac-Fermi sea at Z>170
(Zeldovich, Popov, Migdal)

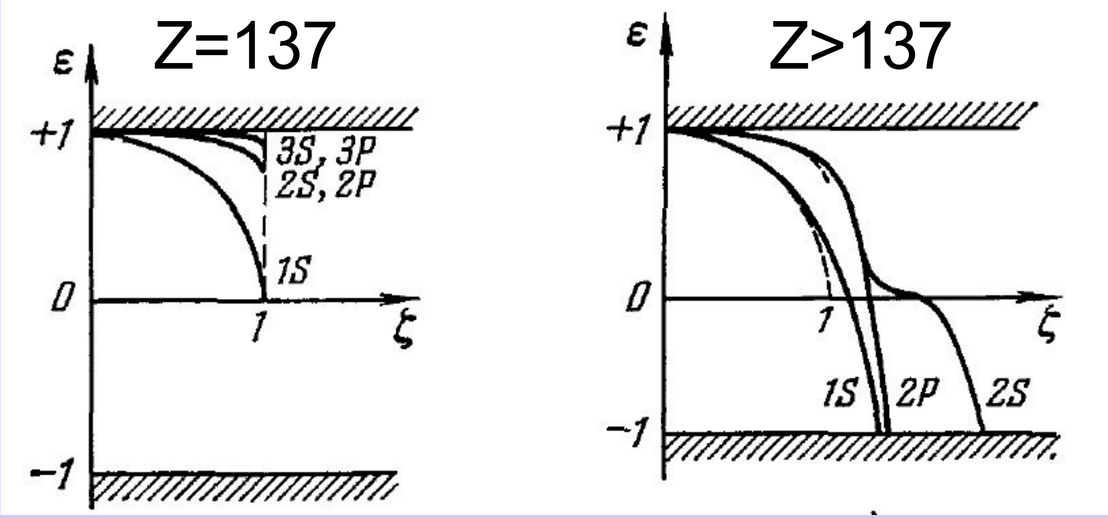

Quasiclassical interpretation:
collapsing trajectories in relativistic Kepler problem at $M < Ze^2/c$

The Dirac-Kepler problem in 2D

$$\hbar v_F \begin{pmatrix} 0 & -i\partial_x - \partial_y \\ -i\partial_x + \partial_y & 0 \end{pmatrix} \psi = \left(\varepsilon - \frac{\beta}{r} \right) \psi,$$

Potential strength

$$\beta \equiv -Ze^2/\hbar v_F$$

In polar coordinates, angular momentum decomposition:

$$\psi(r,\varphi) = \begin{pmatrix} w(r) + v(r) \\ (w(r) - v(r))\, e^{i\varphi} \end{pmatrix} r^{s-\frac{1}{2}} e^{im\varphi} e^{ikr}$$

$$s = \left((m + \tfrac{1}{2})^2 - \beta^2 \right)^{1/2}$$

Incoming and outgoing waves

For each *m*, a hypergeometric equation.

Different behavior: $|\beta| < |m + \frac{1}{2}|$, *s* real, $|\beta| > |m + \frac{1}{2}|$ *s* complex.

Scattering phases found from the relation

$$\frac{v}{w} = \exp\left(2ikr + 2i\beta \ln(2k\rho) - \pi i |m + \tfrac{1}{2}| + 2i\delta_m(k) \right)$$

Scattering phases

The phases δ_m are different in the subcritical and overcritical cases . For $|\beta| < |m + \frac{1}{2}|$,

$$\delta_m = \frac{\pi}{2}(|m + \tfrac{1}{2}| - s) - \arg\Gamma\,(s + 1 + i\beta) + \tfrac{1}{2}\arctan\frac{\beta}{s},$$

while for $|\beta| > |m + \frac{1}{2}|$ the scattering phase is given by

$$e^{2i\delta_m(k)} = e^{\pi i|m+\frac{1}{2}|}\frac{g_{\beta,\gamma} + e^{i\chi(k)}e^{-\pi\gamma}\eta g_{\beta,-\gamma}}{e^{-\pi\gamma}\eta g^*_{\beta,-\gamma} + e^{i\chi(k)}g^*_{\beta,\gamma}},$$

$$\chi(k) = 2\gamma\ln 2kr_0 + 2\tan^{-1}\frac{1+\eta}{1-\eta}, \quad \eta \equiv \sqrt{\frac{\beta-\gamma}{\beta+\gamma}},$$

where $\gamma \equiv \sqrt{\beta^2 - (m + \frac{1}{2})^2}$ and $g_{\beta,\gamma} \equiv \frac{\Gamma(1+2i\gamma)}{\Gamma(1+i\gamma+i\beta)}$.

Subcritical potential strength

Supercritical potential strength.
Use boundary condition on lattice scale $r=r_0$

Subcritical δ's energy-independent

Supercritical δ's depend on energy, π-kinks or no π-kinks

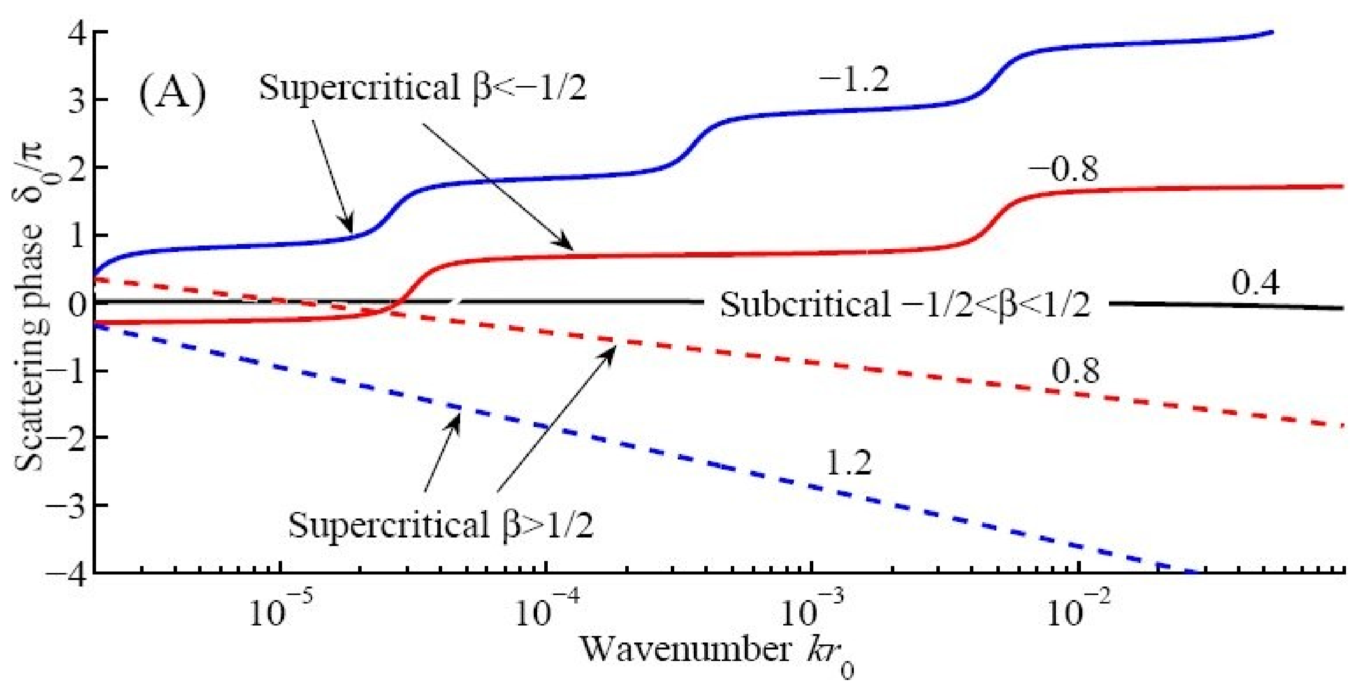

Quasistationary states I

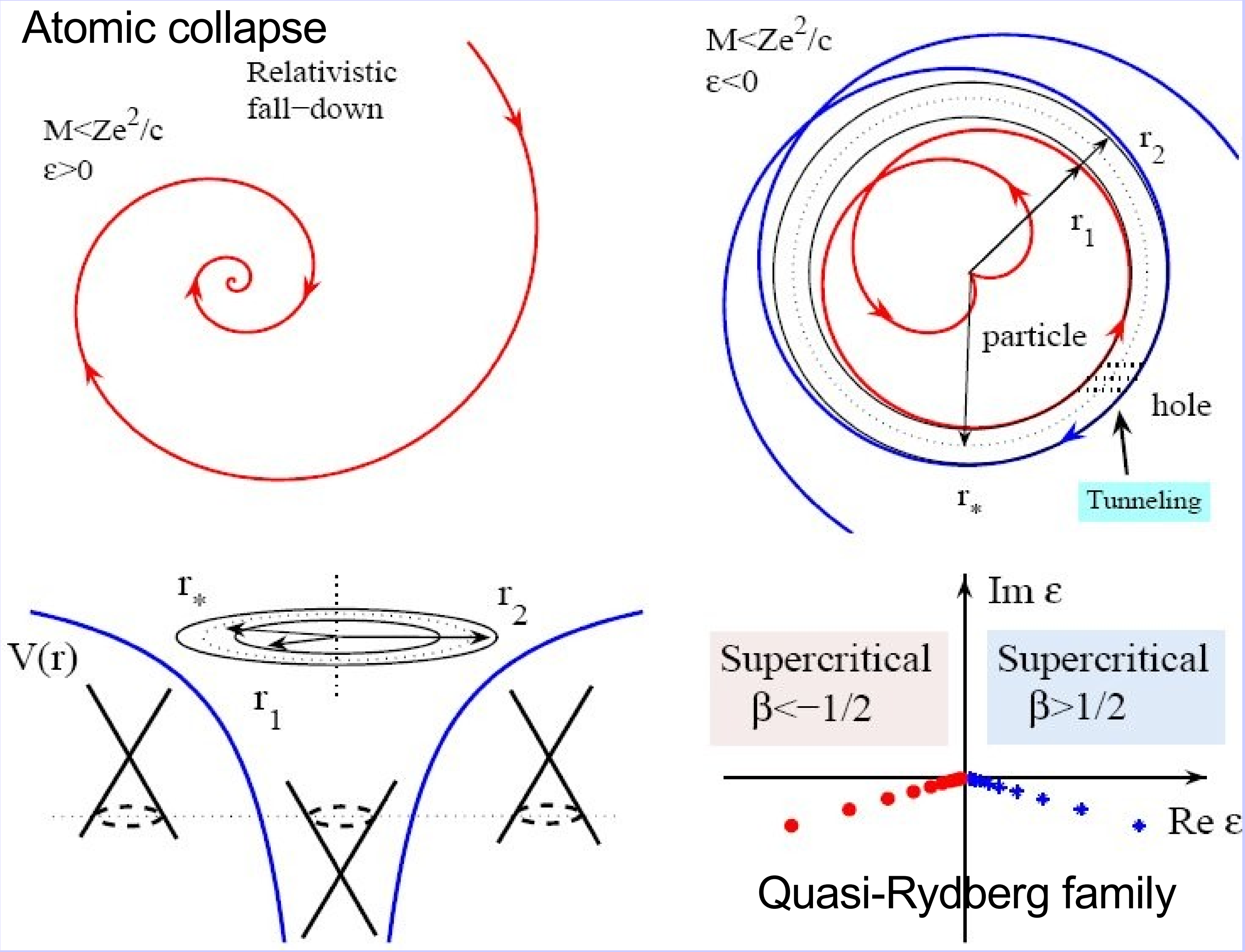

Quasistationary states II

$$p_r^2 = v_F^{-2}\left(\varepsilon + \frac{Ze^2}{r}\right)^2 - \frac{M^2}{r^2}, \quad M < M_c = Ze^2/v_F$$

Classically forbidden region

$$r_1 < r < r_2$$

$$r_{1,2} = (Ze^2 \mp M v_F)/\varepsilon$$

Bohr-Sommerfeld condition:

$$\int_{r_0}^{r_1} p_r dr = \pi\hbar n, \qquad \varepsilon_n \approx \frac{Ze^2}{r_0} e^{-\pi\hbar n/\gamma}, \quad n > 0$$

lattice scale

$$\gamma \equiv (M_c^2 - M^2)^{1/2}$$

Resonance width:

$$\Gamma_n \approx e^{-2S/\hbar} \sim |\varepsilon_n| \exp(-2\pi Ze^2/\hbar v_F)$$

$$S = \int_{r_1}^{r_2} dr \sqrt{\frac{M^2}{r^2} - \left(\frac{\varepsilon}{v_F} + \frac{M_c}{r}\right)^2} = \pi (M_c - \gamma)$$

Transport crossection

Drude conductivity

$$\sigma = \frac{e^2}{h} 2E_F\tau, \quad \tau^{-1} = v_F n_{\text{imp}} \sigma_{\text{tr}}$$

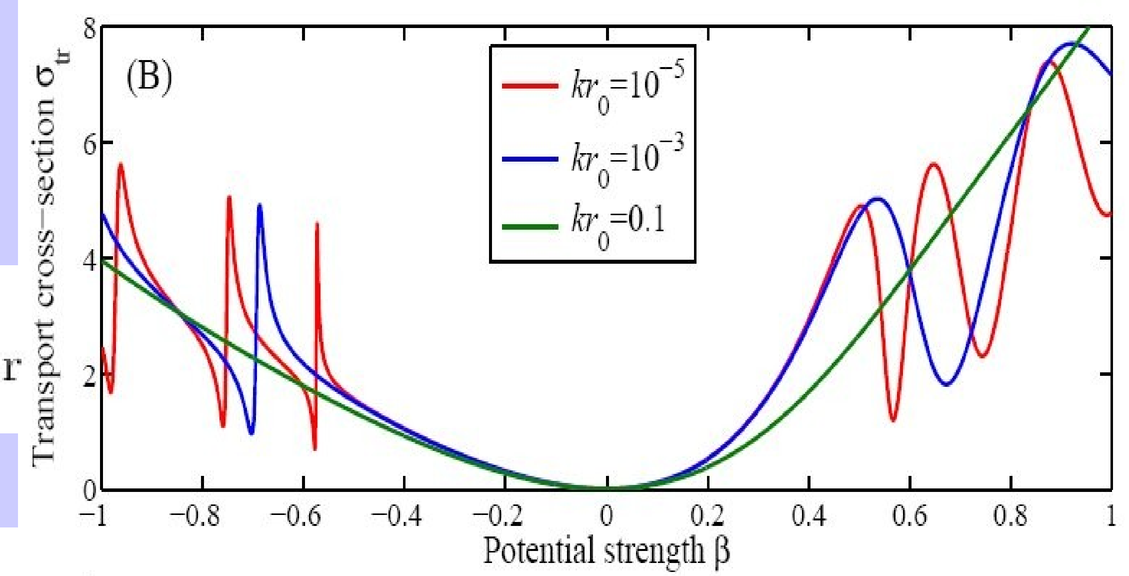

$$\sigma_{\text{tr}} = \int d\varphi (1 - \cos\varphi) |f(\varphi)|^2 = \frac{4}{k} \sum_{m=0}^{\infty} \sin^2(\delta_m - \delta_{m+1})$$

$$f(\varphi) = \frac{2i}{\sqrt{2\pi i k}} \sum_{m=0}^{\infty} (e^{2i\delta_m} - 1)\cos(m + \tfrac{1}{2})\varphi$$

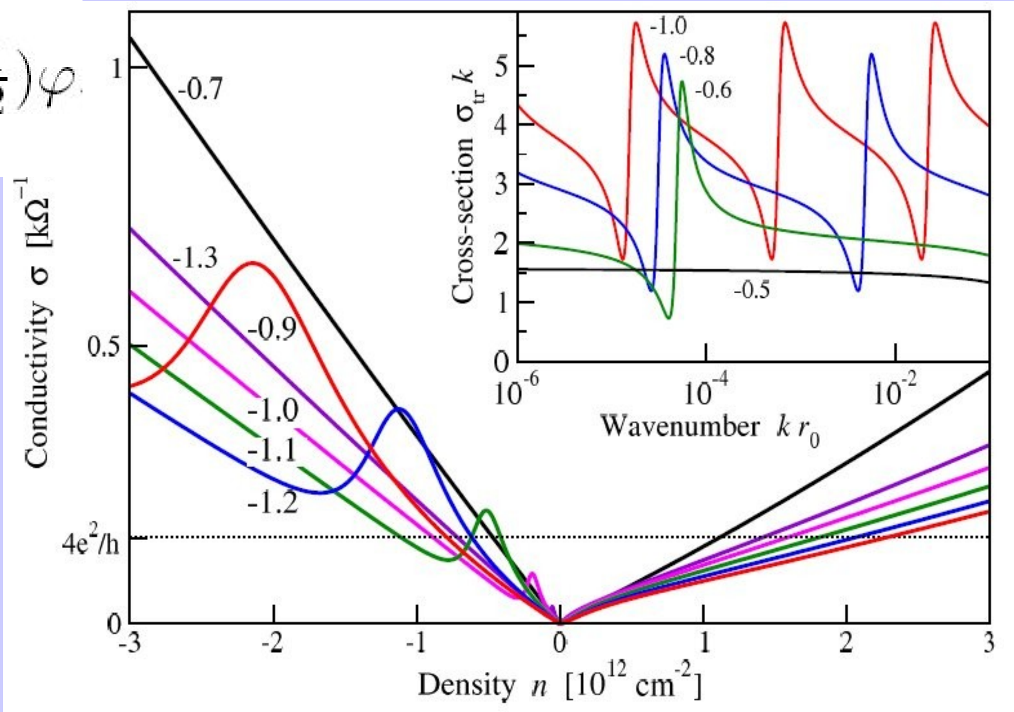

Resonance peaks when
Fermi level aligns with
one of quasiRydberg states

Resonances in the local density of states (LDOS)

Tunneling spectroscopy

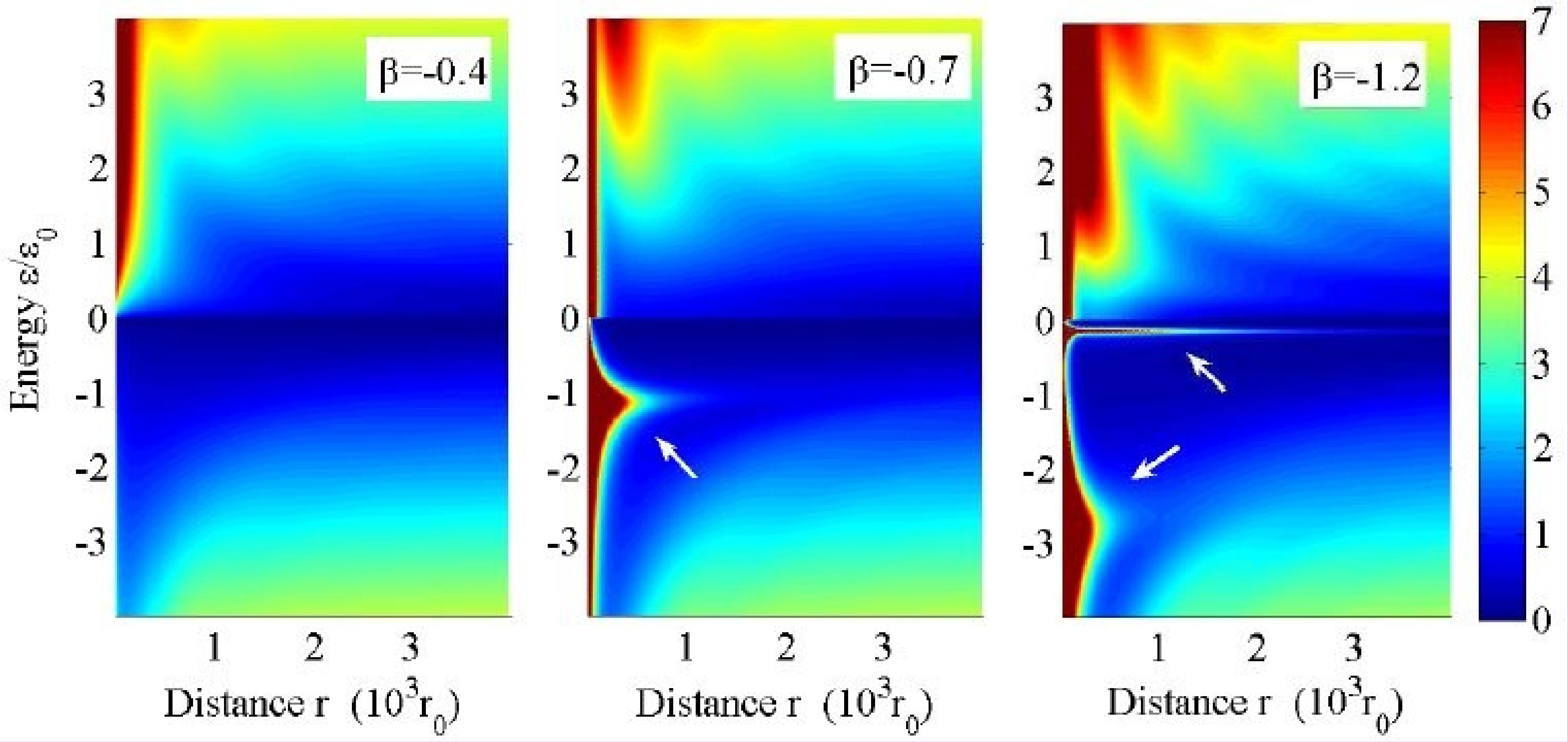

Energy scales as the width Γ and as 1/(localization radius)

Oscillations in LDOS

Standing waves
(not Friedel oscillations)

for overcritical Coulomb potential

period = 1/energy

period > lattice constant, can be probed with STM

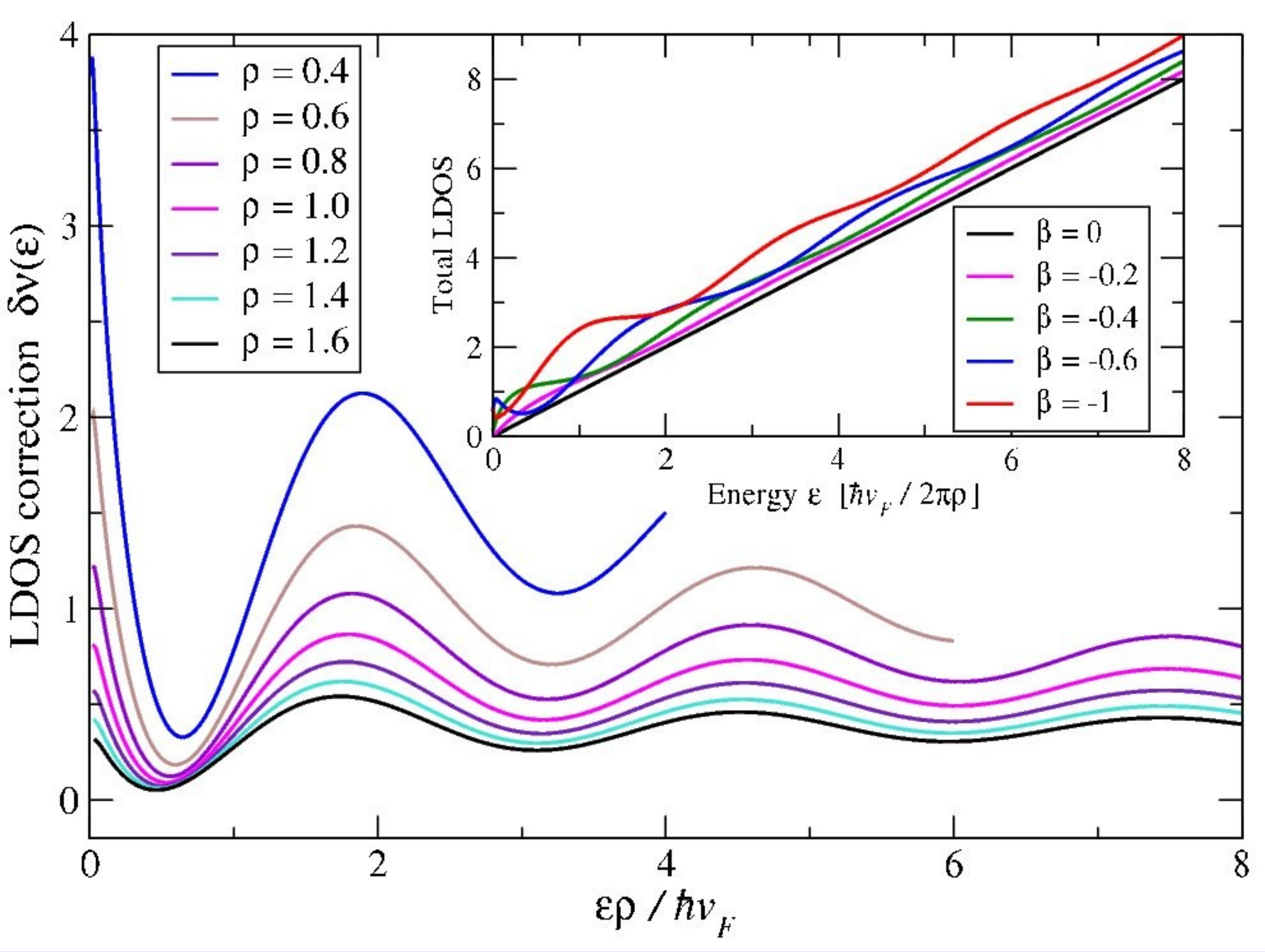

Screening by massless Dirac particles: vacuum polarization

Critical Coulomb potentials in d=2:

$$\beta = \beta_c = \frac{1}{2}, \quad \beta \equiv \frac{Ze^2}{\kappa \hbar v_F}$$

$$Z_c \approx 1$$

In graphene:

$$\frac{e^2}{\hbar v_F} \approx 2.5$$

$$\kappa_{\mathrm{RPA}} \approx 5.$$

Easier to realize than Z>137 for heavy atoms!
Need divalent or trivalent impurities

Polarization charge localized on a lattice scale at $\beta < \frac{1}{2}$

Mirlin et al (RPA), Sachdev et al (CFT)

A power law for overcritical potential:

$$n_{\mathrm{pol}}(\rho) \approx -\frac{N\gamma \,\mathrm{sign}\, \beta}{2\pi^2 \rho^2} + q_0 \delta(\rho), \quad \gamma \equiv \sqrt{\beta^2 - \frac{1}{4}}$$

$$\frac{1}{2} < \beta < \frac{3}{2}$$

Friedel sum rule argument

Use scattering phase to evaluate polarization?

Caution: energy and radius dependence for Coulomb scattering

$$\beta < \beta_c : \quad \theta(k) \approx \beta \ln k\rho$$

$$\beta > \beta_c : \quad \theta(k) \approx \beta \ln k\rho - \gamma \mathrm{sign}\, \beta \ln k r_0$$

Geometric part, not related to scattering, (deformed plane wave)

The essential part

$$Q_{\mathrm{pol}}(\rho) = -N \frac{\theta(k \sim 1/\rho)}{\pi} = -\,\mathrm{sign}\, \beta \frac{\gamma N}{\pi} \ln \frac{\rho}{2r_0}.$$

RG for polarization cloud

Log-divergence of polarization, negative sign,
but no overscreening!

RG flow of the net charge (source+polarization):

$$\frac{d\beta(\rho)}{d\ln\rho} = -\frac{N\,\mathrm{sign}\,\beta}{\pi\kappa}\gamma(\rho), \quad \beta > \beta_c.$$

Polarization cloud radius:

$$\rho_* = r_0 \exp\left(\frac{\pi\kappa}{N}\cosh^{-1}(2\beta)\right)$$

Nonlinear screening of the charge in excess of 1/2

Summary

- Different behavior for subcritical and supercritical impurities
- QuasiRydberg states in the supercritical regime
- Quasilocalized states (resonances), and long-period standing wave oscillations in LDOS around supercritical impurities
- No polarization away from impurity for charge below critical (in agreement with RPA)
- Power law 1/r^2 for polarization around an supercritical charge
- Log-divergence of the screening charge: nonlinear screening of the excess charge Q-1/2, spatial structure described by RG

Atomic collapse, Z>170, can be modeled by divalent or trivalent impurities in graphene

The End

For zigzag edge surface states possible even without B field!

Surface mode propagating along zigzag edge (weak dispersion due to *nnn* coupling)

Momentum space:
(Peres, Guinea, Castro Neto)

zigzag edge

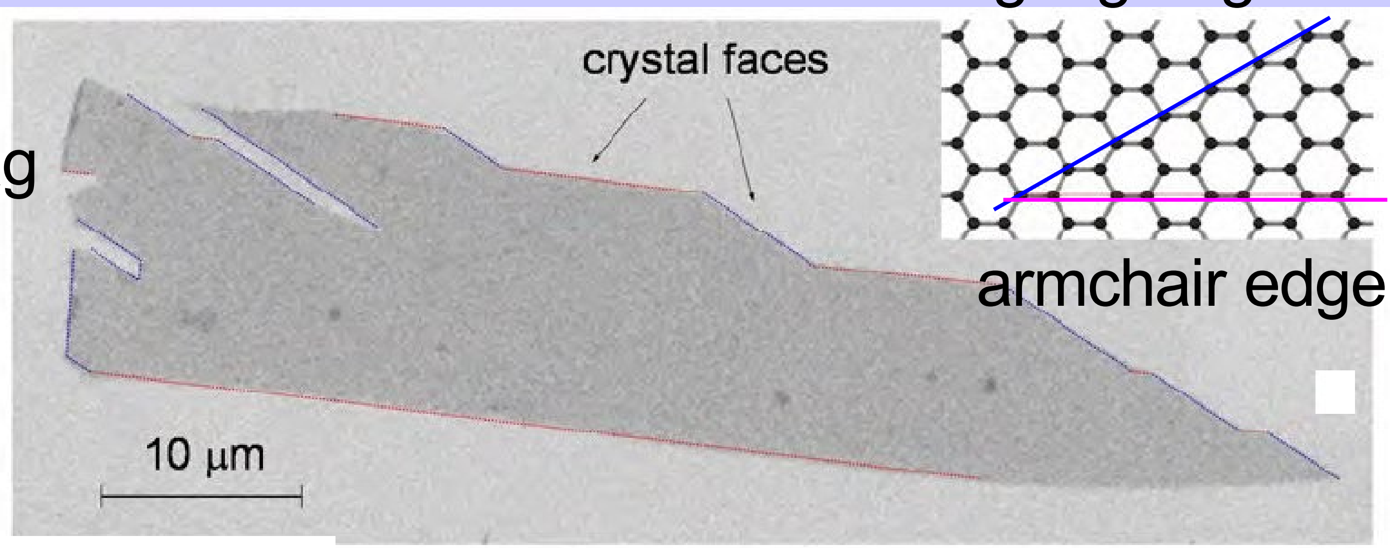

armchair edge

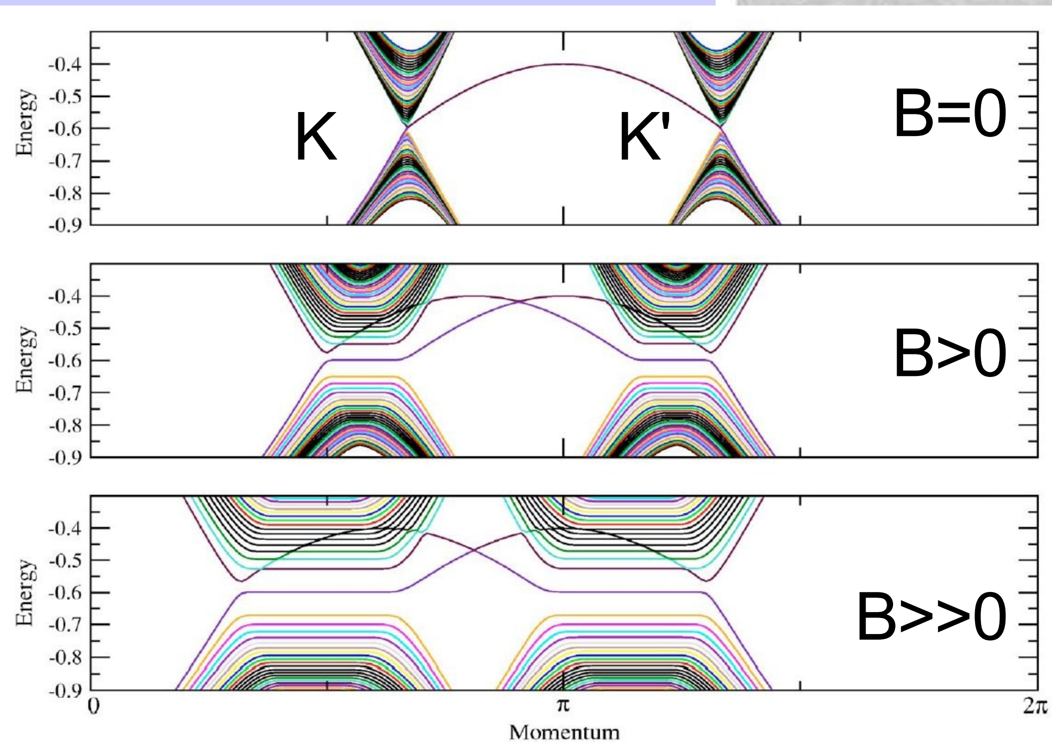

crystallites not just flakes

Scanning tunneling spectroscopy of 3D graphite top layer (Niimi et al 2006)

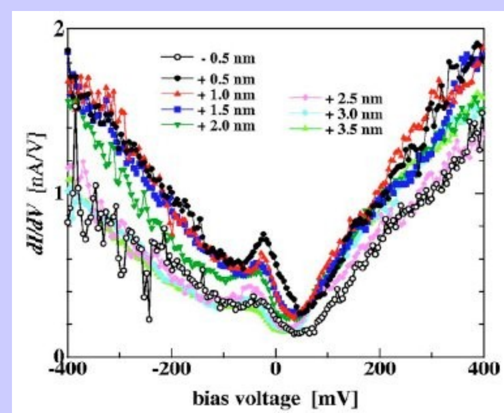

zigzag

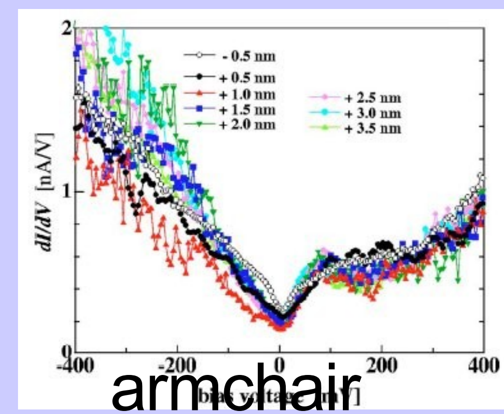

armchair

Reviews on graphene:

Topical volume (collection of short reviews):
Solid State Comm. v.143 (2007)

A. Geim & K. Novoselov “The rise of graphene”
Nature Materials v.6, 183 (2007)